

**CLIMATE IMPACT ON BACTERIAL MENINGITIS OCCURRENCE OVER WEST
AFRICA**

By

DIARRA DIOUF

**B.Sc. (Physics and Chemistry), M.Sc. (Sciences of Meteorology, Oceanography and
Management of Arid area)
(MCS/20/7723)**

A Thesis of the Doctoral Research Programme of the West Africa Climate Systems, under the West Africa Science Service Centre on Climate Change and Adapted Land Use, in the Department of Meteorology and Climate Science submitted to the School of Postgraduate Studies in partial fulfilment of the requirements for the award of the degree of Doctor of Philosophy in Meteorology and Climate Science of the Federal University of Technology, Akure, Nigeria.

June, 2025.

DECLARATION

I hereby declare that this Thesis was written by me and is a correct record of my own researchwork. It has not been presented in any previous application for any degree of this or any University. All citations and sources of information are clearly acknowledged by means of references.

Candidate's Name: Diarra Diouf

Signature:

Date

CERTIFICATION

We certify that this Dissertation entitled “Climate Impact on Meningococcal Meningitis occurrence over West Africa” is the outcome of the research carried out by Diarra Diouf under the WASCAL DRP-WACS in the Department of Meteorology and Climate Science of the Federal University of Technology, Akure.

Prof. A. Akinbobola.....

(Major Supervisor)

Department of Meteorology and Climate Science,
Federal University of Technology,
Akure, Nigeria.

Signature:

Date

Prof. A. T. Gaye.....

(Co-Supervisor)

Ecole Superieur Polytechnique,
Universite Cheikh Anta Diop,
Dakar, Senegal.

Signature:

Date

Dr. M. Martín-Rey.....

(Co-Supervisor)

Departamento de la Fisica de la Tierra y Astrofisica,
Universidad Complutense de Madrid, Spain.

Signature:

Date

Prof. Rodríguez-Fonseca. B.....

(Co-Supervisor)

Departamento de la Física de la Tierra y Astrofísica,
Universidad Complutense de Madrid, Spain.

Signature:

Date

Dr. I. Diouf.....

(Advisor)

Ecole Supérieur Polytechnique,
Université Cheikh Anta Diop,
Dakar, Senegal.

Signature:

Date

Prof .I.A Balogun

(Director)

Doctoral Research Program-West African Climate Systems
West African Science Service Center on Climate Change and
Adapted Land Use (DRP-WACS, WASCAL),
Federal University of Technology,
Akure, Nigeria.

Signature:

Date

ABSTRACT

Bacterial meningitis remains a significant public health concern in West Africa, where seasonal outbreaks are closely linked to environmental factors such as low humidity, high temperatures and exposure to Saharan dust. While the influence of local climatic conditions on meningitis is well documented, the role of large-scale climate variability, particularly that of the El Niño–Southern Oscillation (ENSO), influencing global climates through complex atmospheric and oceanic mechanisms is still not fully understood. These mechanisms may affect Saharan dust activities and local climate conditions which are associated with meningitis outbreaks during the dry season.

This study provides a comprehensive assessment of the relationship between climate and meningitis in West Africa by exploring the interactions between ENSO variability, Saharan dust dynamics and bacterial meningitis incidence in two climatically distinct regions: the Sahel (SAH) and the Gulf of Guinea (GG). This thesis addressed four specific objectives such as: 1) to characterise the seasonal meteorological and dust-related conditions that shape the meningitis cycle; 2) to examine the interannual and spatial variability of these environmental drivers; 3) to identify the large-scale atmospheric and oceanic mechanisms influencing dust variability; and 4) to develop machine learning models for estimating meningitis incidence, using environmental variables and vaccination coverage as inputs.

Weekly environmental and meningitis cases data from 2006 to 2020 were analyzed at seasonal and interannual scale and predict meningitis incidence. At large-scale, monthly Saharan dust, Sea Surface temperature, Sea level pressure and winds components from 1980 to 2020 were employed. Empirical orthogonal function (EOF), lag Spearman correlation, regression map and

composite analyses were applied to reveal a local and large-scale relationship between Saharan dust patterns influencing meningitis dynamics and its ENSO impact.

At seasonal and interannual scale, high concentration of particulate matter (PM₁₀) and aerosol optical depth (AOD) in January reliably precede meningitis outbreaks. The persistence and intensity of the leading mode of dust variability (70.5% in the SAH with peaks in March–April and 70.8% in the GG during January–March) associated with relative humidity (RH) below 20% in the SAH and 45% in the GG, increase the number of cases. At large-scale, SST anomalies in the equatorial Pacific (warm/cool) coincide with elevated dust variability (AOD-PC1) during the JFM–MAM in the GG and FMA–MAM over the SAH. Models like XGBoost in Nigeria ($R^2 = 0.638$), CatBoost in Burkina Faso ($R^2 = 0.619$), Gradient Boosting in Niger ($R^2 = 0.487$) and Random Forest in Mali ($R^2 = 0.355$) identified as the best. However, vaccination status, RH and meridional wind consistently emerged as the most influential predictors across all countries.

These findings advance our understanding of how large-scale climate variability and dust dynamics influence meningitis outbreaks in West Africa. They also demonstrate the utility of machine learning (ML) approaches for forecasting disease risk and support the integration of climate-informed early warning systems, particularly in settings where data is scarce.

ACKNOWLEDGMENTS

I want appreciate God for His grace to successfully complete my Ph.D Degree Programme.

Many thanks to:

the Federal Ministry of Education and Research (BMBF), Germany for sponsoring the WASCAL programme at the Federal University of Technology, Akure (FUTA DRP-WACS);

the Department of Meteorology and Geophysics, Faculty of Physics of the Universidad Complutense de Madrid (UCM) for their support and hospitality toward the student during the research process;

the Laboratory of Atmospheric Physics and Oceanography–Simeon Fongang (LPAO-SF) for their invaluable collaboration and provision of data resources;

the Erasmus+ programme through a Higher Education Learning Agreement for Studies, I completed a 5-month academic stay at Universidad Complutense de Madrid in 2023.

My sincere gratitude goes to my team of supervisors, the major Supervisor **Prof. A. Akinbobola**, Co-Supervisors **Prof. A. T. Gaye**, **Prof. B. R. Fonseca** and **Dr. M. Martin** and Advisors **Dr. I. Diouf** and **Dr. C. Dione**, thank you for always motivating me, for the invaluable advice, encouragement, constructive criticism, insightful suggestions and comments throughout the conduct of this research.

To my host university, the Federal University of Technology Akure, Nigeria through the Doctoral Research Program West African Climate Systems (DRP-WACS) under the Directorship of Professor **I.A Balogun** for the coordination and efforts toward the successful completion of the program.

I would like to show my gratitude to the LABORATOIRE DE PHYSIQUE DE L'ATMOSPHERE ET DE L'OCÉAN Siméon FONGANG (**LPAO-SF/ ESP/ UCAD**)

Departamento de Física de la Tierra, Astronomía y Astrofísica , Universidad Complutense de Madrid Laboratorio de Geofísica y Meteorología,

To my father **Babacar Diouf**, an inexhaustible source of inspiration and wisdom;

To my brave mother **Khady Thiam**, for her unconditional love and the values she passed on to me;

To my brothers and sisters, for the trust they place in my humble self;

To my aunt **Ndeye Thiam**, for her constant love and support;

To my sister **Aissatou Faye**, a wascalian from Batch 3, who has always provided me with comfort and support from the beginning to the end of this thesis;

To my sister **Mariama Diouf**, a Geo-Tech engineer, who has always given me comfort in all circumstances;

To **Moustapha Sow**, who has always helped me in prayers all circumstances and my gratitude also go to my all my fellow WASCAL comrades, especially Dametoti Yamoula, Moussa Ibrahim Maiga, Aissa Sita, Yeo Kolothioloma, Millogo Nadege, Francis, Robert Akum, Gyuk Nehemiah John and Wilson Ilori.

DEDICATION

In the name of ALLAH, the Most Gracious, the Most Merciful.

May peace and blessings be upon the Seal of the Prophets, our Master **MOUHAMAD** (peace and blessings be upon him), a source of light and guidance for all of humanity.

I dedicate this work to **CHEIKH AHMADOU MBAMBA, KHADIMOU RASSOUL** the noble founder of my *confrérie* “**Mouride**”, whose spiritual legacy, teachings, and example have deeply inspired and guided my path. May Allah reward him abundantly and elevate his rank in the hereafter.

To my dear parents, whose unconditional love, prayers, and sacrifices have been the cornerstone of my life and academic journey. Your unwavering support has made this achievement possible.

May this humble work bring honor to you all.

TABLE OF CONTENTS

TITLE PAGE	i
DECLARATION	ii
CERTIFICATION	iii
ABSTRACT	v
ACKNOWLEDGMENTS	vii
DEDICATION	ix
TABLE OF CONTENTS	x
LIST OF TABLES	xvi
LIST OF FIGURES	xvii
LIST OF EQUATIONS	xxiii
LIST OF ACRONYMS	xxiv
CHAPTER ONE	1
INTRODUCTION	1
1.1 Background to the Study	1
1.2 Statement of Research Problems	3
1.3 Aim and Specific Objectives	4
1.4 Justifications	5
1.5 Research scope	7
1.6 Structure of the document	8
CHAPTER TWO	9
LITERATURE REVIEW	9
2.1 Epidemiology of Bacterial Meningitis in West Africa	9

2.2	Transmission of Bacterial Meningitis	12
2.3	Climatic and Environmental Determinants of Meningitis in the African Meningitis Belt	12
2.3.1	Environmental Sensitivity of Meningitis	13
2.3.2	Temporal and Spatial Variability in Meningitis Patterns	13
2.3.3	Forecasting and Modelling Approaches	14
2.3.4	Operationalising Early Warning Systems	15
2.3.5	Recent Evidence and Ongoing Challenges	15
2.4	Environmental and Meteorological Drivers	16
2.4.1	Wind Dynamics and dust transport	16
2.4.2	Temperature	19
2.4.3	Relative Humidity (RH)	20
2.4.4	Saharan Dust and Health Outcomes	21
2.5	Efforts made against meningitis disease	24
2.6	Impacts vaccine against meningitis	25
2.7	Potential Gaps Identified	26
2.8	Large-Scale Climate Drivers and Their Influence on West African Climate and Dust Activity	27
2.9	Predictive Models and Early Warning Systems	28
	CHAPTER THREE	30
	MATERIALS AND METHODS	30
3.1	Description of the Study Area	30
3.2	Data Sources	33

3.2.1	Meningitis Data	33
3.2.2	Aerosols Datasets	33
3. 2.2.1	MERRA-2 Reanalyses	33
3. 2.2.2	CAMS Reanalyses	34
3. 2.3	ERA5 Reanalyses and HadISST	35
3.3	Methods	38
3.3.1	Statistical Methods	38
3.3.1.1	Seasonal and Intra-seasonal Cycle	38
3.3.1.2	Intra-seasonal and Interannual anomalies	39
3.3.1.3	Empirical Orthogonal Functions (EOF)/Principal Component Analysis (PCA)	39
3.3.1.4	Spearman and Lead-Lag Correlation analysis	40
3.3.1.5	Regression maps	41
3.3.1.6	Composite Analysis	41
3.3.2	Artificial intelligence Modeling Techniques	42
3.3.2.1	Description of the models	43
3.3.2.1.1	Ridge regression	43
3.3.2.1.2	Least Absolute Shrinkage and Selection Operator (LASSO)	44
3.3.2.1.3	Elastic net	44
3.3.2.1.4	Random Forest (RF)	45
3.3.2.1.5	Adaptive Boosting (AdaBoost)	46
3.3.2.1.6	Gradient Boosting (GBoost)	46
3.3.2.1.7	Extreme Gradient Boosting (XGBoost)	47
3.3.2.1.8	Categorical Boosting (CatBoost)	48

3.3.2.1.9 Long Short-Term Memory (LSTM)	48
3.3.2.1.10 Shap Values (Shapley Additive explanations)	49
3.3.2.2 Performance Evaluation	50
CHAPTER FOUR	51
RESULTS AND DISCUSSION	51
4.1 Meteorological conditions and Saharan dust effect on meningitis seasonal variability	51
4.1.1 Meningitis belt and climatological environmental conditions	51
4.1.2 Seasonal cycle of meningitis in WAMB before and after the vaccination	54
4. 1.3 Seasonal cycle of environmental parameters and mean cases in WAMB before and after the vaccination	56
4.2 Meteorological conditions and Saharan dust effect on meningitis inter-annual variability	58
4.2.1 Inter-annual variability mode of environmental in SAH and GG before and after vaccination	58
4.2.2 Environmental precursors of meningitis in SAH and GG	68
4.3 Inter-annual Variability and Tele-connections of El Niño–Southern Oscillation and Saharan Dust in Relation to Meningitis over West Africa	72
4.3.1 Interannual variability mode of AOD over West Africa during the dry season	73
4.3.2 Relationship between AOD variability mode and meningitis incidence in SAH and GG zones	75
4.3.3 Interactions between Saharan dust variability mode and global Climate variability	79

4.3.4	Influence of global Climate variability in the Inter-linkage between Saharan AOD and meningitis incidence in the WAMB	84
4.3.5	Identification of ENSO events	89
4.3.6	Intra-seasonal climatology of dust	91
4.3.7	Impact of strong ENSO on Saharan dust in the North African desert.	93
4.3.8	Influence of the ENSO event on wind and dust variability at regional scale: SAH and GG	97
4.3.9	Seasonal fluctuation of SST in the ENSO region, winds and Sharan dust over SAH and GG	103
4.4	Application of AI models	107
4.4.1	Inter-annual and Seasonal cycle of meningitis	107
4.4.2	Environmental precursors of meningitis	110
4.4.3	Relationships between Observed and predicted meningitis	112
4.4.4	Performance of Machine Learning models	115
4.4.5	Distributions of observed and predicted meningitis incidences	118
4.4.6	Model Shapley Additive exPlanations (SHAP) Value Interpretability Analysis	120
4.5	Discussion of Results	122
	CHAPTER FIVE	129
5.	CONCLUSION AND RECOMMENDATIONS	129
5.1	Summary	129
5.2	Conclusion	130
5.3	Recommendations	131
5.4	Contribution to Knowledge	132

5.5	Suggestions for Further Studies	132
	References	134
	Appendix	144

LIST OF TABLES

Table 3.1:	Summary of all datasets used in this study	37
Table 4.1:	Spearman correlation between the leading principal component (PC1) of each environmental variable and the normalized anomalous meningitis cases over the Sahel (SAH) for the periods 2006–2009 (pre-vaccine) and 2010–2020 (post-vaccine). Asterisks (*) indicate statistically significant correlations at the 95% confidence level.	62
Table 4.2:	Spearman correlation between the leading principal component (PC1) of each environmental variable and the normalized anomalous meningitis cases over the Sahel (SAH) for the periods 2006–2009 (pre-vaccine) and 2010–2020 (post-vaccine). Asterisks (*) indicate statistically significant correlations at the 95% confidence level	67
Table 4.3:	One month lagged (lag-1) correlation between PCs of AOD index and meningitis incidence in the SAH (a) and the GG (b) using Spearman method. The PCs for the seasons DJF, and FMA are respectively correlated with the disease during JFM and MAM in the GG and The SAH. The asterisks (*) indicate the statistically significant correlations at 95% confidence level.	77
Table 4.4:	Lagged (lag0) correlation between PCs of AOD index and meningitis incidence in the SAH (a) and the GG (b) using Spearman method. The PCs for the seasons FMA and MAM are respectively correlated with the disease in the SAH during FMA and MAM. The asterisks (*) indicate the statistically significant correlations at 95% confidence level.	77

LIST OF FIGURES

- Figure 2.1:** Meninges inflammation due to meningococcal *meningitidis* and its symptoms 11
- Figure 2.2:** Schematic description of the positions of the African Easterly Jet (AEJ) and the Tropical Easterly Jet (TEJ) over the African continent in August (a) and January (b). Source: Thiam et al., 2024. 17
- Figure 3.1:** West African countries included in the African Meningitis Belt (c), Surface wind and precipitation in Africa: a) in boreal summer and b) in boreal winter 32
- Figure 4.1:** Climatology of the intra-seasonal variability of environmental variables over the West averaged for 2006-2020 WAMB averaged for 2006-2020. 53
- Figure 4.2:** Seasonal cycle of meningitis prevalence between January to June (weeks 1 to 26) between 2006 and 2020 in the two West African climate zones, Sahel (SAH) and Gulf of Guinea (GG), during pre- and post- MenAfriVac periods. 55
- Figure 4.3:** Seasonal cycles of environmental variables (weeks 1 to 26) and mean meningitis cases (brown line) over the Sahel (SAH) and Gulf of Guinea (GG) zones from January to June, before and after the introduction of MenAfriVac. 57
- Figure 4.4.1:** Regression between anomalous environmental variables and the leading mode (PC1) from the principal component analysis (PCA) of the corresponding variables from January to June over the SAH for the period 2006–2009 (a–f, m). 59
- Figure 4.4.2:** Regression between anomalous environmental variables and the leading mode (PC1) from the principal component analysis (PCA) of the corresponding variables from January to June over the SAH for the period 2010–2020 (g–l, n–p). 60

- Figure 4.5.1:** Regression maps showing the relationship between anomalous environmental variables and the leading principal components (PC1) of the corresponding inter-annual variability mode from January to June over the Gulf of Guinea (GG) for the period 2006–2009 (a–f, m). 64
- Figure 4.5.2:** Regression maps showing the relationship between anomalous environmental variables and the leading principal components (PC1) of the corresponding inter-annual variability mode from January to June over the Gulf of Guinea (GG) for the period 2010–2020 (g–l, n–p). 65
- Figure 4.6:** Lagged correlations between the leading principal component (PC1) of each environmental variable and the normalized anomalous meningitis cases, with cases fixed at MAMJ and FMAMJ for the Sahel (SAH, left) and Gulf of Guinea (GG, right), respectively. 70
- Figure 4.7:** Empirical orthogonal function (EOF) analysis of AOD in West Africa. Regression maps of the first (a,d,g,j), second modes (b,e,h,k) and associated Principal Components (c,f,i,l) for the four the seasons DJF, JFM, FMA and MAM during the period 1981–2020. 74
- Figure 4.8:** The lag correlation of the selected PCs of the AOD index (the grey line represents PCs1 and the blue line represents PCs2) with the standardised anomalies of the meningitis cases (b–d: the red line represents SAH and the dashed line represents GG) is shown. 78
- Figure 4.9:** Regression maps of seasonal standardized anomalies of SST (a,d,g,j,m,p,s), SLP (b,e,h,k,n,q,t shaded) and wind at 10m (arrows), and global AOD (c,f,i,l,o,r,u),

with the standardized first leading mode (PCs1) of averaged AOD over WA during the DJF for the period 1981 to 2019. 81

Figure 4.10: Regression maps of seasonal standardized anomalies of SST (a,d,g,j,m,p,s), SLP (b,e,h,k,n,q,t shaded) and wind at 10m (arrows), and global AOD (c,f,i,l,o,r,u), with the standardized first leading mode (PCs1) of averaged AOD over WA during the FMA for the period 1981 to 2019. 82

Figure 4.11: Regression maps of seasonal standardized anomalies of SST (a,d,g,j,m,p,s), SLP (b,e,h,k,n,q,t shaded) and wind at 10m (arrows), and global AOD (c,f,i,l,o,r,u), with the standardized first leading mode (PCs1) of averaged AOD over WA during the MAM for the period 1981 to 2019. 83

Figure 4.12: Regression maps of seasonal standardized anomalies of SST (a,d,g,j,m,p,s), SLP (b,e,h,k,n,q,t shaded) and wind at 10m (arrows), and global AOD (c,f,i,l,o,r,u), with the standardized anomalies of the averaged incidence of meningitis over GG during JFM for the period 2006 to 2019. 86

Figure 4.13: Regression maps of seasonal standardized anomalies of SST (a,d,g,j,m,p,s), SLP (b,e,h,k,n,q,t shaded) and wind at 10m (arrows), and global AOD (c,f,i,l,o,r,u), with the standardized anomalies of the averaged incidence of meningitis over SAH during FMA for the period 2006 to 2019. 87

Figure 4.14: Regression maps of seasonal standardized anomalies of SST (a,d,g,j,m,p,s), SLP (b,e,h,k,n,q,t shaded) and wind at 10m (arrows), and global AOD (c,f,i,l,o,r,u), with the standardized anomalies of the averaged incidence of meningitis over SAH during MAM for the period 2006 to 2019. 88

- Figure 4.15:** Standard deviation and ENSO of the equatorial Pacific SST anomalies over the Niño 3.4 index region: (a) Standard deviation of the Niño 3.4 index over the Niño 3.4 region (5°N–5°S, 120°W–170°W) in each month during 1980–2020; (b) Mean Niño 3.4 index in the preceding winter (December of the previous year to February of the current year). 90
- Figure 4.16:** Variability of global dust mean (a-c) AOD and (b-d) DUCMASS averaged for the years 1980–2020, during the DJF (a-b) and MAM (c-d) seasons. 92
- Figure 4.17:** Composite of global sea surface temperature (SST) anomalies during El Niño–Southern Oscillation (ENSO) events from 1980 to 2020. 94
- Figure 4.18:** Composite of dust (AOD and DUCMASS) in the region (20°W–15°E and 4°N–30°N) during El Niño events from 1980 to 2020. 95
- Figure 4.19:** Composite of dust (AOD and DUCMASS) in the region (20°W–15°E and 4°N–30°N) during La Niña events from 1980 to 2020. 96
- Figure 4.20:** Composite of the SST anomalies in the Niño3.4 region (5°N–5°S, 120°W–170°W), the zonal wind (U10: a–b), the meridional wind (V10: c–d), and dust indices such as AOD (e–f) and DUCMASS (g–h), all averaged over the SAH region (12.22°W–16.04°E and 4.27°N–25.02°N) across the DJF (a, c, e, g) and MAM (b, d, f, h) seasons during the Niño events. 99
- Figure 4.21:** Composite of the SST anomalies in the Niño3.4 region (5°N–5°S, 120°W–170°W), zonal wind (U10: a–b), meridional wind (V10: c–d), and dust indices such as AOD (e–f) and DUCMASS (g–h), all of which are averaged over the SAH region (12.22°W–16.04°E and 4.27°N–25.02°N) across the DJF (a, c, e, g) and MAM (b, d, f, h) seasons during the Niña events. 100

- Figure 4.22:** Composite of the SST anomalies in the Nino3.4 region (5°N–5°S, 120°W–170°W), zonal wind (U10: a–b), meridional wind (V10: c–d), and dust indices such as AOD (e–f) and DUCMASS (g–h), all of which are averaged over the GG region (8.55 °W – 3.88°E and 4.35°N – 12.40°N) across the DJF (a, c, e, g) and MAM (b, d, f, h) seasons during the Nino events . 101
- Figure 4.23:** Composite of the SST anomalies in the Nino3.4 region (5°N–5°S, 120°W–170°W), zonal wind (U10: a–b), meridional wind (V10: c–d), and dust indices such as AOD (e–f) and DUCMASS (g-h), all of which are averaged over the GG region (8.55 °W - 3.88°E and 4.35°N – 12.40°N) across the DJF (a, c, e, g) and MAM (b, d, f, h) seasons during the Nina events. 102
- Figure 4.24:** This boxplot shows the distribution of anomalies in sea surface temperature (SST), zonal wind (zwind), meridional wind (mwind), aerosol optical depth (AOD) and dust xixmass concentration (DUCMASS) during El Niño (a and b) and La Niña (c and d) years, across the SAH and GG regions for winter (DJF) and spring (MAM). 105
- Figure 4.25:** Variability in meningitis incidence across Sahelian countries: Burkina Faso, Mali, Niger and Nigeria. 109
- Figure 4.26:** Spearman's rank correlation coefficients between the normalised anomalies of environmental variables and meningitis cases in Burkina Faso (a), Nigeria (b), Niger (c) and Mali (d). A star (*) indicates statistical significance at the 95% confidence level based on a t-test. 111
- Figure 4.27:** Comparison between the recorded and predicted meningitis prevalence in Burkina Faso (a) and Nigeria (b). 113

- Figure 4.28:** Comparison between the recorded and predicted meningitis prevalence in Niger (c) and Mali (d). 114
- Figure 4.29:** The potential of ML models evaluated and compared in terms of prediction and performance in Burkina (a) and Nigeria (b). 116
- Figure 4.30:** The potential of ML models evaluated and compared in terms of prediction and performance in Niger (c) and Mali (d). 117
- Figure 4.31:** The boxplots of the observed and predicted meningitis incidence in (a) Burkina Faso, (b) Nigeria, (c) Niger and (d) Mali. 119
- Figure 4.32:** The summary plots of the high-ranked SHAP (Shapley) of feature importance for each variable in: (a) Burkina Faso, (b) Nigeria, (c) Niger, (d) Mali. 121

LIST OF EQUATIONS

- Equation 3.1: Covariance Matrix
- Equation 3.2: Ridge Regression Analysis
- Equation 3.3: LASSO Regression using
- Equation 3.4: Elastic Net Regression
- Equation 3.5: Shapley Additive Explanations
- Equation 3.6: R-squared for the S-statistic

LIST OF ACRONYMS

BM	Bacterial meningitis
<i>Spn</i>	<i>Streptococcus pneumoniae</i>
<i>Nm</i>	<i>Neisseria meningitidis</i>
<i>Hib</i>	<i>Haemophilus influenzae</i> type b
USA	Unit States of America
WHO	World Health Organization
AMB	African Meningitis Belt
<i>NmA</i>	<i>Neisseria meningitidis</i> serogroup A
<i>NmW</i>	<i>Neisseria meningitidis</i> serogroup W
<i>NmC</i>	<i>Neisseria meningitidis</i> serogroup C
<i>NmX</i>	<i>Neisseria meningitidis</i> serogroup X
CSM	CerebroSpinal Meningitis
WAMB	West African Meningitis Belt
SAH	Sahel
GG	Gulf of Guinea
EOF	Empirical Orthogonal Function
PC	Principal Component
ENSO	El Niño–Southern Oscillation
AEJ	African Easterly Jet
TEJ	Tropical Easterly Jet
NAO	North Atlantic Oscillation
AOD	Aerosol Optical Depth
DAOD	Dust Aerosol Optical Depth

PM	Particulate Matter
RH	Relative Humidity
MERIT	Meningitis Environmental Risk Information Technologies
ITF	Intertropical Front
ITCZ	Intertropical Convergence Zone
WAM	West African Monsoon
WACS	West African Climate System
WASCAL	West African Science Services Centre on Climate Change and Adapted Land-Use
WRF	Weather Research and Forecast
AI	Artificial Intelligence
ML	Machine Learning
ANNs	Artificial Neural Networks
GMAO	Global Modeling and Assimilation Office
GEOS	Goddard Earth Observing System Model
DUCMASS	Dust Column Mass Density
MERRA2	Modern-Era Retrospective Analysis for Research and Applications
CAMS	Copernicus Atmosphere Monitoring Service
ECMWF	European Centre for Medium-Range Weather Forecasts
u	Zonal Wind
v	Meridional Wind
SLP	Sea Level Pressure
HadISST	Met Office Hadley Centre
JJA	June July August
JJA	June July August
ASO	August September October

SON	September October November
OND	October November December
NDJ	November December January
DJF	December January February
JFM	January February March
FMA	February March April
MAM	March April May
MAMJ	February March April May
FMAMJ	March April May June

CHAPTER ONE

INTRODUCTION

1.1 Background to the Study

Bacterial meningitis (BM) is a serious infectious disease that continues to pose a global public health challenge, particularly in low- and middle-income countries. It is a rapidly progressing condition that can lead to death or permanent disability within 24 hours of symptom onset. Despite being preventable, BM has the highest case-fatality rate among all vaccine-preventable diseases and disproportionately affects children under the age of five (Wright et al., 2021; WHO, 2024). Globally, an estimated 2.5 million new cases of meningitis of all causes were recorded in 2019, including 1.6 million cases attributed to bacterial meningitis, which resulted in approximately 240,000 deaths (Chen et al., 2023; WHO, 2024).

Although BM can occur anywhere in the world, the burden is heaviest in sub-Saharan Africa, particularly in the region known as the **African Meningitis Belt (AMB)**. This region, defined by Lapeyssonnie in 1963, stretches from Senegal in the west to Ethiopia in the east, encompassing 26 countries with recurrent epidemics, especially during the dry season. Since the early 20th century, the AMB has been the site of devastating outbreaks. A notable example is the 1996–1997 epidemic, which affected over 250,000 people and resulted in more than 25,000 deaths, with *Neisseria meningitidis* serogroup A alone accounting for over 11,000 fatalities (Mohammed et al., 2017).

BM is caused by a limited number of bacterial pathogens, most notably *Neisseria meningitidis* (Nm), *Streptococcus pneumoniae* (Spn), *Haemophilus influenzae* type b (Hib), and *Streptococcus agalactiae*. Among the twelve identified Nm serogroups, six (A, B, C, W, X, and Y) have epidemic potential. Humans are the only known reservoir, and the disease is

transmitted through respiratory droplets or close contact with an infected individual (Batista et al., 2017; WHO, 2024). BM outbreaks have also been reported in regions beyond Africa, including Chile, Fiji, Kyrgyzstan, and Tajikistan, underscoring its global relevance.

Efforts to control meningitis in Africa initially relied on reactive immunization strategies using polysaccharide vaccines, which had limited efficacy, particularly among infants and young children, and offered only short-term protection (Martin et al., 2013). In response, a low-cost conjugate vaccine, *MenAfriVac*, targeting serogroup A, was developed and introduced through mass campaigns starting in 2010. This led to a dramatic reduction in NmA cases across the belt. However, other Nm serogroups, particularly C, W135, and Y, have since emerged as the predominant causes of outbreaks, maintaining a high case-fatality rate of 5–6% (WHO, 2015).

The strong seasonality of meningitis outbreaks in the AMB typically beginning with the dry season and subsiding with the onset of rains has long suggested an important role for environmental and climatic factors. Low relative humidity, high temperatures, and dusty atmospheric conditions have been repeatedly associated with epidemic onset. The Harmattan wind, which blows from the northeast during the dry season, carries large quantities of Saharan dust across West Africa, contributing to dry air and high levels of inhalable particulate matter (PM₁₀), which may increase vulnerability to respiratory infections, including BM (Lapeyssonnie, 1963; Molesworth et al., 2003).

Climate change has the potential to exacerbate these risks. Rising temperatures, increased frequency and duration of dry spells, dust storms, and extreme weather events are expected to further influence disease dynamics in West Africa. Fine particles suspended in the air can irritate the respiratory tract and compromise the immune system, while increasing ambient ozone concentrations may aggravate respiratory health conditions. In 2016, WHO estimated

that ambient air pollution caused approximately 456,000 deaths in West Africa alone. Globally, nearly 9 million deaths were linked to air pollution in 2020—accounting for 12% of all recorded deaths.

Northern Africa is recognized as the largest global source of mineral dust, contributing about 60% of the world’s annual aerosol load. During the dry season, dust plumes transported by the Harmattan reach the Gulf of Guinea and surrounding regions, resulting in persistently dusty and dry environmental conditions (Senghor et al., 2016; Diop et al., 2022). These conditions align closely with the peak meningitis season across the West African Meningitis Belt.

In this context, understanding the interactions between environmental variables and meningitis epidemiology is crucial. This study focuses on the **West African Meningitis Belt (WAMB)**, comprising countries such as Senegal, Guinea, Mali, Niger, Nigeria, Côte d'Ivoire, Ghana, Benin, and Togo. The objective is to investigate how climate variability and environmental extremes influence meningitis dynamics in the region, with the goal of contributing to improved forecasting systems and more effective public health preparedness strategies.

1.2 Statement of Research Problems

Bacterial meningitis (BM) continues to pose a significant public health challenge in West Africa, especially within the African Meningitis Belt (AMB), where recurring seasonal outbreaks result in high morbidity and mortality (Lapeyssonnie, 1963; Molesworth et al., 2003; WHO, 2024). While previous research has established a strong seasonal pattern in meningitis incidence closely linked to dry atmospheric conditions, low humidity, high temperatures, and dust concentrations (Greenwood, 1999; Sultan et al., 2005; Martiny & Chiapello, 2013), there remains a limited understanding of how these environmental factors interact with broader,

large-scale climate systems. In particular, the influence of major atmospheric-oceanic drivers such as the El Niño–Southern Oscillation (ENSO) and other teleconnections on Saharan dust emissions and transport has not been sufficiently explored in relation to meningitis dynamics (Sultan et al., 2005; Pandya et al., 2015; Diouf et al., 2025).

Most existing studies have focused on local meteorological variables or have relied on country-level data, overlooking the broader climate mechanisms that influence environmental suitability for meningitis outbreaks (Yaka et al., 2008; Agier et al., 2013; García-Pando et al., 2014). Moreover, the potential for integrating these large-scale drivers into early warning systems has not been adequately investigated. This lack of comprehensive understanding limits the effectiveness of climate-based public health interventions, particularly for anticipating and managing meningitis risk at sub-seasonal to seasonal timescales (Dione et al., 2022; Yarber et al., 2023).

In this context, there is a pressing need to investigate how remote climate systems through their modulation of regional atmospheric circulation, dust transport, and surface weather conditions contribute to the interannual variability of BM outbreaks in West Africa (Sultan et al., 2005; Martiny et al., 2013). By addressing this gap, the present study aims to improve both the scientific understanding of climate-health linkages and the practical development of predictive tools for early warning and disease prevention, thereby contributing to the **WHO Global Roadmap to Defeat Meningitis by 2030** (WHO, 2021).

1.3 Aim and Specific Objectives

The aim of this research is to achieve a complete characterization of climate impact on meningitis incidence over west Africa.

The specific objectives are to:

- i. determine the meteorological conditions and Saharan dust effect on meningitis seasonal cycle;
- ii. analyze meteorological conditions and Saharan dust effect on meningitis inter-annual variability and spatial configuration
- iii. assess the atmospheric and oceanic drivers of dust variability patterns impacting meningitis; and
- iv. develop AI models that can estimate meningitis incidence combine environmental variables and vaccine effects as input.

1.4 Justifications

Despite the widespread use of conjugate vaccines, bacterial meningitis (BM) remains a major global health problem with severe public health and socio-economic impacts (WHO, 2021; Wright et al., 2021). It is characterized by a high case fatality rate; approximately one in ten people with acute BM die, and one in five survivors suffer long-term complications such as hearing loss, seizures, cognitive deficits, and motor impairments (Schiess et al., 2021; WHO, 2024). Global surveillance data indicate that the number of reported BM cases increased between 2006 and 2016, partly due to enhanced case detection and persistent outbreaks in low- and middle-income countries (Bassat et al., 2018).

BM is caused by a small number of bacterial pathogens, including *Neisseria meningitidis*, *Streptococcus pneumoniae*, and *Haemophilus influenzae* type b, each of which includes multiple serogroups or serotypes. This diversity complicates the development of long-term immunization strategies and hinders complete disease control (WHO, 2024; Chen et al., 2023).

Although the introduction of the MenAfriVac vaccine targeting *Neisseria meningitidis* serogroup A (NmA) has resulted in a significant decline in NmA incidence vaccinating over 300 million individuals in 26 African countries since its launch other serogroups continue to cause deadly outbreaks (WHO, 2021; Mohammed et al., 2017).

For instance, serogroup W outbreaks occurred in Burkina Faso in 2002 and 2012, while a large epidemic involving serogroup C (NmC) caused over 11,000 cases and 800 deaths in Niger and Nigeria in 2015 (Kamwamba, T. E. 2017). In 2016, Ghana experienced a significant outbreak involving both NmW and *Streptococcus pneumoniae* (Spn), further illustrating the continued threat posed by multiple serogroups.

Despite strong leadership by the World Health Organization (WHO) and collaborative efforts through the MenAfriNet Consortium and national health institutions, critical challenges remain. Long-term support services for individuals and families affected by post-meningitis complications are often inadequate or entirely absent (WHO, 2024). Furthermore, meningitis epidemics remain difficult to predict and can rapidly overwhelm health systems and communities.

Nevertheless, the progress achieved in recent decades especially the near-elimination of NmA cases in the African Meningitis Belt has inspired renewed optimism about the possibility of defeating the disease. This optimism has culminated in a global call to action, uniting governments, public health agencies, researchers, and affected communities to eliminate meningitis as a public health threat. In response, the **WHO launched the Global Roadmap to Defeat Meningitis by 2030**, which outlines a strategy for improved prevention, diagnosis, surveillance, and support services (WHO, 2021). This roadmap aligns with global efforts to

strengthen primary healthcare, build resilience against health emergencies, and ensure universal health coverage and improved well-being.

1.5 Research scope

The relationship between Saharan dust and meningitis has been extensively examined within the African Meningitis Belt, particularly in sub-Saharan regions, at weekly, intra-seasonal and interannual scales. However, broader global patterns, especially those linked to large-scale climate variability, remain under-explored. As sub-Saharan Africa bears the heaviest burden of meningitis, investigating the spatiotemporal variability of Saharan dust plumes and their role in disease dynamics is essential. This requires a deeper understanding of the environmental and climatic conditions associated with dust emissions, transport and deposition, and their interaction with large-scale atmospheric circulation and local surface characteristics.

The focus of this research is the impact of sea surface temperature (SST) and surface wind coupling on the variability of Saharan dust activity and its association with meningitis outbreaks in West Africa. The first objective is to evaluate the impact of critical environmental factors, such as dust concentration, temperature, wind patterns, and relative humidity, on the timing and severity of meningitis outbreaks throughout the year. The second is to expand the analysis by exploring the role of large-scale climate drivers, particularly the El Niño–Southern Oscillation (ENSO), in modulating dust aerosol variability and its potential link to meningitis patterns.

By identifying the most influential environmental and climatic variables, the study will reconstruct historical meningitis outbreak trends using predicted data and assess the underlying

drivers of interannual variability. Ultimately, this research seeks to enhance the scientific understanding of how dust variability in winter and spring over West Africa influences meningitis dynamics. The findings will inform early warning systems and public health interventions, contributing meaningfully to the implementation of the WHO Global Roadmap to Defeat Meningitis by 2030.

1.6 Structure of the document

The present document is structured in five chapters ranging as follows:

- ✓ Chapter One provides a more detailed description of the research objectives and questions of this thesis.
- ✓ Chapter Two presents a literature review on this topic.
- ✓ Chapter Three illustrates the data and analysis methods used in the study, examining the weekly, interseasonal and interannual variability of environmental variables related to meningitis occurrence in West Africa.
- ✓ Chapter Four presents, analyses and discusses all the results of this work by comparing them with previous findings related to this theme.
- ✓ Chapter Five presents the conclusions of this study and some perspectives for future research.

CHAPTER TWO

LITERATURE REVIEW

2.1 Epidemiology of Bacterial Meningitis in West Africa

The central nervous system includes the brain and spinal cord. It has a layer called the meninges (Figure 2.1.a), which acts as a protective barrier for the brain and spinal cord. Meningitis is the inflammation of these meninges, which can be caused by many pathogens. Viral meningitis is usually caused by enteroviruses, the herpes simplex virus, the varicella zoster virus and the flu virus. BM is one of the deadliest and most disabling forms of meningitis (WHO, 2024). Symptoms of BM include sudden onset of headache, fever, stiff neck, confusion, increased sensitivity to light, fatigue, nausea, seizures, vomiting, colds, sleepiness, skin rashes and loss of appetite (Figure 2.1.b). Although BM affects all ages, young children are most at risk with around half of cases and deaths occurring in children under five of age (WHO, 2024). It can quickly spread among people living or working together in close proximity, for example in the military, boarding schools, and during religious pilgrimages. For instance, an epidemic due to serogroup W135 was recorded worldwide during religious pilgrimages in Arabia in 2000. Of all the pathogens, *Nm* is the most dangerous and is the primary responsible for devastating epidemics worldwide, particularly in the African Meningitis Belt (WHO, 2023; WHO, 2024). It can be identified from other bacteria by the rapid spread of a skin rash, a particular symptom of meningococcal meningitis, also known as cerebrospinal meningitis (CSM).

In the African meningitis belt (AMB), serogroup *NmA* was identified as the leading cause of meningitis epidemics in that region, which it is qualify as an endemic disease. If left untreated, *NmA* can exceed a 50% mortality rate. Furthermore, 8-15% of patients die within one to two

days of experiencing symptoms, and 10-20% of survivors suffer permanent brain damage or disability, including hearing loss, even with early diagnosis and treatment (WHO, 2023).

In 2010, *MenAfriVac*, a conjugate vaccine developed for Africa against *NmA*, was introduced in the meningitis belt, targeting people aged 1–29. Consequently, a 58% decrease in *NmA*-related meningitis was observed from 2017 onward. By around 2019, the epidemics caused by *NmA* appeared to have been eliminated, but the ability of *meningococci* to exchange genetic material responsible for capsule production and switch between serogroups made eliminating the epidemic pattern difficult. Furthermore, the persistence of other serogroups, such as *NmC*, *NmW135*, *NmY* and *NmX*, in inducing epidemics of over 30,000 cases annually across the meningitis belt remains a crucial issue (WHO, 2023). Epidemiological studies have found that the occurrence of invasive meningococcal disease is not solely determined by the introduction of a new virulent bacterial strain, but also by other factors that enhance transmission (Taha et al., 2022).

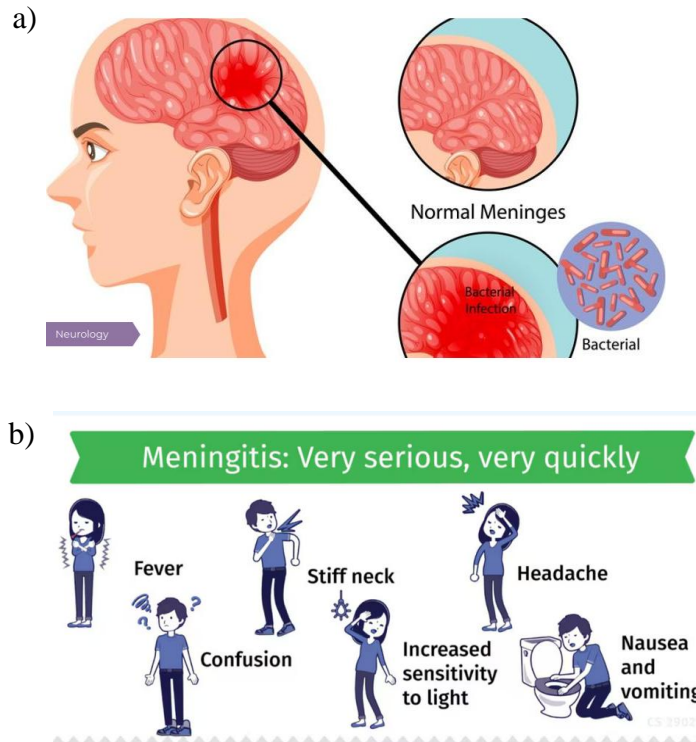


Figure 2.1: Meninges inflammation due to meningococcal *meningitidis* and its symptoms
<https://www.cdc.gov/museum/education/newsletter/2023/jan/index.html>

2.2 Transmission of Bacterial Meningitis

Meningitis bacteria are transmitted from person to person through droplets of respiratory or throat secretions from an infected person, via prolonged close contact such as kissing, sneezing or coughing (WHO). Between 5 and 10% of the population can carry the bacteria in their throat without becoming ill. The carriage rate of meningococci is higher among people in lower socioeconomic classes, military recruits, pilgrims, boarding school students, and prisoners. Symptoms of meningitis can occur within the first week after infection or within 10 days, which is the incubation period. However, the bacteria can also enter the bloodstream from the nasopharynx. Once inside the bloodstream, they can bypass the body's defence mechanisms, pass into the cerebrospinal fluid and reach the meninges. This causes inflammation of the latter. Socioeconomic factors, in conjunction with environmental factors, create a complex framework for predicting meningitis outbreaks and their intensity.

2.3 Climatic and Environmental Determinants of Meningitis in the African Meningitis Belt

The African Meningitis Belt (AMB), as defined by Lapeyssonnie (1963), stretches between latitudes 4°N and 16°N. It is bounded by the 300 mm annual rainfall isohyet in the north and the 1100 mm isohyet in the south. This region is characterized by hot, dry, and dusty conditions, particularly during the dry season from February to late May, when bacterial meningitis (BM) outbreaks are most common. The disease incidence declines during the rainy season, displaying a marked seasonality and hyperendemicity (Greenwood et al., 1984). These dry season conditions are largely influenced by the Harmattan, a northeasterly trade wind that transports large quantities of dust across the region. Given the region's proximity to the

Equator and the desert, high temperatures, low humidity, and frequent dust storms contribute to elevated levels of mineral dust, especially particulate matter (PM10), at ground level.

2.3.1 Environmental Sensitivity of Meningitis

Meningitis is considered one of the most climate-sensitive diseases in Africa (Thomas et al., 2007; Agier et al., 2018), with studies estimating that climate factors account for about 25% of the variability in its incidence (Yaka et al., 2008). A growing body of research has demonstrated that climate conditions and dust levels significantly influence both the timing and intensity of meningitis outbreaks. For instance, Sultan et al. (2005) linked the seasonal onset of meningitis in Mali to large-scale atmospheric circulation, demonstrating that a surface wind speed index could predict epidemic onset with a lead time of approximately six weeks. This suggests potential for early warning systems based on climate indicators.

Thomson et al. (2006) similarly used climate data to build a predictive model for meningitis outbreaks, identifying strong associations between rainfall, dust, and the disease calendar (i.e., pre-, peak-, and post-epidemic seasons). However, they also noted that annual data, though useful, mask important intra-seasonal dynamics crucial for accurate outbreak prediction.

2.3.2 Temporal and Spatial Variability in Meningitis Patterns

Broutin et al. (2007) analyzed long-term data across nine AMB countries, uncovering a periodicity in meningitis outbreaks ranging from 8 to 12 years. Yet this pattern was inconsistent across countries and time periods, partly due to the limitations of low-resolution (yearly) datasets that obscure finer-scale seasonal behavior. Yaka et al. (2008) compared Burkina Faso and Niger, finding a stronger climatic influence in Niger due to enhanced Harmattan winds, while the statistical relationship in Burkina Faso was inconclusive despite similar climatic

conditions in both Sahelian countries. This underlines the need for higher-resolution, localized data to improve understanding of climate–disease interactions.

Agier et al. (2013) addressed this issue by using weekly district-level data in Niger to study the timing of climate signals (dust, temperature, wind, humidity) and meningitis outbreaks. They observed consistent time lags across districts, reinforcing the hypothesis that dust may damage the pharyngeal mucosa and facilitate bacterial invasion. Their findings support integrating dust data into early warning systems.

Martiny and colleagues (2013) explored how varying dust concentrations at different altitudes, along with relative humidity levels, impact the meningitis calendar. They observed that early-year dust loads correlate with epidemic onset, and that meningitis and dust peaks follow each other with short lags (0–2 weeks). Deroubaix et al. (2013) confirmed a one-week lag between dust and meningitis peaks, suggesting that both the duration and intensity of epidemics are closely linked to dust dynamics.

2.3.3 Forecasting and Modelling Approaches

García-Pando et al. (2014) developed statistical models using national and district-level data in Niger. Their models indicated that early dry-season wind and surface dust levels partially explain meningitis seasonality. However, they emphasized that climate alone is insufficient for accurate prediction vaccine effects must also be considered. Diokhane et al. (2016) used WRF model simulations to show elevated dust levels in 2012 in Senegal, a year with high meningitis incidence.

Mueller et al. (2017) assessed health surveillance data from 13 districts in Burkina Faso over a decade, while Jusot et al. (2017) identified high temperatures and reduced visibility as significant risk factors for meningitis in Niger.

Collectively, these studies underscore the importance of integrating climatic risk factors dust, temperature, low humidity alongside social determinants such as human contact rates and co-infections, into comprehensive disease models. This approach is essential for improving outbreak forecasting and tailoring public health responses in the region.

2.3.4 Operationalising Early Warning Systems

Recent advances have focused on operationalizing early warning systems. Dione et al. (2022) co-developed a Meningitis Early Warning System (MEWS) in collaboration with ACMAD and WHO AFRO. By combining sub-seasonal to seasonal (S2S) forecasts of temperature, relative humidity, and dust, they provided a two-week lead time for meningitis alerts across the AMB. Their results showed that dry and warm atmospheric conditions could be predicted in advance, helping public health officials prepare for potential outbreaks.

Similarly, Yarber et al. (2023) identified a two-month lag between the onset of the dust season and meningitis outbreaks in Senegal. The dust season, driven by strong northeasterly winds, starts in February and peaks in early April, while meningitis cases decline by June when humidity rises.

2.3.5 Recent Evidence and Ongoing Challenges

Recent studies continue to clarify regional differences in environmental drivers. Diouf et al. (2025) found that in the Sahel (SAH), meningitis outbreaks are closely associated with high dust levels, elevated temperatures, and relative humidity below 20%. In contrast, in the

Guinean Gulf (GG), outbreaks are linked to high PM10 levels, temperature anomalies, and RH below 45%. These findings emphasize the potential value of environmental monitoring with 2–6 week lead times for outbreak prediction.

Other research (e.g., Pandya et al., 2015) demonstrated that maintaining average RH levels above 40% for several weeks can naturally suppress meningitis outbreaks. Despite this growing body of evidence, climate information remains underutilized in decision-making processes related to epidemic preparedness and control.

As Sultan et al. (2005) noted, a key challenge for modern epidemiology is identifying the spatial and temporal scales necessary to effectively link meningitis patterns with large-scale meteorological phenomena such as the El Niño–Southern Oscillation (ENSO). Progress in this area could significantly enhance our ability to anticipate, prevent, and manage future outbreaks in the African Meningitis Belt.

2.4 Environmental and Meteorological Drivers

2.4.1 Wind Dynamics and dust transport

The African Easterly Jet (AEJ), a strong wind associated with the Harmattan circulation during the boreal winter and spring, has been shown to transport aerosols from the Bodélé Depression in Chad towards the GG region (Thiam et al., 2024). However, vertical mixing is weak during this period, meaning the dusty Saharan air layer remains below 2 km above sea level. The AEJ is located between 500 and 700 hPa (Cook, 1999; Thorncroft and Blackburn, 1999) and is centred near the equator in winter, shifting northwards to around 13–15°N at the height of summer (black arrows). Variations in the AEJ's position and intensity in latitude during winter and spring (Figure. 2.2b) and summer (Figure. 2.2a) lead to changes in precipitation at both intraseasonal and interannual timescales in the Sahel (Jenkins et al., 2005; Sylla et al., 2011).

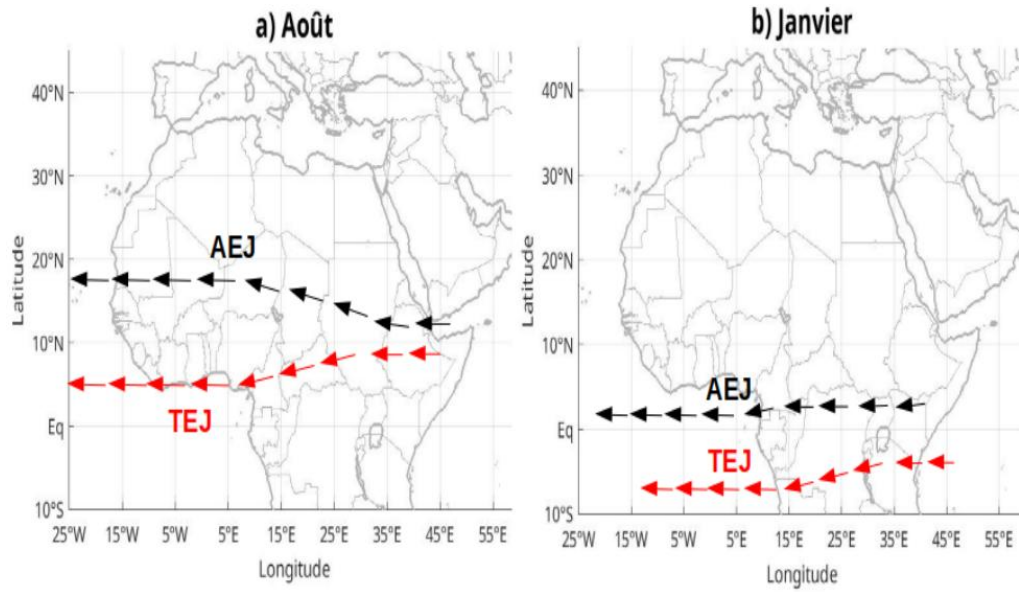


Figure 2.2: Schematic description of the positions of the African Easterly Jet (AEJ) and the Tropical Easterly Jet (TEJ) over the African continent in August (a) and January (b). Source: Thiam et al., 2024.

Wind speed and direction influence the distribution of dust and meningitis pathogens across vast areas. The strong, dry, hot, dusty northeasterly wind known as the Harmattan transports large quantities of Saharan dust from the ground level over the Sub-Saharan region and West Africa in general during the boreal winter and spring (Carlson and Prospero, 1972). This creates a favourable environment for disease transmission by exacerbating the drying of the respiratory tract and reducing visibility and relative humidity (Adedokun et al., 1989), consequently increasing indoor activities. Blowing southward from the Sahara Desert across West Africa during the dry season, the Harmattan wind is driven by a north-south pressure gradient associated with a strengthened subtropical anticyclone (Vallès et al., 2025). This gradient arises from the high-pressure system over the Sahara Desert and the low-pressure system over the Gulf of Guinea, creating a flow of air from north to south. During the winter, the subtropical anticyclone particularly the Azores becomes more intense, amplifying the pressure difference and enhancing the southward air movement. This intensified system transports significant quantities of Saharan dust and dry air across the region (Vallès et al., 2025). It thus significantly influences the weather, climate and air quality in West Africa.

Elsewhere, the migration of the Intertropical Convergence Zone (ITCZ) affects the Harmattan wind and indicates how far south the winds travel, as this is where the two trade winds (the Harmattan and the monsoon) converge and where high dust concentrations are found. The interaction between the Harmattan trade wind and the ITCZ triggers the West African Monsoon (WAM). The latter influences regional climate and weather patterns, and announces the end of the meningitis season in West Africa (Martiny & Chiapello, 2013; Diouf et al., 2025).

Furthermore, in the context of climate change, projections highlight changes in the timing, intensity and geographical extent of the Harmattan season (Prospero, 2002; Pörtner, 2022).

Therefore, a southward shift of the ITCZ due to global warming may delay the onset of the Harmattan season and reduce its duration (Biasutti & Giannini, 2006; Nicholson, 2013). Thus, shifts in wind patterns affect both dust transport and the spread of climate-sensitive diseases on a spatiotemporal scale.

It is important to understand the mechanisms involved in global wind circulation, monitor dust variability around the world depending on the season, and assess its impact on human health.

2.4.2 Temperature

It is widely recognized that the global temperature has increased over the past few decades due to the increased emissions of anthropogenic greenhouse gases, which may be responsible for climate change. Projections of climate variables show an increase in the frequency, severity and duration of extreme weather events. Increasing temperatures influence pathogen survival, host immunity and environmental factors such as humidity and dust emissions. For example, warmer temperatures often reduce humidity, which can desiccate bacteria and reduce their survival rate. In arid and semi-arid regions, higher temperatures associated with dust storms can facilitate the spread of pathogens by providing a medium for their transportation. In winter, fluctuations between rising daytime temperatures, cool nights and reduced relative humidity weaken mucosal barriers, thereby increasing susceptibility to bacterial meningitis. Furthermore, rising temperatures and decreasing precipitation in the sub-Saharan region are likely to exacerbate desertification, resulting in more intense surface dust events (Mulitza et al., 2010; Evan et al., 2014) and consequently increasing the risk of meningitis. In summary, temperature patterns and their influences, combined with the circulation of dust monitored by wind

dynamics, are crucial for understanding the spatiotemporal distribution of *Neisseria meningitidis* in the sub-Saharan region.

2.4.3 Relative Humidity (RH)

Relative humidity (RH) is defined as the amount of water vapour present in the air, expressed as a percentage of the amount needed for saturation at the same temperature. It plays a critical role in maintaining healthy indoor environments by regulating moisture levels and preventing the growth of harmful microorganisms. Low RH promotes the formation of indoor ozone, which irritates the mucous membranes and respiratory tract, making individuals more susceptible to infection. Dry air desiccates the mucosal membranes of the respiratory tract, reducing their ability to defend against bacteria. When RH is too high, it can create a damp environment that encourages the growth of harmful microorganisms, such as bacteria and viruses. Historically, RH has received less attention than Saharan dust in terms of studies on the relationship between climate and meningitis. Thus, it is challenging to estimate the appropriate RH threshold for any country. For example, Diouf et al. (2025) found that these thresholds were 20% and 40% for countries in the Sahel and Gulf of Guinea regions, respectively.

Beyond dust, humidity, temperature and wind dynamics, rainfall patterns also play a significant role in the meningitis calendar. For example, the onset of the rainy season often marks the end of meningitis outbreaks, as increased moisture reduces dust concentration and improves mucosal hydration. Improved vegetation cover during the wet season helps stabilize the soil and reduce dust generation.

Furthermore, anthropogenic activities such as urbanization and changes in land use, which affect air quality and dust emissions, have been found to indirectly influence meningitis

patterns. Indeed, advanced modeling efforts increasingly integrate these variables to predict meningitis risk, emphasizing the importance of environmental surveillance for early warning systems. Therefore, in light of the potential intensification of these environmental conditions under the effects of climate change, there is an increasing need to understand and mitigate the interactions between meningitis and its environmental drivers. This knowledge is crucial for optimizing vaccination campaigns, public health interventions and predictive modeling, and for ensuring better disease management in affected regions.

2.4.4 Saharan Dust and Health Outcomes

Aerosols, especially mineral dust, have emerged as a key component of the climate system and a major contributor to the natural aerosol load in the atmosphere (Wagner et al., 2016). They are also one of the most important environmental risk factors for meningitis epidemics (Figures. 2.3a and 2.3b). Higher concentrations of these particulates have been linked to an increased number of meningitis cases, highlighting their role as environmental stressors in the spread of disease. Aerosols are tiny particles suspended in the air, either as solids or liquid droplets. They can originate from human activities or natural sources. The Harmattan wind, which blows from the northeast from winter to spring, brings dust and biomass burning from the semi-arid regions of the GG and beyond. This creates a conducive environment for bacterial invasion and increases disease transmission (Agier et al., 2013). Thus, the particulate matter intensifies, deteriorating air quality and increasing respiratory diseases such as meningitis. Dust combined with hot, dry air can irritate the respiratory system and weaken the mucous membrane, enabling bacteria to enter the bloodstream more easily (Mueller & Gessner, 2010). Based on their size, aerosol particles are classified as particulate matter, such as PM10 and

PM_{2.5} (microscopic) and ultra-fine particles (nanoscopic). According to the World Health Organization (WHO, 2022), exposure to particulate matter concentrations of 10–25 $\mu\text{g}/\text{m}^3$ can trigger inflammation. Furthermore, iron oxides embedded in dust particles may increase the risk of infection by promoting bacterial growth. This, in conjunction with hot and dry weather, exacerbates the situation by damaging the mucosal lining of the nose and throat, creating an environment conducive to bacterial meningitis, cardiovascular disorders and cancer. However, areas with strong pressure gradients, which are often associated with cyclones, experience wind speeds that elevate dust concentrations to levels exceeding 150 $\mu\text{g}/\text{m}^3$, which is far above the limits recommended by the WHO. At such concentrations, daily mortality rates are estimated to rise by 5%, highlighting the urgent need for mitigation strategies.

On the other hand, dust can absorb and reflect solar and terrestrial radiation, inducing surface cooling and altering the lifetime and albedo of clouds by acting as ice and cloud condensation nuclei. This results in the stabilization of the planetary boundary layer, which suppresses trans-boundary transport of air pollutants and leads to an explosive rise in near-surface particulate matter concentrations. Additionally, anthropogenic pollutant concentrations originating from traffic patterns and sunlight-driven chemical reactions (through diurnal variations) can be indirectly elevated by dust through an alteration of the atmospheric circulation.

a)



b)

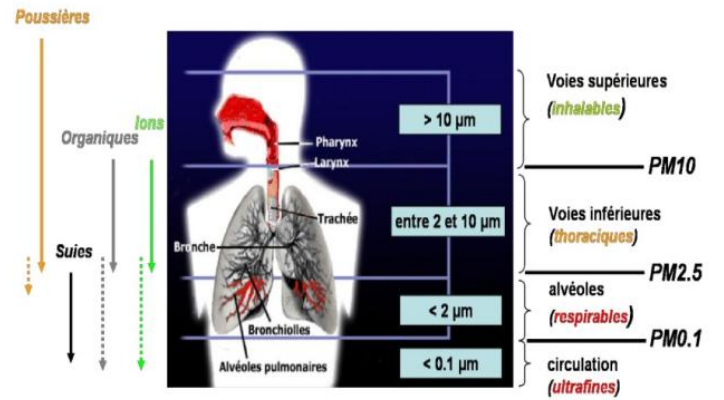


Figure 2.3: Figure 2.3: Impact of airborne particulate matter during dust events on human health.

2.5 Efforts made against meningitis disease

Previous studies have already demonstrated an association between environmental conditions and meningitis occurrence. Creating healthier environments with zero meningitis cases has become one of the most pressing issues of our time. Efforts have been made to combat meningitis. The Bill and Melinda Gates Foundation has provided funding specifically earmarked for the manufacture and deployment of conjugated meningococcal vaccines in the African 'meningitis belt'. In 2007, the Meningitis Environmental Risk Information Technologies (MERIT) project was initiated to reduce the burden of meningitis epidemics in Africa. Led by the World Health Organization (WHO), MERIT has initiated disease modelling activities in some WA countries like Niger, Ghana, and is extending its efforts across the entire meningitis belt. Opportunities have been identified to integrate valuable climate, environmental and other information into meningitis prevention and control by developing the following:

i) Current and future risk maps

ii) Early warning systems

iii) Improved impact assessment methodologies for prevention efforts In particular, one of MERIT's partners, the IRI, supports its problem-focused, demand-led, multi-stakeholder project by: i) providing climate expertise on monitoring and predicting the dry season, as well as on characterising dust, specific humidity and temperature, and the onset of the rainy season in the Meningitis Belt; ii) testing the means and implications of integrating climate information into the decision-making tools of the WHO and relevant Ministries of Health, which began in January 2010; and iii) education, training and outreach, specifically through implementing interdisciplinary workshops, such as the Summer Institute on 'Climate Information for Public Health'. The 'Defeating meningitis by 2030' global roadmap was approved by the World Health

Assembly in November 2020. The roadmap sets out a comprehensive vision for 2030: 'Towards a world free of meningitis', with three overarching goals:

- Elimination of bacterial meningitis epidemics;
- Reduction of cases of vaccine-preventable bacterial meningitis by 50% and deaths by 70%;
- Reduction of disability and improvement of quality of life after meningitis due to any cause.

2.6 Impacts vaccine against meningitis

Polysaccharide and polysaccharide-protein conjugate vaccines have been used to combat meningitis (Greenwood et al., 1999). These vaccines provide long-lasting immunological and immunogenic memory to young children. Since December 2010, a conjugate meningitis vaccine called *MenAfriVac* has been recommended to protect people in sub-Saharan Africa against serogroup A. Over 277 million people aged 1–29 years old in 26 countries were immunised against *NmA*. More recently, *NmCVs* containing various combinations of serotypes A, C, W and Y have been licensed, as have safe and effective vaccines against *Streptococcus pneumoniae* (Spn) and *Haemophilus influenzae type b* (Hib). Although vaccination has significantly reduced the burden of meningitis, it remains a significant challenge. As recognized in the World Health Organization's (WHO) Immunization Agenda 2030, too many children have insufficient access to vaccines, partly due to the high cost of some of the most effective conjugate vaccines, which limits their availability in low- and middle-income countries. Furthermore, existing vaccine formulations do not necessarily reflect the serogroups of the disease most prevalent in countries with the highest burden. Even in countries where vaccines are accessible, there is no standard approach to vaccination. However, bacterial

meningitis (BM) induced by *NmC*, *NmW* and *NmX* remains an important public health concern, highlighting the need for a strategic, multi-sectorial approach to integrating new methods in order to achieve the WHO Immunization Agenda 2030.

2.7 Potential Gaps Identified

Many studies focus on specific countries, usually those most severely affected or where the disease is endemic. The differences in meningitis patterns across countries involved in the AMB, which may be a consequence of differences in climate and weather conditions between the Sahel (dry air and hot conditions) and the Gulf of Guinea (wet air and cool conditions), are poorly documented. Most studies concentrate on short-term or specific years, failing to consider the long-term impact of climate variability on environmental and socioeconomic variables. There is a need for more high-resolution spatial analyses that consider local and global variations in disease outbreaks and burden. While several studies highlight the key influence of Saharan dust on meningitis outbreaks, understanding the mechanisms involved in aerosol dynamics, such as emission, transport and deposition, is of vital importance in order to better prevent dust events and anticipate support, awareness, preparedness and response actions for meningitis outbreaks. Predictive models that combine the effects of environmental, climatic, weather and socio-economic factors simultaneously could enhance understanding and guide public health interventions. For this, an artificial intelligence approach is crucial.

2.8 Large-Scale Climate Drivers and Their Influence on West African Climate and Dust Activity

The association between surface dust load and meningitis cases is particularly strong, making dust an essential component in predictive outbreak models. The climate of West Africa is not only shaped by local weather conditions but also by large-scale atmospheric and oceanic phenomena such as El Niño–Southern Oscillation (ENSO), commonly referred to as climate drivers. It influence the distribution of rainfall, surface temperature, relative humidity, wind patterns and the mobilization and transport of Saharan dust, which is a key environmental determinant of BM outbreaks in the AMB. However, Saharan dust has been shown to induce lower tropospheric warming and stabilisation by blocking shortwave radiation, which leads to strong sea surface warming off the coast of northwestern Africa (Roy et al., 2001; García et al., 2017). In addition, warm sea surface temperatures (SSTs) cause a release of heat flux: the air above warms and rises, creating a low-pressure area. Conversely, on the cold side, the air cools and becomes denser, resulting in the development of a high-pressure zone. This pressure gradient influences the direction of the wind, which shifts from high-pressure to low-pressure zones. As the wind enters a region of low pressure and accelerates towards high pressure, it tends to slow down. Consequently, massive mineral dust deposition is observed at equatorial latitudes in winter and in spring between 5°N and 10°N, while in summer, high dust concentrations are carried towards the Canary Islands (17°N–30°N) (Rodríguez et al., 2023). Researchers like Prospero et al. (2003), DeFlorio et al. (2016) and Vallès et al. (2025), demonstrated the mechanism by which ENSO events alter the wind regime of the tropics, affecting dust production and transport over the Sahara, through a negative correlation between Dust Aerosol Optical Depth (DAOD) anomalies in JFM (winter) and the El Niño3 index.

According to Prospero et al. (1996), Nakamae et al. (2013) and Vallès et al. (2025), similar atmospheric patterns in the North Atlantic, such as the North Atlantic Oscillation (NAO), can influence the transport of dust across the tropical Atlantic. Furthermore, the positions of the Intertropical Convergence Zone (ITCZ), where the two trade winds (Harmattan and monsoon) converge, indicate how far the winds may travel. Here, the West African Monsoon (WAM) originates, and it is highly affected by El Niño–Southern Oscillation (ENSO) events. Consequently, the WAM not only influences regional climate and weather patterns, but also signals the end of the meningitis season in West Africa.

Therefore, understanding atmospheric and oceanic forcing through surface wind direction and intensity could be invaluable for meningitis prediction, the development of early warning systems, and the planning of targeted vaccination campaigns to mitigate future occurrences.

2.9 Predictive Models and Early Warning Systems

Over the past six decades, artificial intelligence (AI) has become widely used in various areas of medical research and clinical practice (Tran et al., 2019; Mousavi et al., 2023). In recent years, numerous studies have employed these approaches to forecast infectious outbreaks. These studies have demonstrated that machine learning (ML) algorithms can predict the onset and spread of infectious illnesses with an accuracy comparable to or better than that of traditional statistical methods (Santangelo et al., 2023). Healthcare organizations also use AI methods such as artificial neural networks (ANNs) to enhance data analysis, clinical diagnosis, the prediction of cancer and other illnesses, image analysis and interpretation, patient care, and the creation of diagnostic and prognostic models for forecasting the course of disease transmission (Lalmuanawma et al., 2020; Sear et al., 2020). These methods consume less

energy (Kostic et al., 2019; Shah et al., 2019). ML is a branch of artificial intelligence that can analyse large and complicated datasets to spot patterns and trends that may be difficult for people to identify. Supervised learning involves training a model using a variety of inputs (or features) connected to a predetermined result. Models trained by supervised learning can produce discrete predictions, such as positive or negative, benign or cancerous, or continuous predictions in the form of a score ranging from 0 to 100.

In this thesis, we employed ML algorithms to forecast meningitis patterns under various climate scenarios, and then reconstructed past meningitis incidences by using historical environmental datasets for simulation.

CHAPTER THREE

MATERIALS AND METHODS

3.1 Description of the Study Area

The study area includes West African countries within the AMB, such as Senegal, Guinea, Mali, Niger, Nigeria, Burkina Faso, the Ivory Coast, Ghana, Benin and Togo (Fig 3.1c). The climate in West Africa is mostly linked to the movement of the inter-tropical front, also known as the Intertropical Convergence Zone. This is the interface between warm, humid air masses and cold, dry ones. It migrates annually from north to south based on the sun's position and marks the different seasons in West Africa. Countries south of the Sahara, in the humid coastal region, experience one rainy season lasting from one to six months. Only the southernmost coastal regions, from Liberia to Nigeria, experience two rainy seasons: a long one and a shorter one. Furthermore, as it is in the northern hemisphere, between December and March, the anticyclonic (high-pressure) zone centred over the Sahara generates a dry, dusty harmattan wind that blows almost constantly from the northeast. This dries out all landscapes down to the Atlantic coast and transports large quantities of ground-level Saharan dust over the Sahelian and Gulf of Guinea regions. During this period, temperatures initially cool from December to February alongside the coastal regions, but then gradually rise to excessive levels, reaching up to 45°C in the shade in April and May. Meanwhile, the atmosphere becomes drier by the day, with relative humidity fluctuating between 10% and 20% in the months preceding the rainy season. West Africa is one of the most densely populated regions. In summer, the anticyclone is replaced by a low-pressure zone that brings warm, humid winds from the Gulf of Guinea (Zwarts et al., 2009; Arbonnier, 2000). These two seasons characterise the onset and offset of

the meningitis season, suggesting the important role of climate factors in driving the occurrence and calendar of the disease.

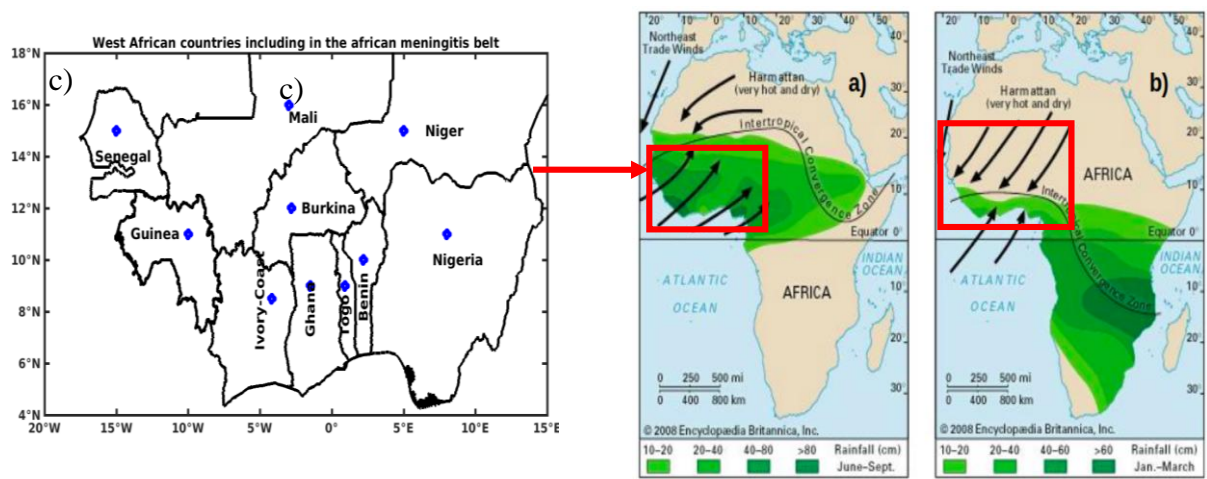


Figure 3.1: West African countries included in the African Meningitis Belt (c), Surface wind and precipitation in Africa: a) in boreal summer and b) in boreal winter

3.2 Data Sources

3.2.1 Meningitis Data

Weekly meningitis case data are collected at country level and shared with the World Health Organization (WHO), which makes this information publicly available via the following link: <https://www.menafrinet.org/>. For our study, we downloaded the data for the period from January to June (26 weeks per year), spanning the years from 2006 to 2020. However, data for Senegal and Guinea were only available from after 2010. The months selected were based on previous studies reporting the seasonal occurrence of meningitis in most countries within the AMB (Martiny and Chiapello, 2013; Deroubaix et al., 2013; Sultan et al., 2005).

3.2.2 Aerosols Datasets

This study utilises three dust aerosol indices: Aerosol Optical Depth (AOD at a wavelength of 550 nm), Dust Column Mass Density (DUCMASS) and the Particulate Matter index (PM10). AOD and DUCMASS are taken from the Modern-Era Retrospective Analysis for Research and Applications (MERRA, version 2), and PM10 comes from Copernicus.

3. 2.2.1 MERRA-2 Reanalyses

MERRA-2, provided by NASA's Global Modeling and Assimilation Office (GMAO) (Bosilovich et al., 2016; Gelaro et al., 2017), is the latest atmospheric reanalysis including aerosols for the satellite era after 1979. It is based on the latest version of the Goddard Earth Observing System Model (GEOS-5, 5th edition) data assimilation system (Rienecker et al., 2008), incorporating an updated model (Molod et al., 2015) and a global statistical interpolation scheme (Wu et al., 2002). The MERRA-2 aerosol assimilation component (Randles et al.,

2017) provides various variables relating to different aerosol species, including black carbon, organic carbon, mineral dust, sea salt and sulphurous aerosols (SO₂ and SO₄) (da Silva et al., 2015). Information on the procedure and validation of the MERRA-2 aerosol data assimilation, as well as the results of comparisons with observations, can be found in Randles et al. (2017) and Buchard et al. (2017). In this study, we extracted the dust column mass density (DUCMASS) in kg m⁻² to represent the atmospheric dust content from the MERRA-2 `tavgM_2d_aer_Nx` product (GMAO, 2015), as well as the aerosol optical depth (AOD) at a wavelength of 550 nm, to quantify the amount of aerosols present in an atmospheric column. Both MERRA-2 dust data files can be downloaded from the Goddard Earth Sciences Data and Information Services Center (<https://disc.gsfc.nasa.gov/>) and (<https://goldsmr4.gesdisc.eosdis.nasa.gov/data/MERRA2/M2I3NXGAS.5.12.4/>) respectively. MERRA-2 has a time coverage from 1980 to the present and a horizontal resolution of 0.5° × 0.625°, with a temporal resolution of 3 hours. The choice of the 550 nm wavelength is justified by its proximity to visible radiation, which affects visibility during dust events.

3. 2.2.2 CAMS Reanalyses

The Copernicus Atmosphere Monitoring Service (CAMS) provides two reanalysis products: the CAMS global reanalysis (EAC4), which currently covers the period from 2003 to December 2023; and the CAMS global greenhouse gas reanalysis (EGG4), which currently covers the period from 2003 to 2020. The CAMS reanalysis is the latest global atmospheric composition (AC) reanalysis dataset produced by the Copernicus Atmosphere Monitoring Service. It consists of three-dimensional, time-consistent AC fields, including aerosols, chemical species, and greenhouse gases. The CAMS reanalysis was produced using 4DVar data

with 12-hour assimilation windows from 09:00 UTC to 21:00 UTC and from 21:00 UTC to 09:00 UTC in CY42R1 of ECMWF's Integrated Forecast System (IFS). It has 60 hybrid sigma/pressure levels in the vertical, with the top level at 0.1 hPa. Atmospheric data are available at these levels, which are also interpolated to 25 pressure levels, 10 potential temperature levels and 1 potential vorticity level. The parameter used is PM10, which quantifies air pollution concentration (Deroubaix et al., 2013). Daily time-step PM10 data is available at <https://ads.atmosphere.copernicus.eu/cdsapp/>. According to Deroubaix et al., (2013), a high correlation exists between PM10 and AOD at 550 nm during the boreal winter and spring, peaking in March and April. We combined both parameters to explore the relationship between dust and meningitis. PM10 has a time step of three hours and a horizontal resolution of $0.75^{\circ} \times 0.75^{\circ}$.

3. 2.3 ERA5 Reanalyses and HadISST

This study uses the following meteorological variables: temperature; zonal (u) and meridional (v) wind components; sea level pressure (SLP); and relative humidity (RH). Wind stress is responsible for transferring momentum from the atmosphere to the ocean; therefore, it can be interpreted as the surface wind that modifies the surface of the ocean (Stewart, 2008). These data were obtained from ERA5 hourly pressure level data from 1940 to the present day. ERA5 is the fifth-generation reanalysis from the ECMWF (European Centre for Medium-Range Weather Forecasts), providing comprehensive global climate and weather data from the past eight decades. ERA5 datasets offer high temporal and spatial resolutions, with hourly data and $0.25^{\circ} \times 0.25^{\circ}$ grid spacing respectively. For our analysis, we selected the 1000 hPa pressure

level, which is closest to the Earth's surface. These datasets can be downloaded via the following link:

<https://cds.climate.copernicus.eu/cdsapp#!/dataset/reanalysis-era5-pressure-levels?tab=overview>

The Sea Surface Temperature (SST) data are from the Met Office Hadley Centre (HadISST). This data is used to identify global teleconnections with Sahara dust activity. The data span the period from 1870 to the present on a monthly basis, with a horizontal longitude/latitude resolution of $1^{\circ} \times 1^{\circ}$ (Rayner et al., 2003; Mohino et al., 2015).

Satellite and reanalysis data provide a more comprehensive and reliable perspective on the variability of climatic parameters.

Table 3.1: Summary of all datasets used in this study

Datasets Sources	Parameters	Units	Spatial resolutions	Temporal resolutions
WHO	Cases meningitis		Country level	Weekly
MERRA-2	AOD	nm	0.25° X 0.625°	3 Hours
	DUCMASS	Kg.m ⁻²		
Copernicus	PM10	Kg.m ⁻³		
ERA5	Temperature	K	0.25° X 0.25°	6 Hours
	Relative Humidity	%		
	Zonal wind component	m.s ⁻¹		
	Meridional wind component	m.s ⁻¹		
	Mean Sea Level Pressure	Pa	1° X 1°	Monthly
HadISST	Sea Surface Temperature	°C	1° x 1°	Monthly

3.3 Methods

To this end, we employed a variety of statistical methods to gain a better understanding of how environmental conditions influence the temporal and spatial distribution of meningitis.

To achieve the objectives one and two, we employed various statistical methods to better understand how environmental conditions influence the temporal and spatial distribution of meningitis over WAMB. The analysis was divided into two main periods based on the introduction of *MenAfriVac*: the pre-vaccination period (2006–2009) and the post-vaccination period (2010–2020). In addition, the study area was divided into two distinct regions, the SAH and the GG, in which climatic factors and meningitis cases are spatially averaged for the associated countries (Fig 2a–d).

3.3.1 Statistical Methods

3.3.1.1 Seasonal and Intra-seasonal Cycle

To explore the seasonal cycle, we use weekly values ranging from week 1 to week 26 (January–June) for both environmental variables and meningitis incidence. To investigate the intra-seasonal variability of environmental conditions, we focused on:

- boreal winter (December, January, February: DJF): during this period, the Sahel is dry and affected by the Harmattan trade winds, while the Gulf of Guinea experiences dry but humid conditions with dust events originating from Bodélé Depression.
- boreal spring (March, April, May: MAM): is characterized by extreme heat with increasing humidity in the SAH, whereas the GG enters in the rainy season.

3.3.1.2 Intra-seasonal and Interannual anomalies

The weekly meningitis data were converted to monthly data and averaged for the Sahelian countries (Burkina Faso, Niger, Nigeria and Mali) to represent the Sahel region (SAH). Guinea and Senegal which available data started in 2010 and 2012 respectively were not considered in this case in order to avoid more bias. The same approach was used to address the GG regions including, Ivory Coast, Benin, Togo and Ghana. We then computed the seasonal anomalies by subtracting the seasonal cycle for dust and climate variables from 1980 to 2020 and for the meningitis data from 2006 to 2020. To isolate interannual and interseasonal variability, we applied the detrend methodology to the anomalies. To investigate the teleconnection between climate variables and Saharan dust, we considered the period from 1980 to 2020. To highlight their influence on meningitis in the SAH and GG regions, however, we considered the period from 2006 to 2020.

3.3.1.3 Empirical Orthogonal Functions (EOF)/Principal Component Analysis (PCA)

For the inter-annual variability analysis, we applied the Empirical Orthogonal Functions (EOF) analysis, also known as Principal Component Analysis (PCA) (Each pattern is associated with a principal component (PC) time series, which describes the temporal evolution of the EOF patterns (Von Storch and Zwiers, 2001; Marta et al., 2016; Diouf et al. 2025). Each variability mode explains a fraction of the total variance of the original field (Von Storch and Zwiers, 1999; Sultan et al., 2005). Given an environmental variable Y with (space, time), dimensions, the PCA methodology involves the following step:

1. Calculating the weekly standardized anomalies of Y by subtracting for each grid point, the mean of each week over all years from the respective weekly values.

2. Calculating the covariance matrix of Y as $C = Y*Y'$ (3.1)

where Y' being the transpose of Y and Y dimensioned in [space (rows), time (columns)].

3. Diagonalizing the matrix C computing the the eigenvalues, eigenvectors (EOFs), and principal components (PCs) of Y, considering the SAH and GG regions separately over the entire study period.

4. Selecting the leading modes of variability of Y and investigating their impact on meningitis, relating the PCs with the standardized weekly anomalies of cases.

3.3.1.4 Spearman and Lead-Lag Correlation analysis

To quantify the relationship between environmental variability and meningitis incidence, we performed a Spearman correlation analysis between the first PCs of each environmental variable and the weekly standardized anomalies of meningitis cases (w1–w26).

To explore the precursor role of environmental variables on the disease incidence, a led-lag correlation analysis was conducted.

- For the SAH region, the anomalous meningitis cases index was fixed in MAMJ (week 9 to week 24) while the lags were calculated over a period of 16 weeks, moving backward one week at a time. For instance, lag -1 is corresponds to weeks 8–23, lag -2 to weeks 7–22, and so on.
- For the GG region, the anomalous cases index was fixed in FMAMJ (week 5 to week 24) with lags calculated over 20 weeks, shifting one week backward. Thus, lag -1 corresponds to weeks 5–23, lag -2 to weeks 4–22 and so on.

Finally, a Student's t-test was applied to assess the statistical significance of the correlations calculated at a 90% confidence level.

3.3.1.5 Regression maps

To determine the leading patterns of interannual aerosol optical depth (AOD) variability over West Africa (4°N–18°N, 20°W–15°E) from 1980 to 2020, we applied EOF analysis (see objectives 1 and 2) to decompose the spatiotemporal AOD into orthogonal modes in terms of EOF patterns. We then identified the AOD variability mode significantly associated with meningitis incidence and performed a lag correlation analysis using the Spearman method with a 95% confidence level between the AOD PCs and the standardised meningitis case anomalies. We then selected the identified PCs of AOD and explored the precursor role of sea surface temperature (SST), sea level pressure (SLP) and wind direction on dust distribution through lagged regression map analysis. Statistical significance was assessed using a Monte Carlo approach involving the generation of 100 random regressions with an equal number of positive and negative events drawn from the entire time series. This large number of iterations enables implementation of a 90% confidence level based on a two-tailed t-test. Analogue regression maps were computed using the time series of the disease in GG and SAH, as well as the global SST, SLP and wind component in the same seasons, which are significantly correlated with the PCs of AOD. Comparing these maps with those of the climate variables and the PCs of AOD can provide useful information about the interlinkage between the different patterns of AOD and bacterial meningitis.

3.3.1.6 Composite Analysis

To support the results of the regression map of climate indices such as ENSO modulating the seasonal variability of Saharan dust and its impact on the meningitis calendar, we analysed the Ocean Niño Index (ONI). According to Huang et al. (2017) and Xu et al. (2024), the ONI is

calculated as the three-month running mean of SST anomalies in the Niño 3.4 region (5°N–5°S, 120°W–170°W), based on centred 30-year reference periods updated every five years (Climate Prediction Center, 2020). The phase and intensity of ENSO events are characterised by monthly sea surface temperature (SST) anomalies in the Niño 3.4 region (5°N–5°S, 120°W–170°W) (Trenberth, 1997). The three-month running mean of the monthly SST was averaged over the Niño 3.4 region to represent the Oscillation Niño Index (ONI). The standard deviation of the ONI index was then calculated for each month from 1980 to 2020. As shown in Figure 4.15a, December has relatively large standard deviations (1.3), so we consider the December–February (DJF) season to characterise ENSO events, which peak in winter. Five typical ENSO events were identified during 1980–2020: 1982–1983, 1991–1992, 1997–1998, 2009–2010, and 2015–2016. The corresponding La Niña (LN) events were 1988–1989, 1998–1999, 1999–2000, 2007–2008, and 2010–2011.

A composite analysis was applied based on these ENSO events in order to identify and describe the processes associated with large-scale climate indices and Sahara dust variabilities (von Storch and Zwiers, 2001). Global sea surface temperature (SST) and regional aerosol optical depth (AOD) and dust load mass (DLM) distribution were constructed for the ENSO years to reveal differences in spatial distribution patterns.

3.3.2 Artificial intelligence Modeling Techniques

The complexity of developing numerical models that combine environmental and socioeconomic factors with meningitis incidence poses a significant challenge to scientists involved in predicting meningitis, particularly in tropical systems such as the African meningitis belt. In this context, researchers have recommended using machine learning (ML)

models to produce sensible disease predictions. To identify potential climate variables associated with the disease in West Africa at a country level, various ML models were developed using the climate indices and environmental data mentioned above. Regularisation approaches such as Ridge Regression, Least Absolute Shrinkage and Selection Operator (LASSO) and ElasticNet are often used to address the issue of multicollinearity, whereby there is a high degree of correlation among the predictor variables. Meanwhile, boosting algorithms such as adaptive boosting (AdaBoost), gradient boosting (GBoost), categorical boosting (CatBoost) and extreme gradient boosting (XGBoost) can prevent overfitting and optimise computational resources. However, random forests (RF) rely on the diversity of independently trained trees.

3.3.2.1 Description of the models

3.3.2.1.1 Ridge regression

Ridge regression, developed by Hoerl and Kennard (1970a), is used to reduce the impact of multicollinearity between environmental variables. It is an extension of the ordinary least squares (OLS) regression method, improving the stability of parameter estimates by adding a regularisation term (L2) that penalises large coefficients (Arief et al., 2024).

Although ridge regression introduces slight bias into the estimation process, it enhances model robustness and provides better generalisation performance (Fanny et al., 2018).

The main steps in ridge regression analysis include:

- a) Selecting the optimal λ (regularization strength) via cross-validation.
- b) Performing ridge regression with the selected λ using the following formula:

$$\widehat{\beta}_{ridge} = \arg \min \left\{ \sum_{i=1}^n \left(y_i - \beta_0 - \sum_{j=1}^p \beta_j x_{ij} \right)^2 + \lambda \sum_{j=1}^p \beta_j^2 \right\} \quad (3.2)$$

3.3.2.1.2 Least Absolute Shrinkage and Selection Operator (LASSO)

The Least Absolute Shrinkage and Selection Operator (LASSO) is a regularised regression technique that performs both parameter estimation and feature selection. Unlike Ridge regression, which only shrinks coefficients, LASSO adds a penalty based on their absolute values. This penalty can reduce some coefficients to zero, effectively removing less important predictors from the model.

This simplifies the model, improving its interpretability while mitigating the effects of multicollinearity among predictors (Sartika et al., 2020; Arief et al., 2024).

The main steps in LASSO regression analysis are:

- a) Selecting the optimal λ (regularization parameter) through cross-validation.
- b) Performing LASSO regression using the optimal λ , following the formula:

$$\widehat{\beta}_{lasso} = \arg \min \left\{ \sum_{i=1}^n \left(y_i - \beta_0 - \sum_{j=1}^p \beta_j x_{ij} \right)^2 + \lambda \sum_{j=1}^p |\beta_j| \right\} \quad (3.3)$$

3.3.2.1.3 Elastic net

Elastic Net is a regularised regression technique that combines the strengths of Ridge regression and LASSO. By incorporating L1 (LASSO) and L2 (Ridge) penalties into a single loss function, Elastic Net efficiently handles multicollinearity and performs variable selection (Zou & Hastie, 2005; Arief et al., 2024). This dual regularisation framework strikes a balance by shrinking coefficient estimates for greater stability while permitting some coefficients to be reduced to zero, thereby simplifying the model. The main steps in Elastic Net regression are:

a) Selecting the optimal λ (regularization parameter) through cross-validation, along with an α value between 0 and 1, which controls the balance between L1 and L2 penalties.

b) Performing Elastic Net regression with the optimal λ and α using the following loss function:

$$\widehat{\beta}_{EN} = \operatorname{argmin} \left\{ \sum_{i=1}^n \left(y_i - \beta_0 - \sum_{j=1}^p \beta_j x_{ij} \right)^2 + \left(a \sum_{j=1}^p |\beta_j| + (1-a) \sum_{j=1}^p \beta_j^2 \right) \right\} \quad (3.4)$$

3.3.2.1.4 Random Forest (RF)

Random Forest (also known as Random Decision Forest) is an ensemble learning technique used for both classification and regression tasks. It operates by constructing a large number of decision trees during the training phase and outputs the mean prediction (for regression) or the majority vote (for classification) of the individual trees (Amit & Geman, 1997; Breiman, 2001; Ho, 1998; Fernández-Delgado et al. 2014; Caruana and Niculescu-Mizil 2006; Rokach 2016).

Random Forest addresses the tendency of individual decision trees to overfit their training data by introducing randomness through two mechanisms:

Bootstrap sampling: each tree is trained on a random subset of the training data (with replacement).

Random feature selection: at each split in a tree, a randomly selected subset of features is considered, which introduces diversity among the trees.

This ensemble approach enhances generalization performance and makes Random Forest robust to noise and overfitting (Wager, 2016; Borup et al., 2023).

3.3.2.1.5 Adaptive Boosting (AdaBoost)

AdaBoost is an ensemble learning technique that improves the performance of weak learners (typically decision trees with shallow depth) by combining them into a single strong predictive model. AdaBoost works by sequentially training weak learners, where each subsequent model focuses more on the instances that were misclassified by previous ones. The final prediction is a weighted sum of the individual learners' outputs, with higher weights assigned to more accurate models (Mishra et al., 2020).

This adaptive mechanism allows AdaBoost to progressively reduce errors and improve prediction performance. For example, Mishra et al. (2020) successfully applied AdaBoost to forecast crop production under climate variability. In another study, Walker et al. (2019) demonstrated that AdaBoost models were more accurate and reliable than traditional logistic regression models for similar prediction tasks.

3.3.2.1.6 Gradient Boosting (GBoost)

Gradient boosting is a powerful algorithm for building predictive models, which works by optimising a specified loss function in a stage-wise fashion. This concept was extensively developed by Friedman (2021), who introduced the Gradient Boosting Machine (GBM) framework.

Gradient boosting works by fitting new weak learners (typically decision trees) to the residual errors made by the ensemble of previously trained learners. This additive, sequential approach involves adding a new learner at each iteration to reduce the prediction error of the overall model.

The algorithm uses a gradient descent optimisation framework, which iteratively updates the model to minimise the loss function. The direction of steepest descent (the negative gradient) guides the algorithm in correcting its previous mistakes. When the gradient approaches zero, the model has either reached a local minimum of the loss function or is close to doing so. An important hyperparameter in this process is the learning rate, which determines the size of each step in the iterations. A smaller learning rate improves the model's ability to generalise, but requires more iterations to converge.

3.3.2.1.7 Extreme Gradient Boosting (XGBoost)

XGBoost is an advanced and more regularized variant of the Gradient Boosting algorithm. It incorporates L1 (Lasso) and L2 (Ridge) regularization to control model complexity and enhance generalization performance (Xiang et al., 2022; Liu et al., 2024).

As a tree-based algorithm in the supervised learning category, XGBoost follows a sequential tree-building process, but with optimized parallel computation to speed up training. This combination of speed, scalability, and accuracy makes XGBoost highly effective and widely adopted in various domains, including health, agriculture, finance, and climate science (Nalluri et al., 2020; Shafay et al., 2020; Chen et al., 2020; Lee et al., 2022).

Compared to traditional Gradient Boosting, XGBoost offers better performance due to its regularization, efficient handling of missing data, and built-in mechanisms for preventing overfitting.

3.3.2.1.8 Categorical Boosting (CatBoost)

CatBoost is a gradient boosting algorithm developed by engineers at Yandex and specifically optimized for handling categorical features (Zhang et al., 2020). Unlike other boosting algorithms, CatBoost uses symmetric trees, meaning that the same feature is used to split the data at each level of the tree. This design produces a tree of depth k with exactly 2^k leaves, which improves efficiency and consistency during both training and inference.

During model training, a sequence of decision trees is built iteratively, with each new tree aiming to reduce the loss compared to the previous one (Shao et al., 2024). To avoid overfitting, the number of trees and other hyperparameters (such as tree depth and learning rate) are set during initialization.

CatBoost is particularly effective in datasets with many categorical variables and is known for requiring minimal preprocessing, making it well-suited for real-world structured data application.

3.3.2.1.9 Long Short-Term Memory (LSTM)

Long Short-Term Memory (LSTM) is a type of Recurrent Neural Network (RNN) designed specifically to analyze time series data and capture long-term dependencies. Originally proposed by Hochreiter and Schmidhuber (1997) and further refined in later works such as Gers et al. (2020), the LSTM architecture addresses the limitations of traditional RNNs, particularly the vanishing gradient problem.

Unlike standard RNNs, which rely solely on the previous hidden state for computation, LSTMs introduce a cell state that acts as long-term memory. This cell state is regulated by three gates input, output, and forget gates that control the flow of information in and out of the cell. These

mechanisms allow the model to retain or discard information across time steps, making LSTM highly effective for sequential prediction tasks like disease incidence modeling.

In this study, the LSTM model was implemented and evaluated using hyperparameter optimization techniques, including cross-validation and GridSearchCV, to identify the most effective configuration for predicting meningitis incidence based on time-dependent environmental data.

3.3.2.1.10 Shap Values (Shapley Additive explanations)

SHAP is a method for interpreting complex predictive models and understanding the relationship between input features and predicted outcomes (Yang et al., 2024). Based on principles from cooperative game theory, SHAP assigns each feature an importance value that quantifies its contribution to a given prediction. SHAP values allow modelers to decompose a prediction into the sum of individual feature contributions, providing a transparent explanation for how each variable influenced the model's output. This helps not only in ranking feature importance but also in identifying whether a feature had a positive or negative impact on the prediction.

Mathematically, a SHAP value represents the conditional expectation of a model's prediction, averaged over all possible combinations of feature inputs. They are solutions to the following Shapley value equation from cooperative game theory:

$$\phi_i(f, x) = \sum_{z \subseteq x} \frac{|z|!(M-|z|-1)!}{M!} [f_x(z) - f_x(z \setminus i)] \quad (3.5)$$

where $f_x(z) = f(h_x(z)) = E[f(z) | z]$ and s is the set of non-zero indices in z . SHAP used to increase the transparency and interpretability of machine learning models.

3.3.2.2 Performance Evaluation

The selection of the best-performing model is based on goodness-of-fit metrics, primarily the coefficient of determination, commonly known as R-squared (R^2) (Gujarati, 2021). This metric evaluates how well a model replicates observed data by measuring the proportion of variance in the dependent variable that is explained by the independent variables in the model.

Mathematically, R^2 is defined as the ratio of the variance explained by the model to the total variance in the data. It is computed on the test dataset to assess the model's generalization ability using the following formula:

$$R^2 = 1 - \frac{RSS_E}{TSS_R} \quad (3.6)$$

The numerator represents the residual sum of squares (RSS), or the unexplained variance, the denominator is the total sum of squares (TSS), or the total variance in the observed data. A higher R^2 value (closer to 1) indicates better model performance, while lower values suggest poor predictive capability. Although R^2 is widely used, it should be complemented with other metrics such as Mean Squared Error (MSE) and Root Mean Squared Error (RMSE) to obtain a more comprehensive evaluation of model accuracy.

CHAPTER FOUR

RESULTS AND DISCUSSION

The aim of this study is to achieve a complete characterization of the impact of climate on the incidence of meningitis in West Africa, and to determine the effect of meteorological conditions and Saharan dust on the seasonal cycle of meningitis. The study will also analyze the effect of meteorological conditions and Saharan dust on the interannual variability and spatial configuration of meningitis.

4.1 Meteorological conditions and Saharan dust effect on meningitis seasonal variability

4.1.1 Meningitis belt and climatological environmental conditions

The spatial extension of the meningitis belt in West Africa, along with the climatological values of key environmental variables (temperature, RH, surface winds) in boreal winter and spring is depicted in Figure 4.1. Countries within the “West African meningitis belt” extending from Senegal in the Nigeria are also shown. This region includes countries such as Mali, Niger, Nigeria, Burkina Faso, Ivory Coast, Ghana, Togo, and Benin (Figure 4.1a).

During boreal winter (DJF), warm temperatures ranging from 28°C to 32°C are observed in the northern and central parts of the GG. These conditions are associated with relative humidity levels between 30% and 80% and high dust concentrations originating from the Bodélé Depression, which increase from the northern GG region towards the south (Figure 4.1b-c).

During boreal spring (MAM), temperatures rise progressively from the GG region to the SAH, where they exceed 37°C. Conversely, relative humidity increases from 20% to 40% in the SAH, while it remains between 50% and 80% in the GG zone. However, Aerosol Optical Depth (AOD) increases significantly in the SAH, indicating higher dust concentrations (Figure 4.1d-e).

The position of the Intertropical Front (ITF) located at 8°N during DJF, and shifts northward to approximately 13°N in MAM (Figure 4.1c - e).

In conclusion, dust particles observed at the surface during DJF, are lifted into higher atmospheric layers by the end of May, significantly influencing meteorological conditions during the dry season.

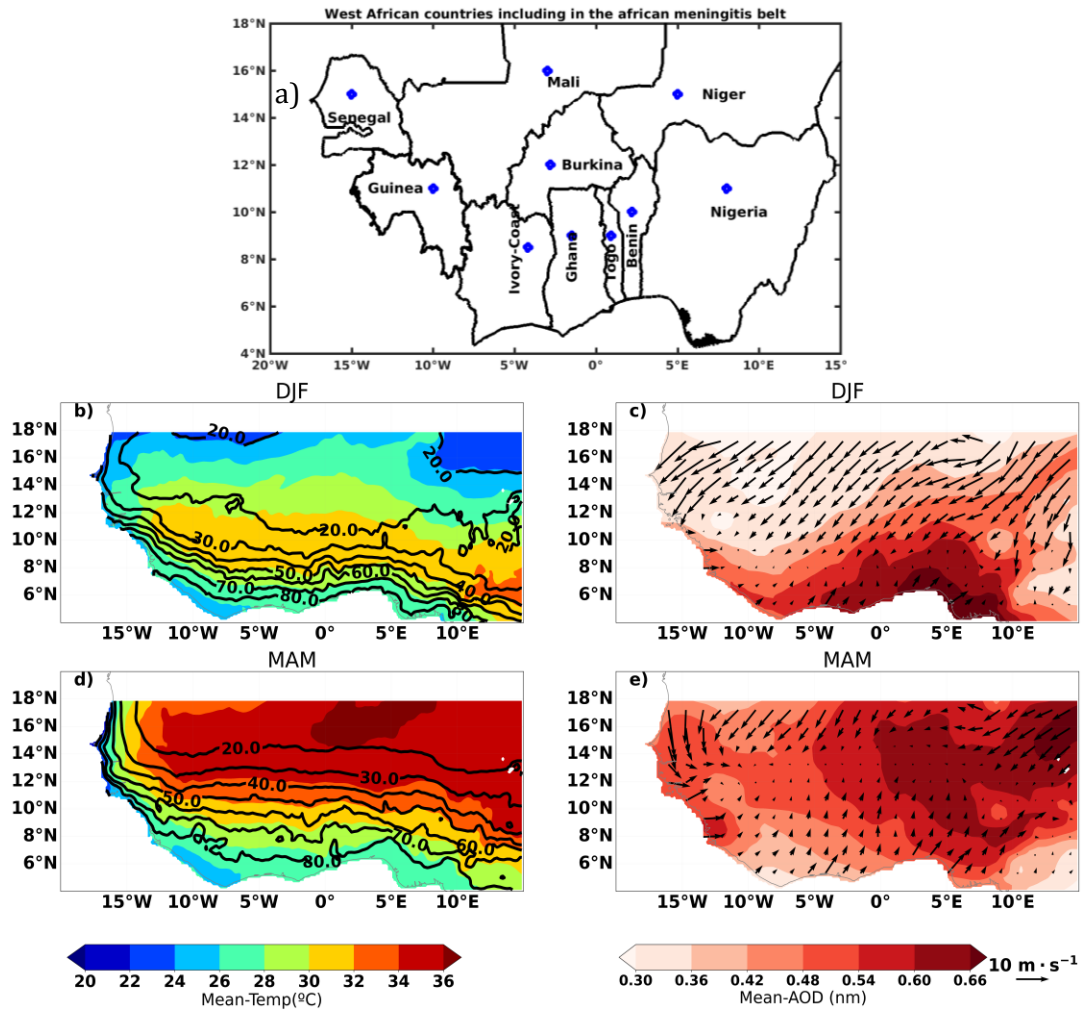


Figure 4.1: Climatology of the intra-seasonal variability of environmental variables over the West averaged for 2006-2020 WAMB averaged for 2006-2020.

4.1.2 Seasonal cycle of meningitis in WAMB before and after the vaccination

Weekly meningitis cases reported from 2006 to 2009, prior to the introduction of *MenAfriVac*, reveal that the SAH countries (Figure 4.2.a) experienced the highest burden of the disease, with a weekly average exceeding 2,000 cases, whereas the GG countries (Figure 4.2.c) recorded a significantly lower incidence, averaging fewer than 100 cases per week. The epidemic peak in the SAH region occurred between the 4th week of March and the 2nd week of April, in contrast to the GG region, where peaks were observed earlier, between the 3rd and 4th weeks of February.

From 2010 onward, a shift in the disease pattern is evident, with a significant reduction in the number of recorded meningitis cases in the SAH (Figure 4.2.b), due to the introduction of the vaccination.

Conversely, the GG experienced an increase and extension in the duration of the epidemic, with a consistent average number of cases between 2006–2009 and 2010–2020, except in Ivory Coast where the trend differed (Figure 4.2.b). The maximum number of cases were recorded from the 2nd week of February to the 4th week of May in the SAH and from the week 4 of January to week 4 of April (corresponding to W13) in the GG region.

In summary, the periods 2006–2009 and 2010–2020 show notable changes in meningitis patterns, both in terms of the weekly number of cases and the overall magnitude of the disease throughout the season.

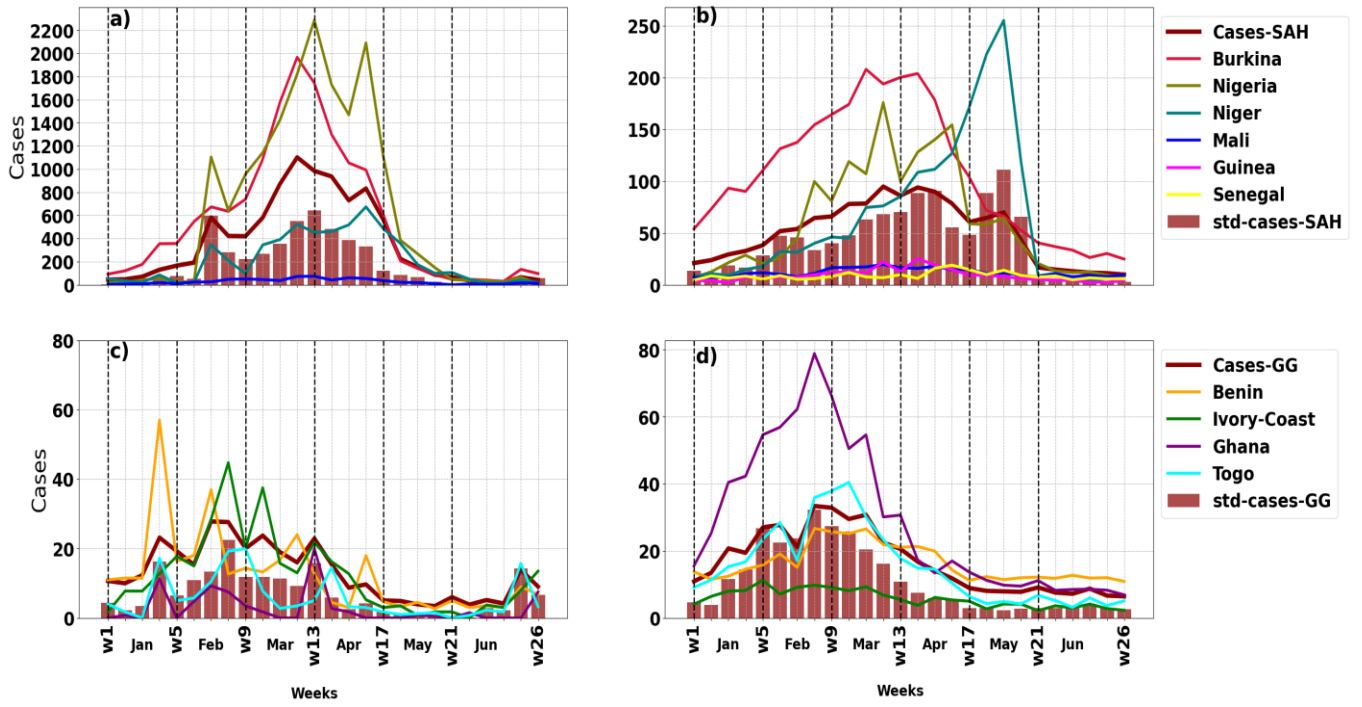


Figure 4.2: Seasonal cycle of meningitis prevalence between January to June (weeks 1 to 26) between 2006 and 2020 in the two West African climate zones, Sahel (SAH) and Gulf of Guinea (GG), during pre- and post- MenAfriVac periods.

4. 1.3 Seasonal cycle of environmental parameters and mean cases in WAMB before and after the vaccination

Figure 4.3 presents a cross-analysis of environmental variables and meningitis cases in the Sahel (SAH, left panel) and Gulf of Guinea (GG, right panel) regions. The results indicate that the onset of the meningitis season is preceded by high dust concentration events in January in both regions (Figure 4.3e & f), corresponding to an increase in temperature and a decrease in RH (Figure 4.3a- b). Remarkably, the increase in surface dust concentration until boreal spring seems to influence in the duration and intensity of the meningitis season (Figure. 4.3e-f). Peak PM10 concentrations are observed in March, while AOD peaks in April. In the SAH, meningitis cases peak at week 12, typically preceded by a peak in PM10 at week 11 and coinciding with the AOD peak for the period 2006–2009, when RH begins to exceed 38%. In contrast, meningitis peaks occur earlier, around week 8, in the GG region and are associated with RH levels above 45%.

A reversal in the surface wind direction (Figure 4.3c-d) together with increased RH (Figure 4.3a-b) mark the end of the meningitis season. In the GG region, the meningitis season concludes earlier, around the 4th week of April, when PM10 concentrations have already decreased significantly.

Notice that from 2010, the number of cases substantially decrease in SAH region because of vaccination (dashed brown line, Figure 4.3a). Nevertheless, there is still a seasonal cycle of the cases in which dry, and dusty environmental conditions enhance the meningitis along both study periods and wet, and reduced dust conditions reduce the disease.

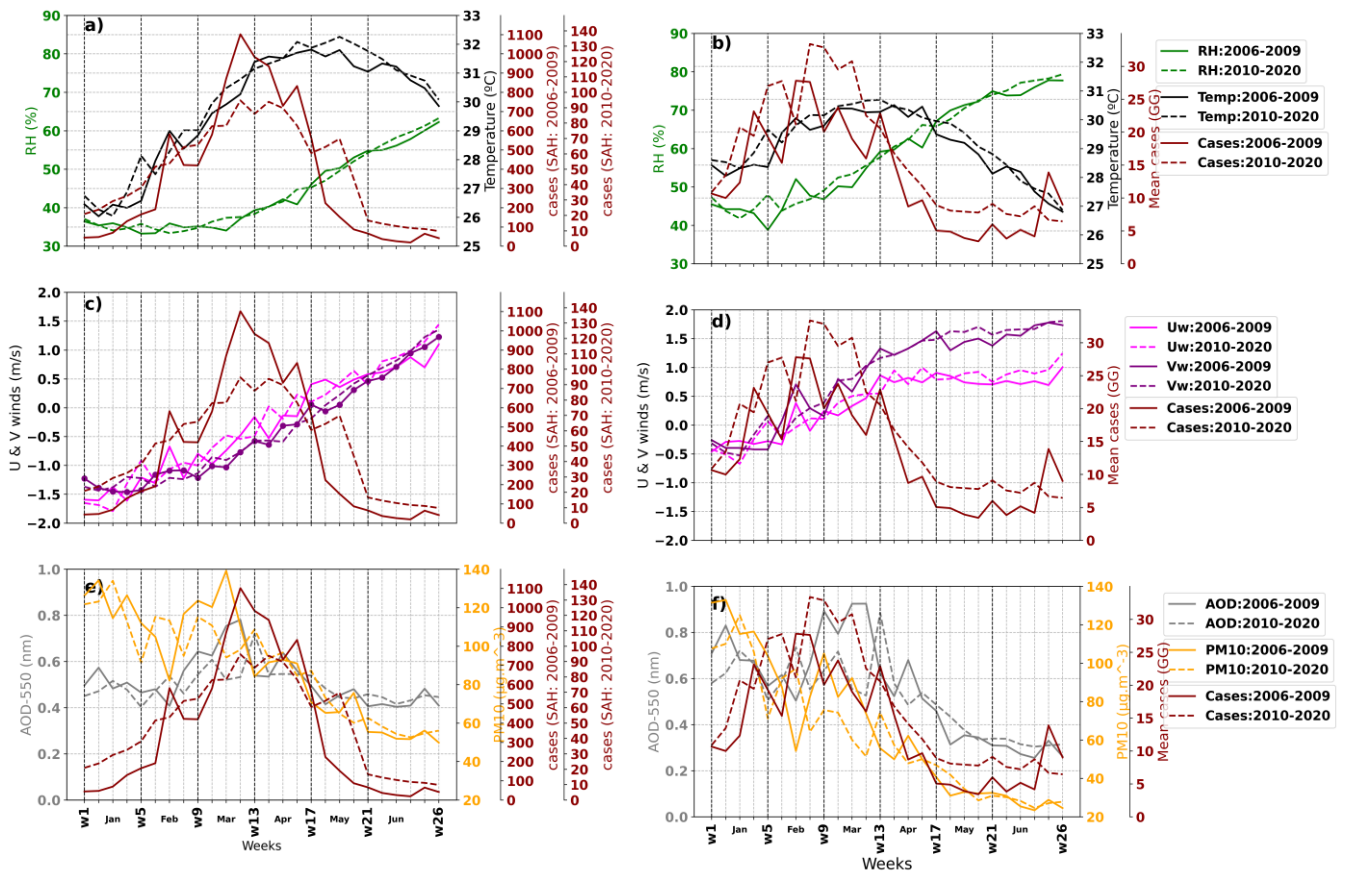


Figure 4.3: Seasonal cycles of environmental variables (weeks 1 to 26) and mean meningitis cases (brown line) over the Sahel (SAH) and Gulf of Guinea (GG) zones from January to June, before and after the introduction of MenAfriVac.

4.2 Meteorological conditions and Saharan dust effect on meningitis inter-annual variability

4.2.1 Inter-annual variability mode of environmental in SAH and GG before and after vaccination

In this section, we explore the climatic patterns driving the emergence of meningitis outbreaks over the SAH and GG regions. To this end, the leading modes of inter-annual variability of environmental factors were computed before and after the introduction of vaccines (Figure 4.4). During 2006–2009, the dominant environmental mode, which accounts for 56%–79% of the total variability, is characterized by anomalous northeasterly winds (Figure 4.4c,f), lower relative humidity (RH) (Figure 4.4a), higher concentrations of PM10 and AOD (Figure. 4d-e), and elevated air temperatures (Figure 4.4b). Notably, air temperature and dust patterns exhibit a meridional gradient, with maximum positive values in the northeastern SAH region (Figure 4.4b, d-e). This spatial configuration aligns with Saharan dust transport by Harmattan winds, inducing local warm and dry conditions.

Interestingly, a similar mode of environmental variability persists after vaccination (Figure 4.4g-l), although with a reduction in meridional wind intensity (Figure 4.4l), leading to less southward transport of Saharan dust between 2010 and 2020 (Figure 4.4J-k).

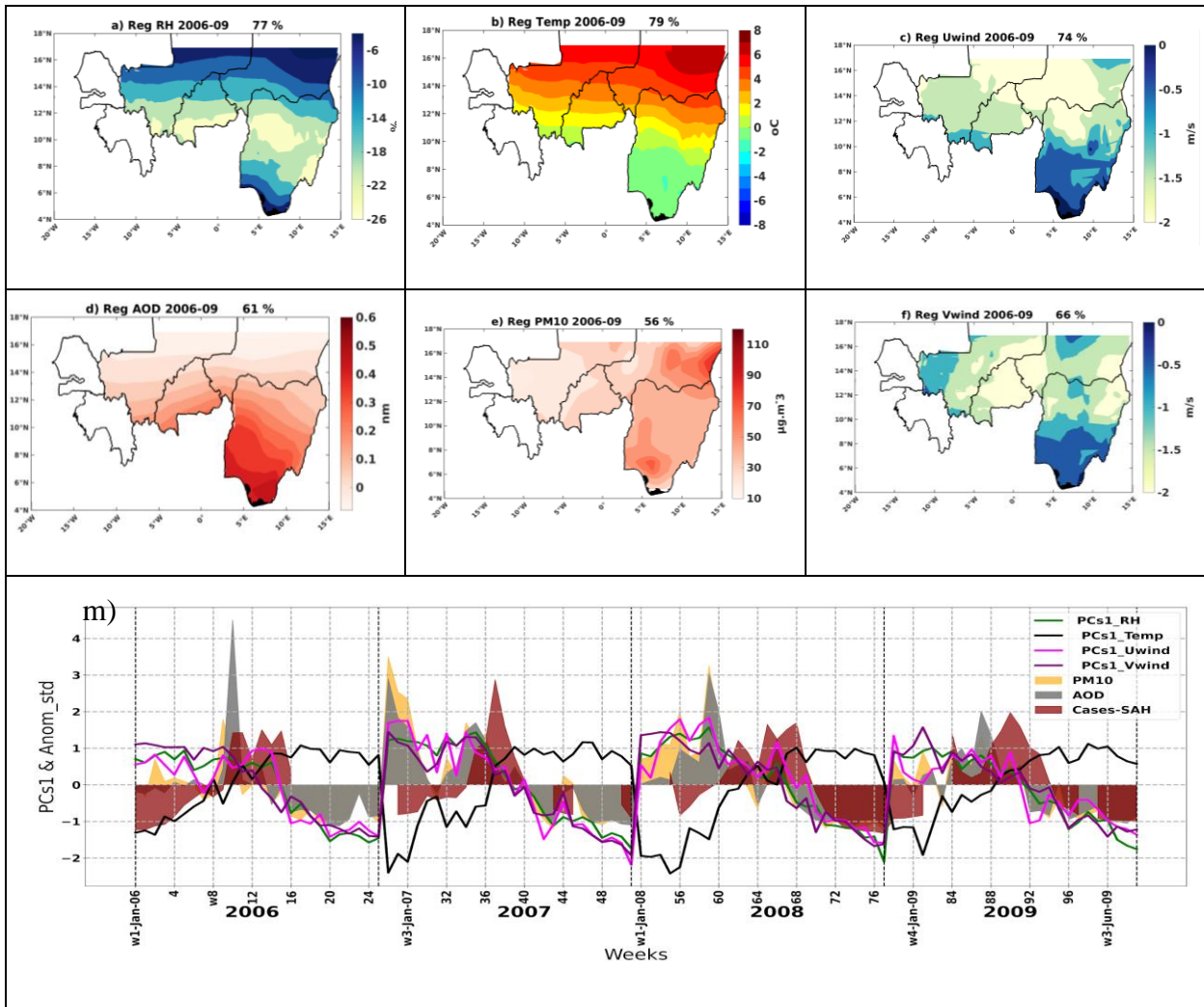


Figure 4.4.1: Regression between anomalous environmental variables and the leading mode (PC1) from the principal component analysis (PCA) of the corresponding variables from January to June over the SAH for the period 2006–2009 (a–f, m).

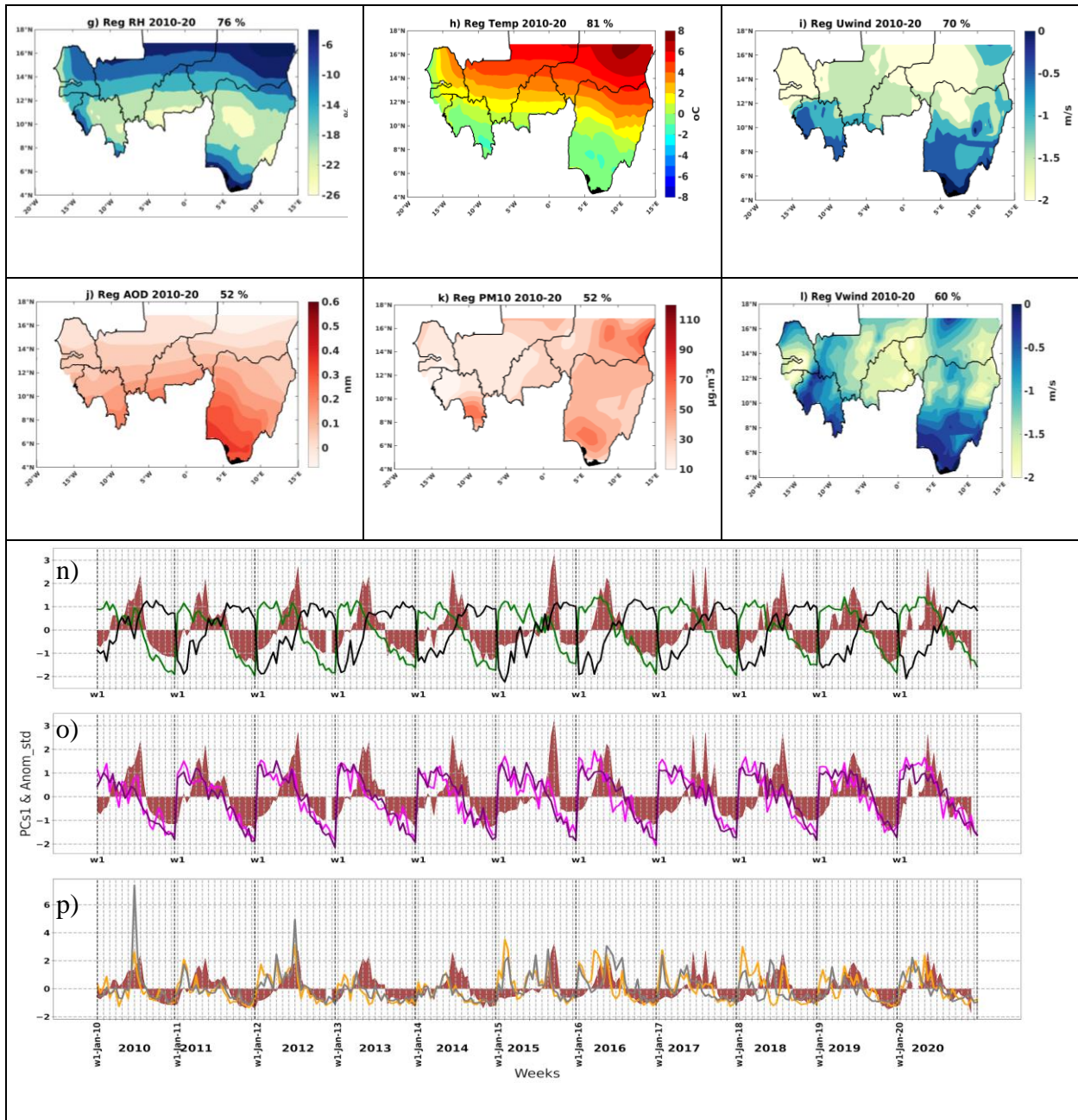


Figure 4.4.2: Regression between anomalous environmental variables and the leading mode (PC1) from the principal component analysis (PCA) of the corresponding variables from January to June over the SAH for the period 2010–2020 (g–l, n–p).

Regarding temporal evolution, these climate variability modes appear to precede meningitis outbreaks in both study periods in the SAH (Figure 4.4m–p). Before vaccination programmes, only dust concentrations and zonal wind exhibited significant correlations with meningitis cases, while the association with air temperature was negligible (Table 4.1). However, during 2010–2020, all environmental factors showed stronger and more significant correlations with meningitis cases (Table 4.1) emphasizing the precursor role of climatic factors in the emergence of the disease.

Notably, the timing and intensity of meningitis outbreaks display considerable variability, with early outbreaks in 2011 and 2016 contrasting with delayed ones in 2015 and 2017 (Figure. 4.4n). Interestingly, the most intense meningitis outbreaks coincide with persistent northeasterly winds and prolonged dusty conditions, as observed in 2012, 2015, and 2017, among other years (Figure. 4.4o–p).

In summary, our findings demonstrate a strong and persistent influence of environmental factors on the timing and magnitude of meningitis outbreaks in the SAH region, even after the introduction of vaccines.

Table 4.1: Spearman correlation between the leading principal component (PC1) of each environmental variable and the normalized anomalous meningitis cases over the Sahel (SAH) for the periods 2006–2009 (pre-vaccine) and 2010–2020 (post-vaccine). Asterisks (*) indicate statistically significant correlations at the 95% confidence level.

SAH	2006-2009	2010-2020
PM10 & Men	0.28*	0.45*
AOD & Men	0.38*	0.51*
RH & Men	0.17	0.51*
Temp & Men	0.10	0.28*
Uw & Men	0.25*	0.43*
Vw & Men	0.11	0.44*

In the GG region, the leading mode of variability, which accounts for 60%–88% of the total variance, is characterized by northeasterly winds weakening toward the equator. These winds tend to converge over the 6°N–8°N latitudinal band, where maximum dust concentrations are observed (Figure 4.5c–f, i–l). The GG region experiences low relative humidity and warm conditions, with maximum values recorded in the northernmost area (Figure 4.5a–b, g–h).

This spatial configuration highlights the transport of substantial amounts of dust from the desert to the GG region, contributing to warm and dry local conditions. Despite these similarities, after vaccination, dust concentration anomalies were weaker and shifted northward (Figure 4.5j–k), accompanied by an intensification of drier conditions (Figure 4.5g).

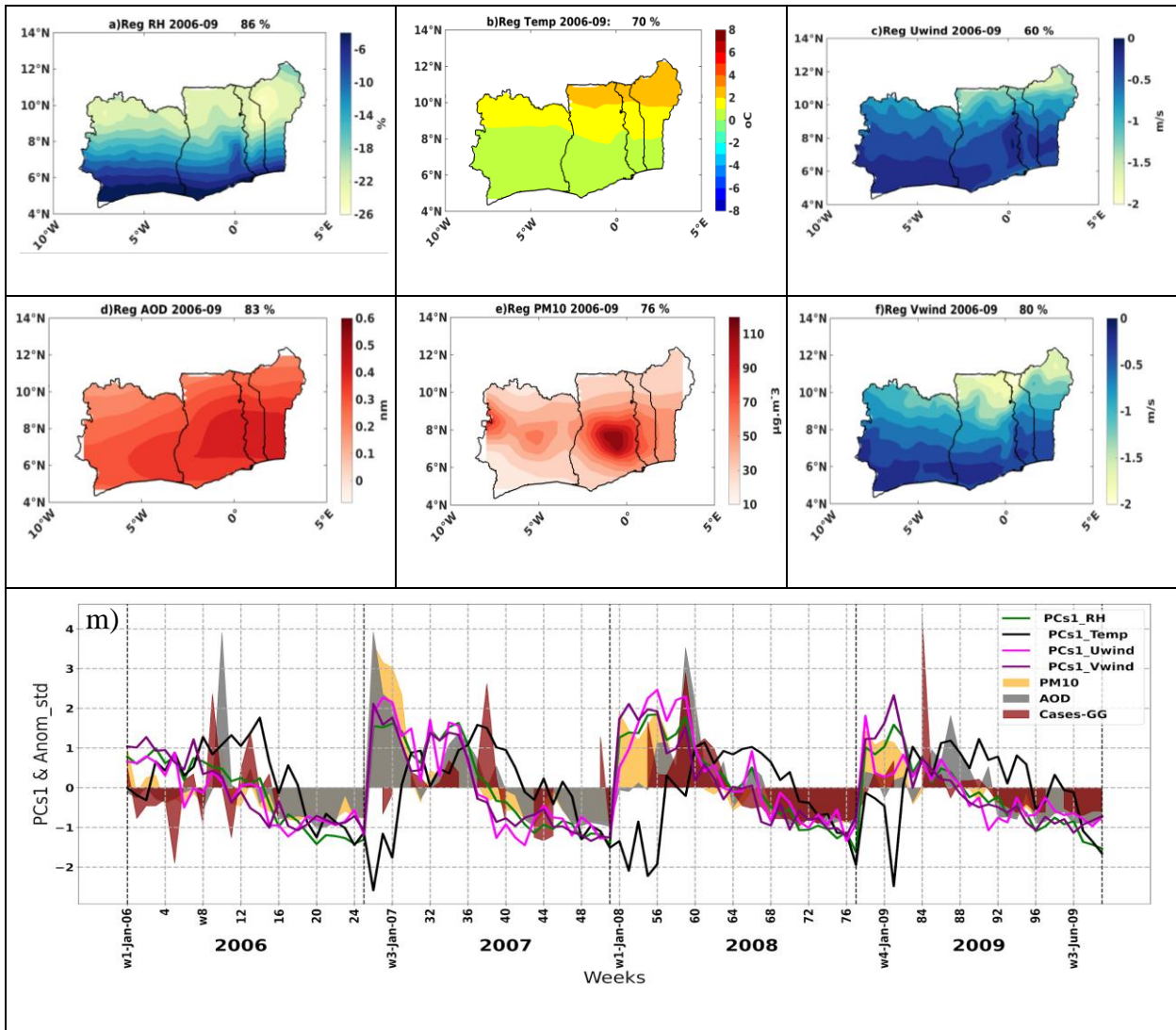


Figure 4.5.1: Regression maps showing the relationship between anomalous environmental variables and the leading principal components (PC1) of the corresponding inter-annual variability mode from January to June over the Gulf of Guinea (GG) for the period 2006–2009 (a–f, m).

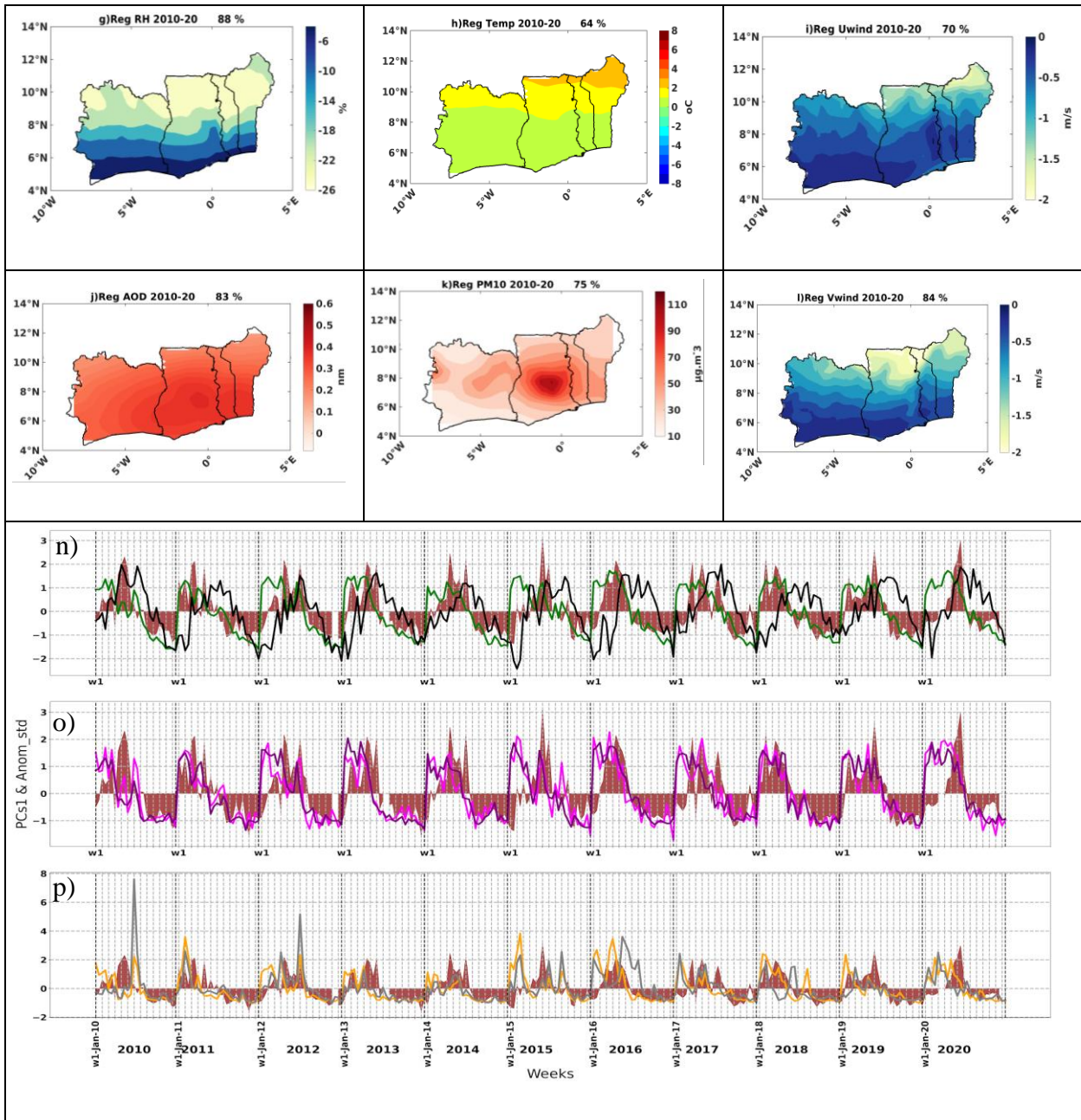


Figure 4.5.2: Regression maps showing the relationship between anomalous environmental variables and the leading principal components (PC1) of the corresponding inter-annual variability mode from January to June over the Gulf of Guinea (GG) for the period 2010–2020 (g–l, n–p).

It is worth noting that these favorable climatic factors not only precede but also persist during disease outbreaks (Figure 4.5m–p). In fact, environmental interannual variability exhibits a pronounced and persistent impact on meningitis in the GG region, as reflected in the high and significant correlation scores observed both before and after vaccination (Table 4.2). Notably, the influence of air temperature on meningitis became significant only in the post-vaccination period (2010–2020).

Similar to the SAH region, GG countries exhibit substantial variability in meningitis timing, with certain outbreaks occurring early in the dry season (e.g., 2011 and 2018), shorter episodes in late spring (e.g., 2015 and 2020), and prolonged meningitis outbreaks extending throughout the entire dry season (e.g., 2012, 2017, and 2019) (Figure. 4.5n).

Our results demonstrate the key role of climatic variables in meningitis incidence across the whole West African Meningitis Belt, independent of the vaccination campaign. These findings open new opportunities for anticipating disease outbreaks. In this sense, the relative contribution of each environmental factor and the associated lead time are explored in the following section.

Table 4.2: Spearman correlation between the leading principal component (PC1) of each environmental variable and the normalized anomalous meningitis cases over the Sahel (SAH) for the periods 2006–2009 (pre-vaccine) and 2010–2020 (post-vaccine). Asterisks (*) indicate statistically significant correlations at the 95% confidence level

GG	2006-2009	2010-2020
PM10 & Men	0.46*	0.56*
AOD & Men	0.49*	0.56*
RH & Men	0.43*	0.67*
Temp & Men	0.18	0.33*
Uw & Men	0.35*	0.59*
Vw & Men	0.35*	0.60*

4.2.2 Environmental precursors of meningitis in SAH and GG

In the previous section, we provided evidence about the precursor role of environmental in meningitis outbreaks in both the SAH and GG regions. However, it is necessary to determine the lead times for each climatic predictor more precisely, as this information is crucial for integration into early warning systems. To this end, anomalies in meningitis cases were fixed in FMAMJ for GG and MAMJ for SAH, based on the disease peak identified in Figure (4.2). The environmental PC1s were then lagged from 0 to week 4 (GG) and from 0 to week 8 (SAH). These represent negative lags, as they evaluate environmental conditions preceding meningitis incidence.

In SAH, during 2006–2009, significant positive correlations were found between surface winds, dust (AOD and PM10), and RH from lag -8 to lag -2, and from lag -8 to lag 0, respectively (solid lines, Figure. 4.6a). Notably, maximum correlation scores occur at lag -6, except for PM10, which peaks at lag -3, suggesting that climatic information up to six months in advance could help anticipate disease emergence. Notably, air temperature exhibits significant positive scores only at lag 0 (solid dark line), indicating its limited predictive role.

During 2010–2020, zonal and meridional winds, along with RH, continue to show significant positive correlations with meningitis cases from lag -8 to lag 0 (dashed pink, purple, and green lines, Figure 4.6a). However, dust concentrations display shorter lead times, correlating with meningitis cases from lag -4 to lag 0 (dashed gray and orange lines, Figure 4.6a). Consequently, after vaccination, the strongest correlations (ranging from 0.5 to 0.8) for environmental precursors occur approximately two months before the meningitis peak (Figure 4.6). No significant correlation is observed between air temperature and meningitis cases after vaccination (dashed dark line, Figure 4.6a).

In GG, before vaccination, significant correlations were observed for surface winds (lag -4 to lag -2), PM10 (lag -3 to lag -2), and RH (lag -4 to lag 0) (solid lines, Figure 4.6b). However, AOD and air temperature do not exhibit significant correlations with meningitis cases (gray line). The optimal lead time for early warning systems appears to be lag -3, based on the highest correlation scores.

During the 2010–2020 period, similar to SAH, positive correlations between zonal wind, meridional wind, PM10, and RH persist from lag -1 to lag -4 (dashed pink, purple, and green lines). Maximum correlation scores occur at lag -2 (ranging from 0.5 to 0.7), suggesting that meningitis outbreaks could be predicted approximately two weeks in advance based on environmental information (Figure 4.6b). Regarding air temperature, significant correlations emerge at lag -1, suggesting its contribution to a favorable environment for meningitis outbreaks after vaccination (dashed dark line, Figure 4.6b).

In summary, our results highlight climatic factors as fundamental drivers of meningitis outbreaks in SAH and GG. Moreover, environmental information from 2 to 6 weeks in advance could aid in anticipating meningitis outbreaks in these vulnerable regions.

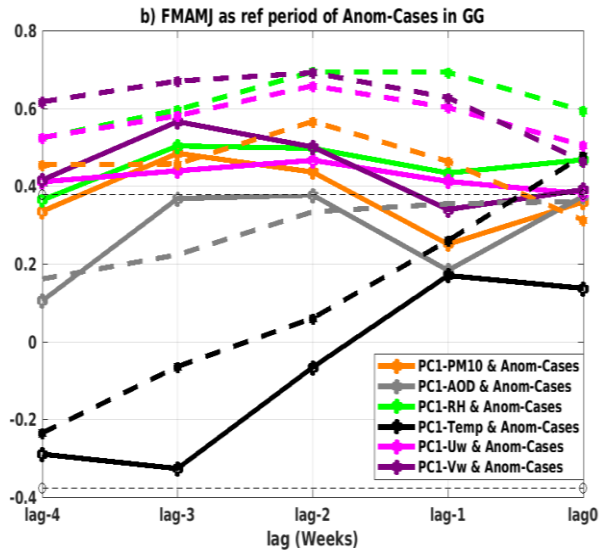
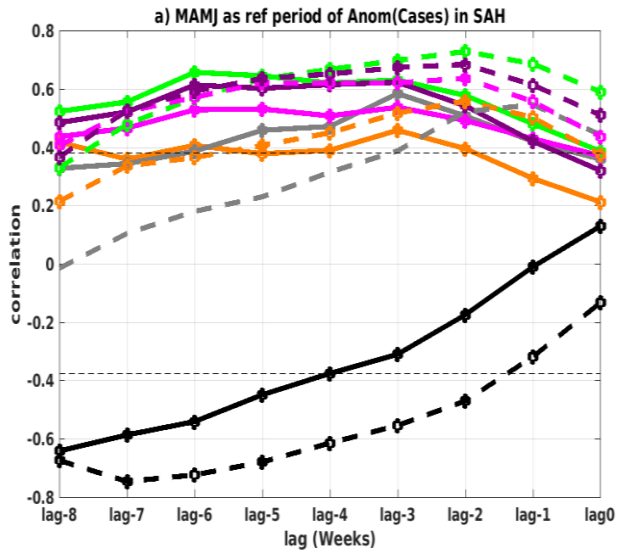


Figure 4.6: Lagged correlations between the leading principal component (PC1) of each environmental variable and the normalized anomalous meningitis cases, with cases fixed at MAMJ and FMAMJ for the Sahel (SAH, left) and Gulf of Guinea (GG, right), respectively.

Summary

The present study examines the incidence of meningitis and the influence of environmental factors across countries in the West African Meningitis Belt (WAMB) from 2006 to 2020. This region encompasses diverse climatic zones and has undergone several vaccination campaigns since 2010. The analysis integrates a robust statistical framework, including principal component analysis (PCA) and lead-lag correlation methods, to assess the relationship between environmental variables and meningitis outbreaks. This study provides critical insights into meningitis dynamics in West Africa, emphasizing the significant impact of vaccination on extending disease duration and delaying transmission. Additionally, it identifies dust events in January as key triggers for meningitis outbreaks in both the SAH and GG regions. However, in the SAH region, the persistence of high temperatures, low relative humidity (<20%), and intensified surface dust concentrations prolongs disease prevalence.

Meanwhile, in the GG region, PM10, moderate relative humidity (<45%), and maximum temperatures though generally lower than in SAH are critical factors shaping the meningitis season. At the inter-annual scale, dominant climatic modes are linked to northeasterly winds transporting high dust concentrations over WAMB, creating a dry and warm environment that favors meningitis outbreaks. Notably, anomalous PM10, AOD, RH, and surface winds emerge as key drivers of meningitis incidence, with predictive lead times of 3–6 weeks.

Our findings align with previous studies highlighting the role of environmental conditions in infectious respiratory diseases (Sultan et al., 2005; Martiny at Chiapello 2013; Yaber et al., 2023; Dione et al 2022). However, our study provides additional insights:

- A comprehensive climate-meningitis analysis across the entire WAMB region. Changes in the seasonal cycle and variability of environmental factors before and after vaccination.

- The robustness of the climate-meningitis relationship despite the presence of multiple vaccines against bacterial meningitis, predominantly caused by *Neisseria meningitidis* (*Nm*) and *Streptococcus pneumoniae* in the African meningitis belt.
- More importantly, surface winds, dust concentrations, and relative humidity serve as key precursors of meningitis outbreaks. These climatic variables enable early anticipation of meningitis cases 2–3 weeks in advance for dust concentrations and 4–6 weeks in advance for winds and relative humidity (Figure 4.6).

Unlike previous studies, our results suggest a weak relationship between air temperature and meningitis emergence in SAH and GG (Ayalande et al., 2020; Yaber et al., 2023). Changes in surface winds and dust transport over WAMB may be linked to large-scale atmospheric patterns, influenced by local and remote climatic forces such as the El Niño-Southern Oscillation (ENSO) (Li et al., 2021), the Intertropical Convergence Zone (ITCZ), and the North Atlantic Oscillation (NAO) (Ridley et al., 2014; Le et al., 2022). These relations should be checked in future studies.

4.3 Inter-annual Variability and Tele-connections of El Niño–Southern Oscillation and Saharan Dust in Relation to Meningitis over West Africa

In this section, we examine the teleconnection between the interannual variability of global atmospheric Saharan dust and ENSO events using MERRA-2 atmospheric aerosol reanalysis data such as AOD-550nm and DUCMASS.

4.3.1 Interannual variability mode of AOD over West Africa during the dry season

Figure 4.7 illustrates the EOF analysis of AOD conducted over West Africa (WA), considering the DJF (December–February), JFM (January–March), FMA (February–April) and MAM (March–May) seasons. The first and second EOF modes of AOD are represented in the left-hand panel, and their associated PCs are represented in the right-hand panel (the first modes are represented in figures (4.7a, d, g and j); the second modes are represented in figures (4.7b, e, h and k). The variability in the distribution of AOD shows the permanent presence of dust across WA during the dry season. The main leading modes of variability appear during JFM and MAM in the GG and SAH, respectively, accounting for 70.8% and 70.5% of the total variability. However, it is known that surface dust concentration usually peaks during JFM in the GG, while the SAH dust event reaches its maximum amplitude during MAM. The standardised principal components associated with the leading EOF modes vary on an interannual timescale (Figure 4.7c, f, i, l). The year 1992 had more dust events in both seasons, while 2015 was identified as the dustiest year from 2006 to 2020.

In summary, the JFM and MAM seasons exhibit the greatest AOD variability in the GG and SAH, respectively.

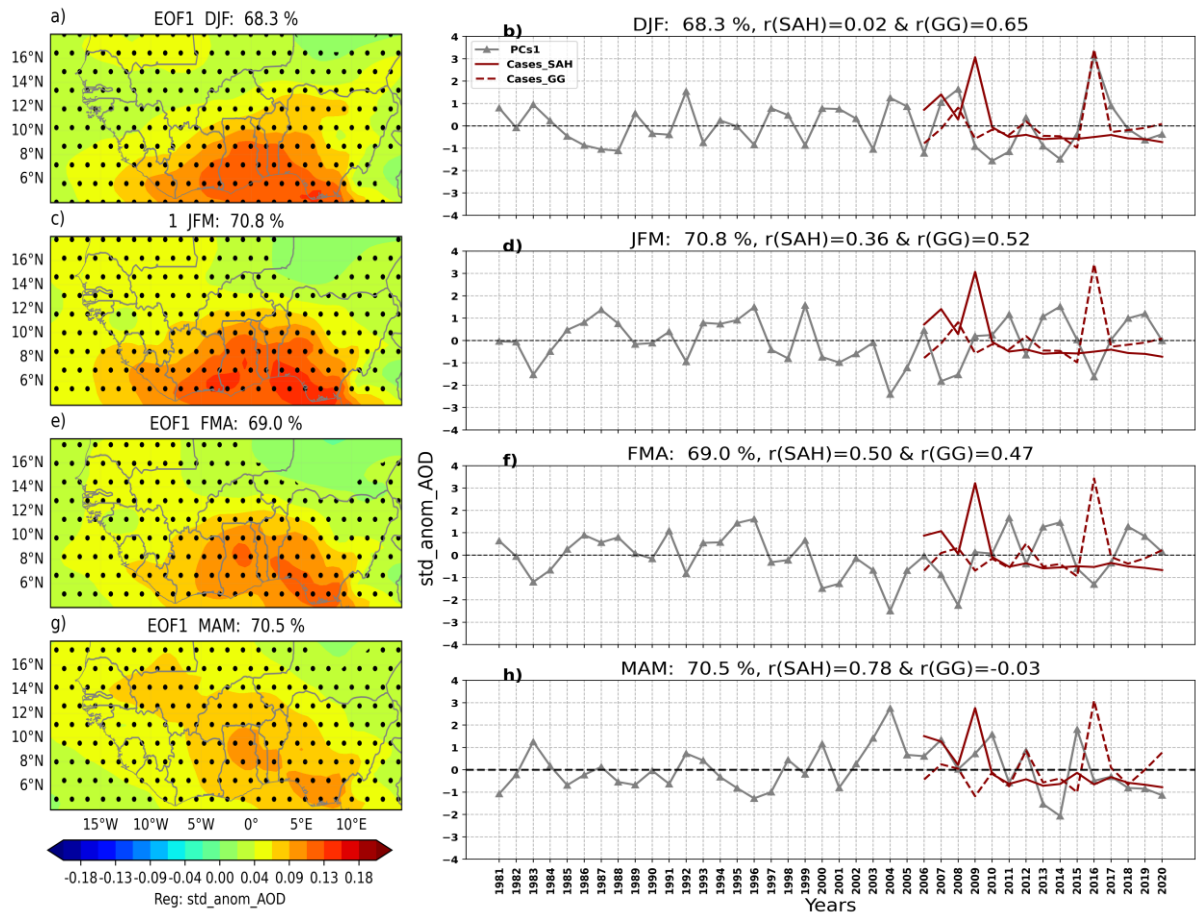


Figure 4.7: Empirical orthogonal function (EOF) analysis of AOD in West Africa. Regression maps of the first (a,d,g,j), second modes (b,e,h,k) and associated Principal Components (c,f,i,l) for the four the seasons DJF, JFM, FMA and MAM during the period 1981–2020.

4.3.2 Relationship between AOD variability mode and meningitis incidence in SAH and GG zones

The Spearman correlations between the PCs of AOD and the standardised anomalies of meningitis incidence, conducted in Tables (4.3 and 4.4), show the lag between the dust and disease seasons considered, respectively, at -1 and 0. A positive and significant relationship between dust and meningitis is illustrated in both phases (lag -1 and lag 0). However, across Table 4.3, only the leading principal component (PC1) shows an important relationship between these variables. For example, the previous dust event during the DJF season preceded the JFM meningitis season in the GG, showing a high correlation ($r = 0.45$) compared to the others. Meanwhile, the SAH meningitis season during the MAM season showed a strong and significant link ($r = 0.53$) with the AOD variability during the FMA season. Table 4.4, representing phase 0 of these correlations, shows that only SAH exhibited significant correlations with PCs 1 and 2 of AOD during FMA ($r = 0.51$ and $r = 0.6$, respectively), and with PC1 during MAM, exhibiting the highest correlation ($r = 0.85$).

Figure 4.8 highlights the interannual variability of both parameters, such as the PCs of AOD, which show a significant correlation (see Tables 4.3 and 4.4), and the disease patterns in both areas. The identified and selected lead mode of AOD and the corresponding seasons show a significant correlation with disease at lags -1 and 0. This indicates that 2016 was a year of high meningitis incidence in the GG (Figure. 4.8a), coinciding with the dustiest year between 2006 and 2020 in that area.

Regarding disease patterns in SAH (Figure. 4.8b–d), three years with a notable meningitis incidence were identified. In 2007, there was less incidence, and the peak of the disease during the FMA season coincided with the peak of dust variability (PC2) and an increase through

PCs1 for the same season (Figure. 4.9b). This was followed by 2015, when the peak of the disease in MAM coincided with an increase in dust variability during the FMA season (Figure. 4.8.b) and a peak in MAM (Figure. 4.8.d). The year 2009 represents the year with the highest incidence of meningitis over the SAH during the period 2006–2020, while AOD variability was less significant compared to the years 2007 and 2015. However, the dust patterns closely resemble the increase in incidence of the disease when the dust variability reaches around 1. In summary, the meningitis season appears to be led by AOD variability during winter in the GG and during both winter and spring in the SAH.

Table 4.3: One month lagged (lag-1) correlation between PCs of AOD index and meningitis incidence in the SAH (a) and the GG (b) using Spearman method. The PCs for the seasons DJF, and FMA are respectively correlated with the disease during JFM and MAM in the GG and The SAH. The asterisks (*) indicate the statistically significant correlations at 95% confidence level.

Lag -1	a) SAH		b) GG
	corr		corr
PCs1_DJF/MenJFM	0.018		0.65*
PCs1_JFM/MenFMA	0.4		0.60*
PCs1_FMA/MenMAM	0.47*		0.50

Table 4.4: Lagged (lag0) correlation between PCs of AOD index and meningitis incidence in the SAH (a) and the GG (b) using Spearman method. The PCs for the seasons FMA and MAM are respectively correlated with the disease in the SAH during FMA and MAM. The asterisks (*) indicate the statistically significant correlations at 95% confidence level.

Lag 0	a) SAH		b) GG
	corr		corr
PCs1_JFM/MenJFM	0.36		0.52*
PCs1_FMA/MenFMA	0.50*		0.47
PCs1_MAM/MenMAM	0.78*		-0.03

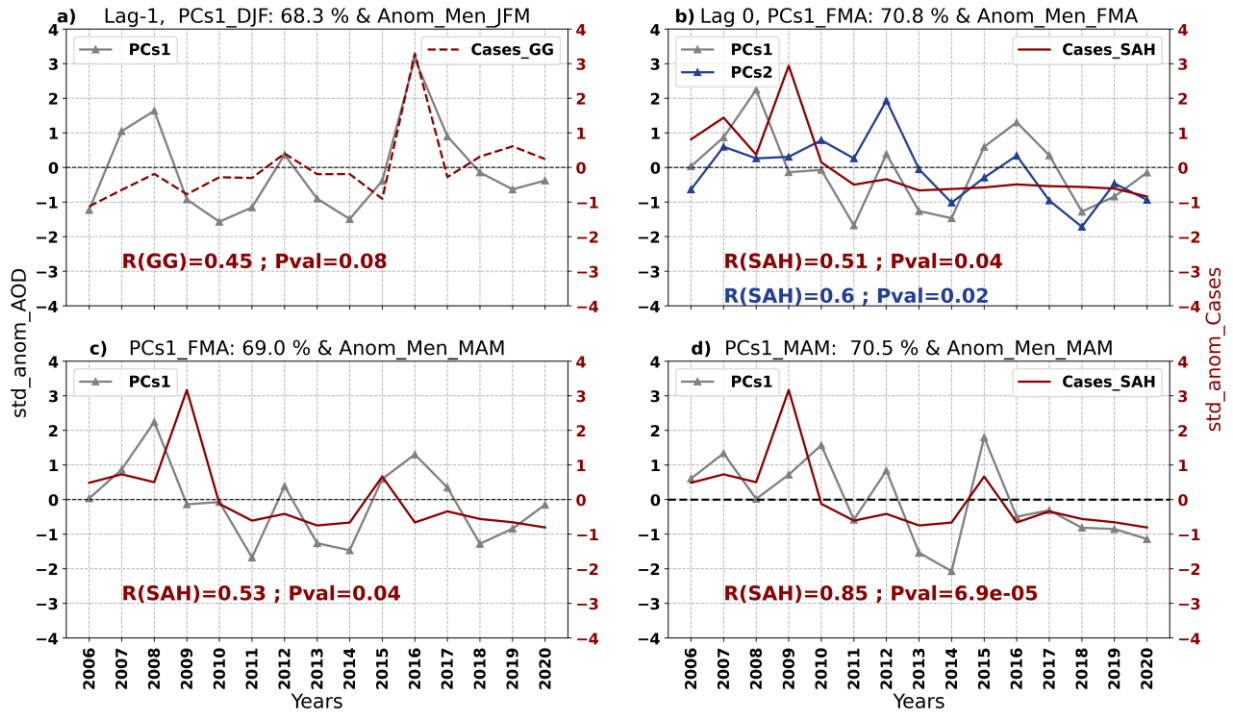


Figure 4.8: The lag correlation of the selected PCs of the AOD index (the grey line represents PCs1 and the blue line represents PCs2) with the standardised anomalies of the meningitis cases (b–d: the red line represents SAH and the dashed line represents GG) is shown.

4.3.3 Interactions between Saharan dust variability mode and global Climate variability

In this section, the selected AOD PCs during the DJF and FMA seasons (PCs 1 and 2) and the MAM season over WA, which were significantly correlated with meningitis in the SAH and GG, were regressed with the anomalies of global SLP (Figure 4.9-4.11: b,e,h,k,n,q,t shaded) combine with the winds direction (Figure 4.9-4.11: b,e,h,k,n,q,t arrows), SST (Figs 4.9-4.11: a,d,g,j,m,p,s) and AOD (Figure 4.9-4.11: c,f,i,l,o,r,u). Six seasons in advance from lag 0 were taken into account.

Figures 4.9–4.11 represent a lagged regression analysis conducted to reveal the sequence of teleconnected atmospheric processes that link tropical Pacific SST anomalies to dust variability over West Africa.

Figure 4.9 shows the DJF season of PCs 1 of AOD fixed and the SST, SLT and wind components lagged from DJF to JJA.

Figure 4.10 illustrates the seasonality of the PCs1 of AOD, with the SST, SLT and Winds components lagged from lag 0 (FMA), lag -1 (JFM), lag -2 (DJF), lag -3 (NDJ), lag -4 (OND), lag -5 (SON) and lag -6 (ASO).

Figure 4.11 shows the seasonality of the PCs1 of AOD, with the SST, SLT and Winds components lagged from lag 0 (MAM), lag -1 (FMA), lag -2 (JFM), lag -3 (DJF), lag -4 (NDJ), lag -5 (OND) and lag -6 (SON).

The results show that, in boreal winter and spring, the warming (El Niño) in the Pacific is evident in all Figure 4.9, Figure 4.10, and Figure 4.11 (from lag -2 to lag0: for panel m,p,s). This SST anomaly pattern evolves into a high-pressure system (Figure 4.9, Figure 4.10, and Figure 4.11; from lag -2 to lag0: for panel n,q,t) over northern Africa and the subtropical Atlantic, accompanied by intensified northeasterly wind anomalies over the Sahara and West

Africa. These wind patterns favour the southward transport of Saharan dust, leading to enhanced aerosol optical depth (AOD) concentrations over the Gulf of Guinea and the equatorial region (Figure 4.9, Figure 4.10, and Figure 4.11 from lag -2 to lag0: for panel o,r,u), and consequently to cooling of the sea surface temperature (SST) close to the north Atlantic equatorial region. This can be attributed to the ability of dust to scatter and absorb solar radiation, thereby reducing shortwave radiation in the equatorial North Atlantic SST. In response, the trade winds blowing over West Africa appear to be weak and dust-poor, and the reduced scattering and absorption of solar radiation by dust aerosols cools the ocean surface.

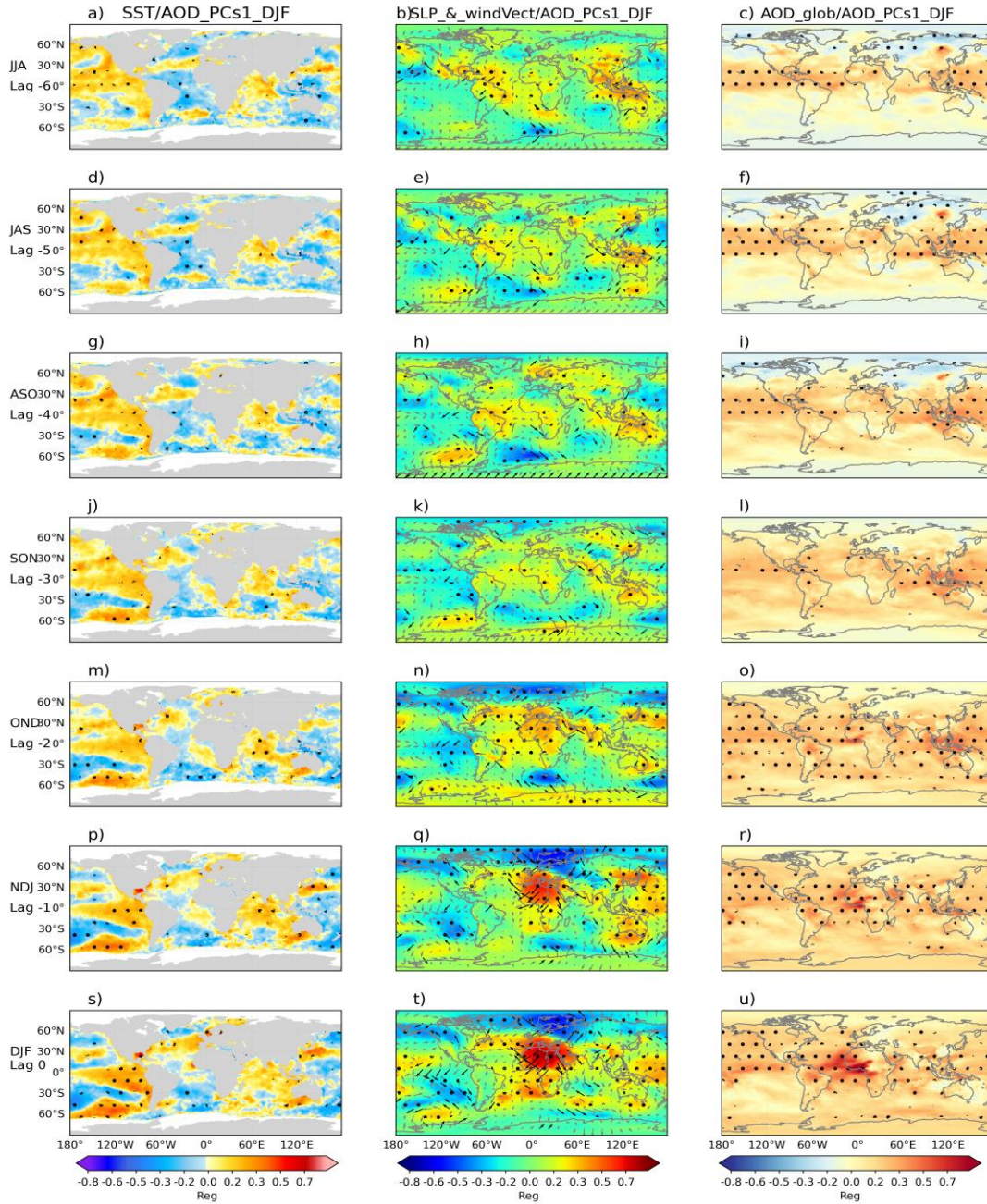


Figure 4.9: Regression maps of seasonal standardized anomalies of SST (a,d,g,j,m,p,s), SLP (b,e,h,k,n,q,t shaded) and wind at 10m (arrows), and global AOD (c,f,i,l,o,r,u), with the standardized first leading mode (PCs1) of averaged AOD over WA during the DJF for the period 1981 to 2019.

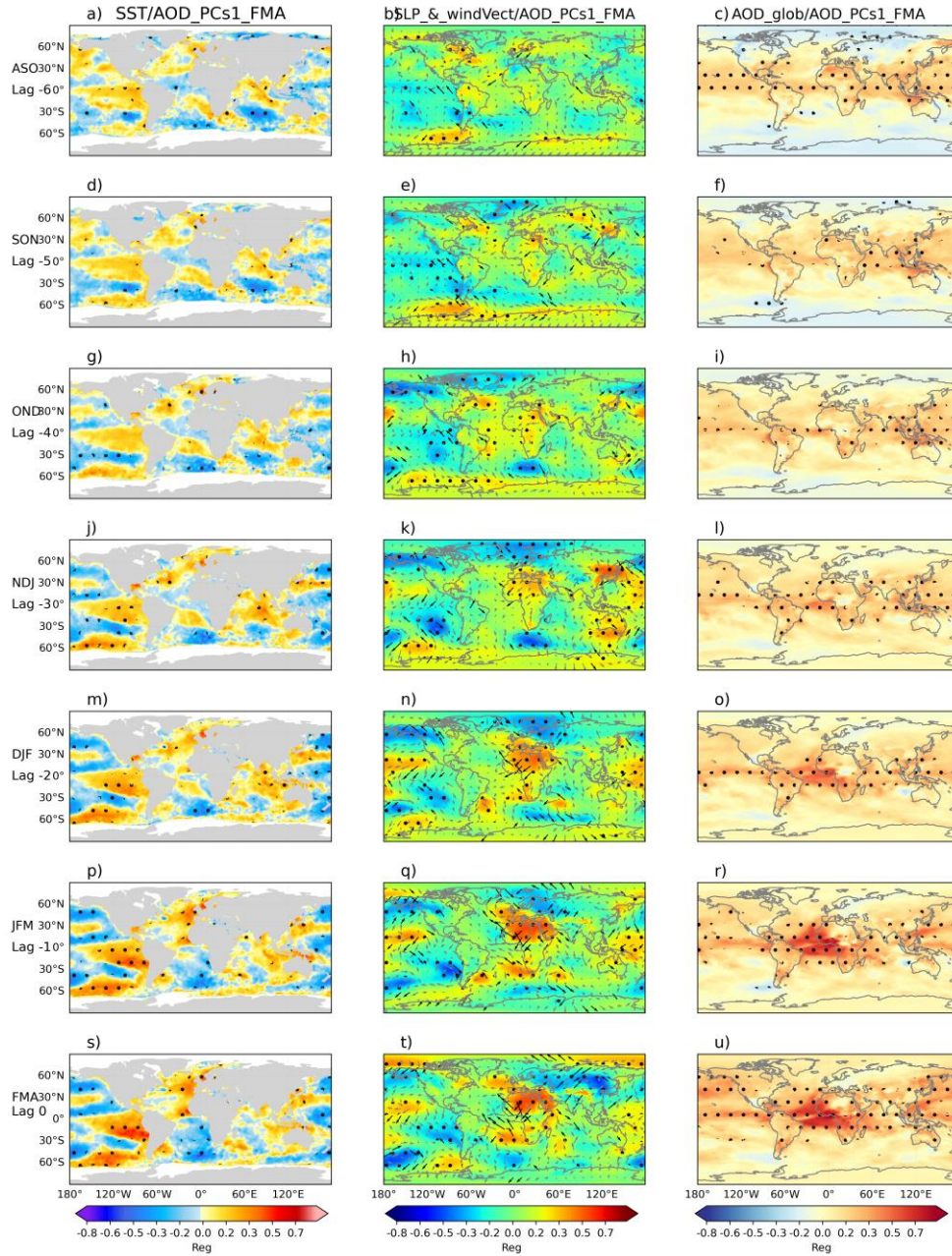


Figure 4.10: Regression maps of seasonal standardized anomalies of SST (a,d,g,j,m,p,s), SLP (b,e,h,k,n,q,t shaded) and wind at 10m (arrows), and global AOD (c,f,i,l,o,r,u), with the standardized first leading mode (PCs1) of averaged AOD over WA during the FMA for the period 1981 to 2019.

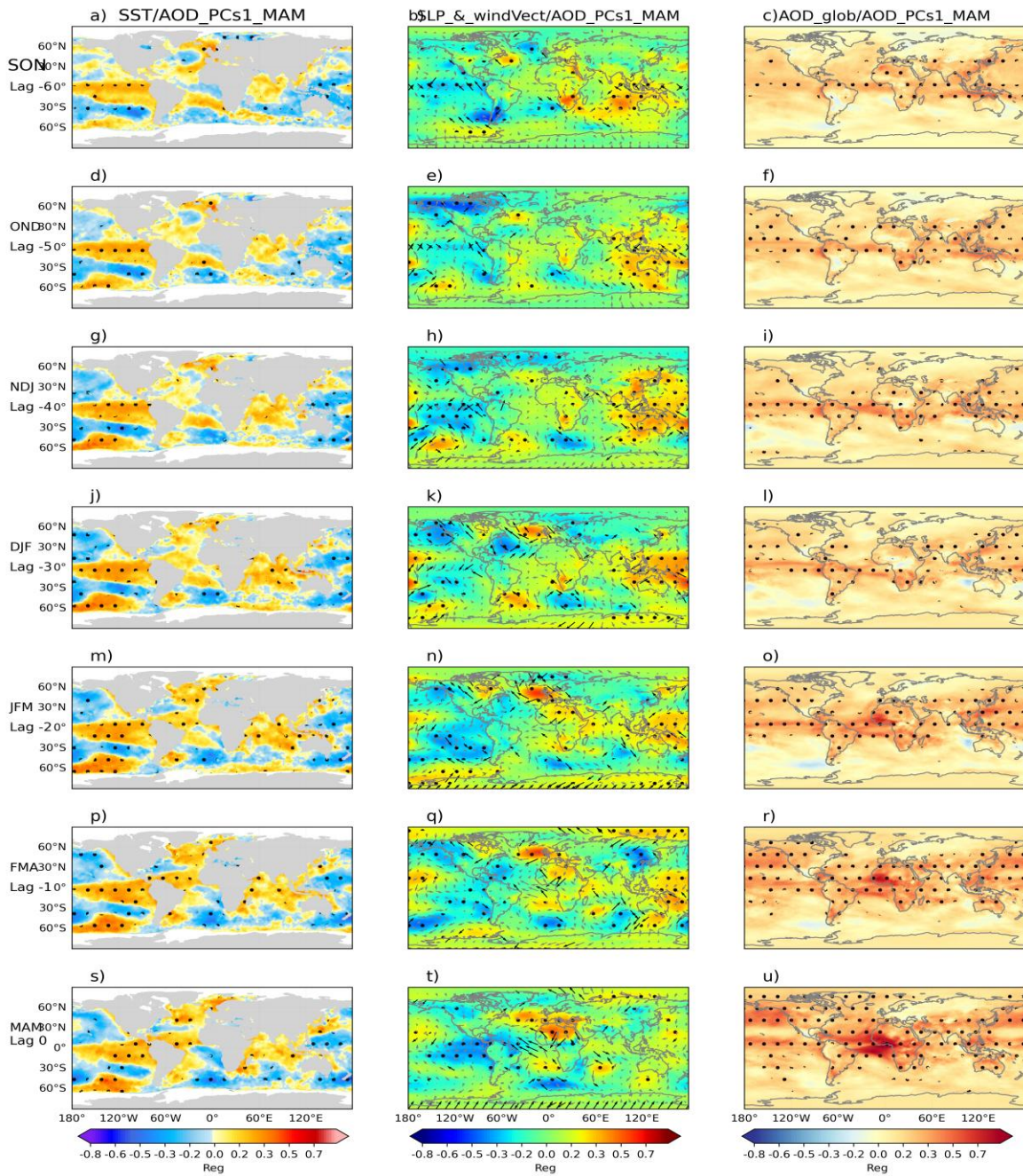


Figure 4.11: Regression maps of seasonal standardized anomalies of SST (a,d,g,j,m,p,s), SLP (b,e,h,k,n,q,t shaded) and wind at 10m (arrows), and global AOD (c,f,i,l,o,r,u), with the standardized first leading mode (PCs1) of averaged AOD over WA during the MAM for the period 1981 to 2019.

4.3.4 Influence of global Climate variability in the Inter-linkage between Saharan AOD and meningitis incidence in the WAMB

This paragraph addresses analogous regression maps to previous ones (Figure. 4.9–4.11), but using the time series of the disease in GG and SAH (considering the seasons that are significantly correlated with the PCs of AOD), the global SST, SLP, wind and AOD were investigated in order to compare the results with those in Figure (4.9–4.11) and to provide useful information about the interlinkage between AOD and disease. The lagged regression patterns relating to meningitis anomalies in the Sahel (MenSAH) for the FMA and MAM seasons, as well as in the Gulf of Guinea (GG) during the JFM season, are shown in Figures (4.12–4.14).

Figure 4.12 shows the meningitis incidence anomalies over GG fixed in the JFM season and then regressed against the SST (a,d,g,j,m,p,s), SLP(b,e,h,k,n,q,t shaded) combine with the winds direction (b,e,h,k,n,q,t arrows), and AOD (c,f,i,l,o,r,u), with a 6-month lag time. Lag 0 corresponds to JFM, lag -1 to DJF, lag -2 to NDJ, lag -3 to OND, lag -4 to SON, lag -5 to ASO, and lag -6 to JAS. Figures (4.13 and 4.14) illustrate the regression analysis of meningitis incidence in the Sahel. The latter, covering the February–May season, is highly related to Saharan dust events from the boreal winter, which persist throughout the spring season, including the peak (maximum dust concentration) over the Sahel (0.51/0.6 for PCs1/PCs2 of AOD during FMA and 0.85 during MAM). The FMA season for meningitis (Figure. 4.13) is fixed, while SST (a,d,g,j,m,p,s), SLP (b,e,h,k,n,q,t shaded) combine with the winds direction (b,e,h,k,n,q,t arrows), and AOD and the global AOD pattern (c,f,i,l,o,r,u), are lagged from lag 0 (FMA), lag -1 (JFM), lag -2 (DJF), lag -3 (NDJ), lag -4 (OND), lag -5 (SON) and lag -6 (ASO). Similarly, MAM was fixed and atmospheric and ocean variables were lagged with MAM as lag

0 and with the other seasons as negative lags: FMA as lag -1, JFM as lag -2, DJF as lag -3, NDJ as lag -4, OND as lag -5 and SON as lag -6.

In the case of the GG (Figure 4.12), warm SST anomalies (Figure 4.12a,d,g,j,m,p,s) over the equatorial Pacific, indicative of El Niño conditions, is associated with elevated aerosol concentrations and meningitis cases in the GG with a maximum in DJF (Figure 4.12r). This sequence begins with low sea-level pressure over the tropical Pacific, evolving into a high-pressure anomaly over the Atlantic and North Africa. This is accompanied by intensified northeasterly winds that promote the mobilization and transport of Saharan dust towards the Gulf of Guinea and the Sahel.

Conversely, in the FMA and MAM seasons, regression patterns linked to Sahelian meningitis incidence (see Figure 4.13 and 4.14) are associated with cool SST anomalies (Figure 4.13 & Figure 4.14 for panels a,d,g,j,m,p,s) in the equatorial Pacific indicative of La Niña conditions. This is associated with low pressure around the equator and over West African regions. Consequently, a weak variability in dust concentrations is observed in this region and at high altitudes. The conditions observed in figure 4.13, with FMA as the meningitis season in SAH, persist in MAM (Figure. 4.14). In both periods, cool SST anomalies over the equatorial Pacific, typically occurring several months prior, contribute to increased precipitation in southern Africa and drought in West Africa, indirectly increasing the occurrence of meningitis outbreaks over the Sahel.

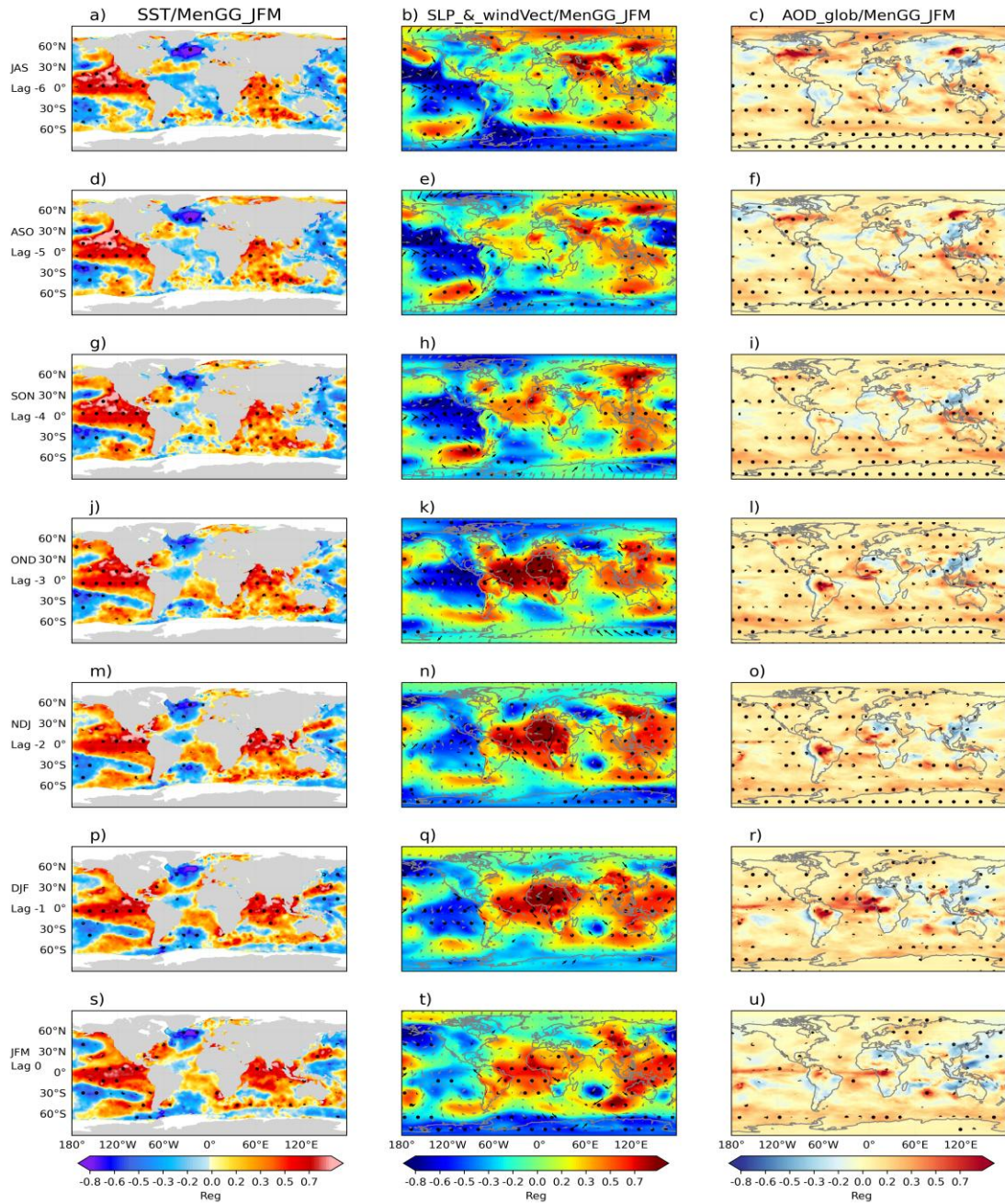


Figure 4.12: Regression maps of seasonal standardized anomalies of SST (a,d,g,j,m,p,s), SLP (b,e,h,k,n,q,t shaded) and wind at 10m (arrows), and global AOD (c,f,i,l,o,r,u), with the standardized anomalies of the averaged incidence of meningitis over GG during JFM for the period 2006 to 2019.

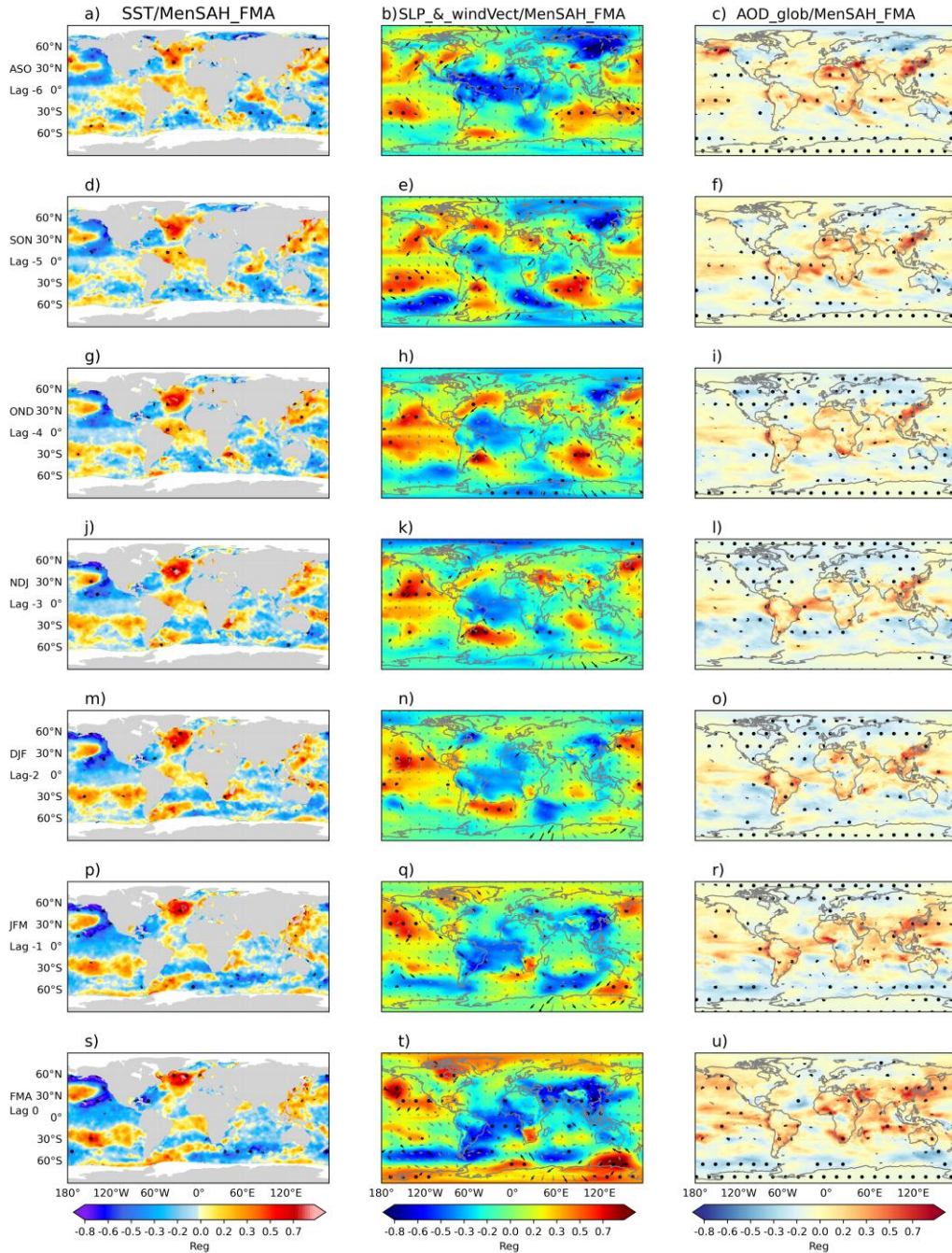


Figure 4.13: Regression maps of seasonal standardized anomalies of SST (a,d,g,j,m,p,s), SLP (b,e,h,k,n,q,t shaded) and wind at 10m (arrows), and global AOD (c,f,i,l,o,r,u), with the standardized anomalies of the averaged incidence of meningitis over SAH during FMA for the period 2006 to 2019.

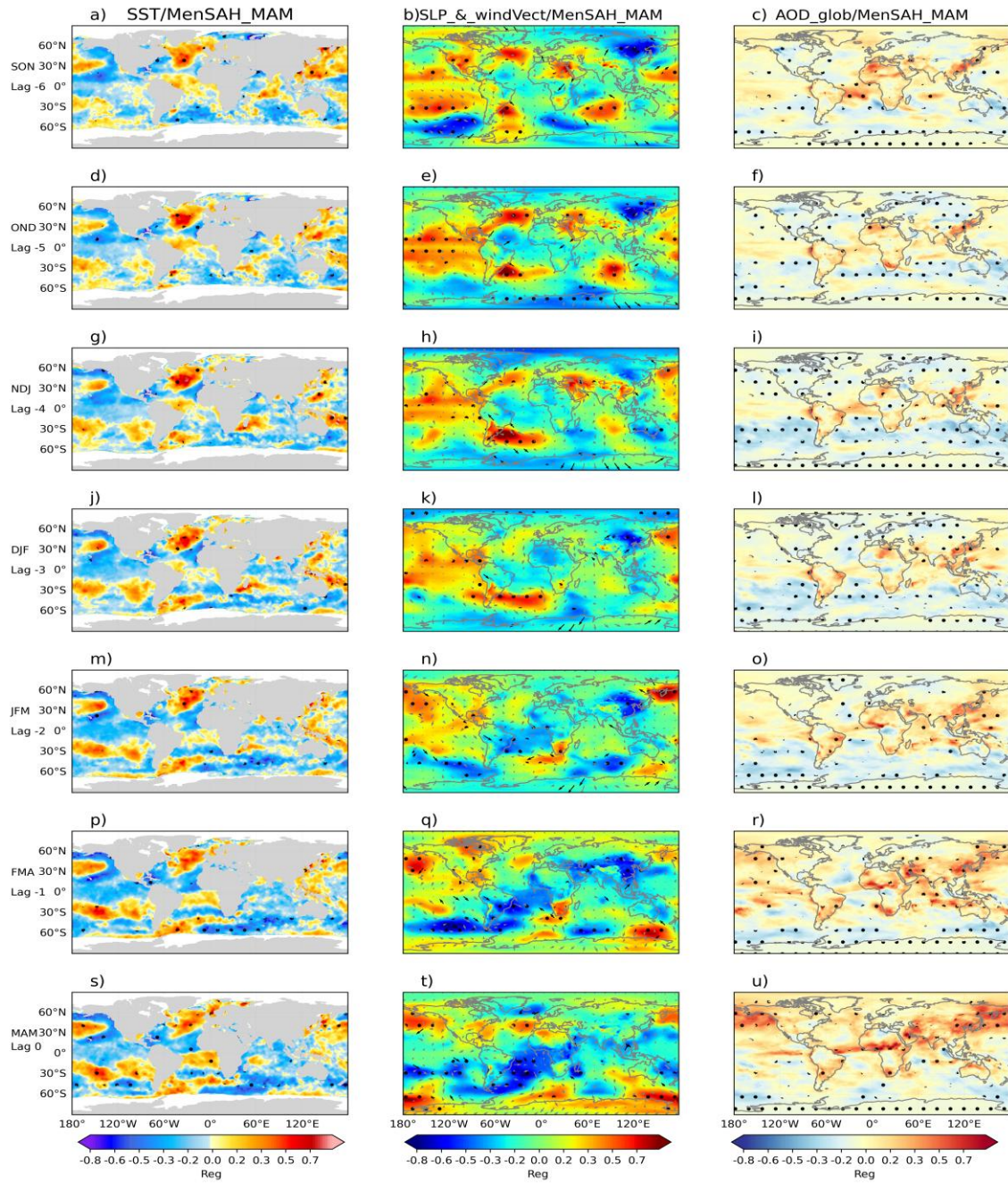


Figure 4.14: Regression maps of seasonal standardized anomalies of SST (a,d,g,j,m,p,s), SLP (b,e,h,k,n,q,t shaded) and wind at 10m (arrows), and global AOD (c,f,i,l,o,r,u), with the standardized anomalies of the averaged incidence of meningitis over SAH during MAM for the period 2006 to 2019.

To support the results of the regression analysis, which illustrate the mechanisms involved in the teleconnection between ENSO and global Saharan dust, we performed a composite analysis. This analysis highlights the spatial variability of Saharan dust during ENSO events, and will help us to predict the future occurrence of meningitis based on climate projections.

4.3.5 Identification of ENSO events

Figure 4.15a shows the annual cycle of the standard deviation of sea surface temperature (SST) in the Niño 3.4 region (5°N – 5°S , 120°W – 170°W). The peak of SST variability in this region occurs in December, with an approximate variability of 1.3°C . Based on this result, and given that ENSO events tend to peak during the winter season (DJF), the Ocean Niño Index (ONI) was calculated using a three-month running mean of monthly SST averaged over the Niño3.4 region. Indeed, SST anomalies greater than $+1.3$ standard deviations defined El Niño (EN) events and those lower than -1.3 standard deviations defined La Niña (LN) events during 1980–2020 (see Figure. 4.15b). Five EN and LN events were identified as follows: (1982/1983, 1991/1992, 1997/1998, 2009/2010 and 2015/2016) and (1988/1989, 1998/1999, 1999/2000, 2007/2008 and 2010/2011), respectively (see Fig 4.14b).

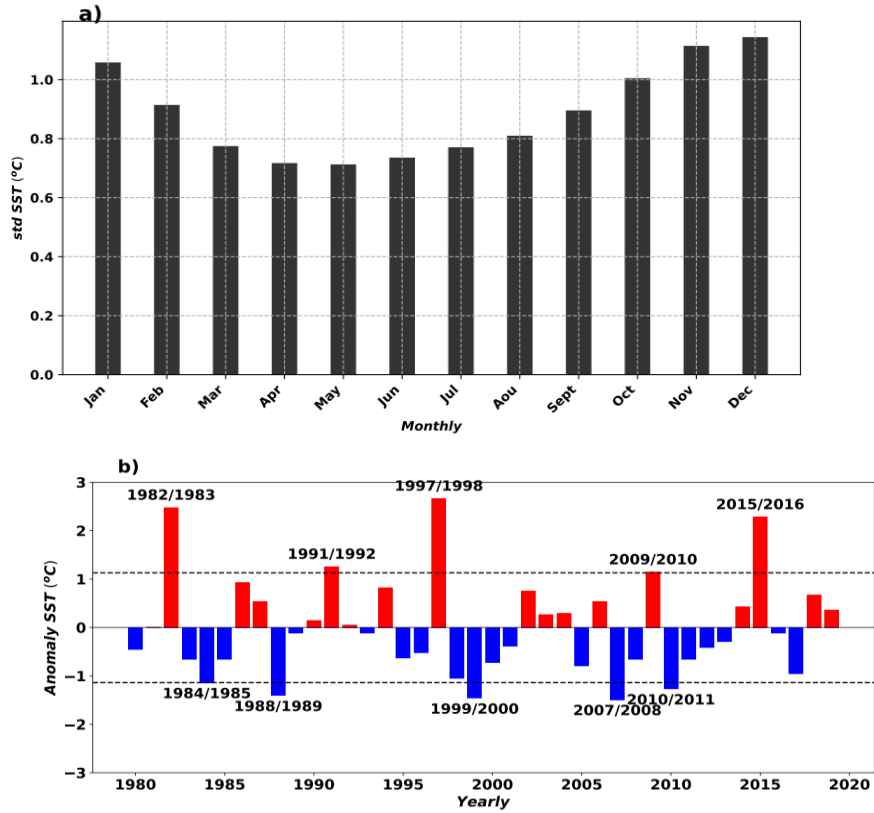


Figure 4.15: Standard deviation and ENSO of the equatorial Pacific SST anomalies over the Niño 3.4 index region: (a) Standard deviation of the Niño 3.4 index over the Niño 3.4 region (5°N–5°S, 120°W–170°W) in each month during 1980–2020; (b) Mean Niño 3.4 index in the preceding winter (December of the previous year to February of the current year).

4.3.6 Intra-seasonal climatology of dust

To identify the seasons and regions with high dust concentrations during the dry season, including the meningitis season in the WAMB, we calculated the mean dust aerosol, such as AOD and DUCMASS, from December to February and MAM. Figures 4.16a–d show the global distribution of these dust aerosols during the boreal winter and spring seasons. They reveal high levels of dust aerosols in the GG during DJF and over the Saharan and sub-Saharan regions in MAM, with the highest concentrations in the Sahel zone. The Bodélé Depression is clearly shown to be not only a high-emitting source, but also a persistent emitting source throughout the dry season, with emissions being more intense from December to March. Figures (4.16c and 4.16d) show that the dust plume begins in late spring in North Africa and moves towards Asia and the Caribbean, with high values tending to concentrate in East Africa, Sub-Saharan Africa, the Arabian Peninsula and Central Asia.

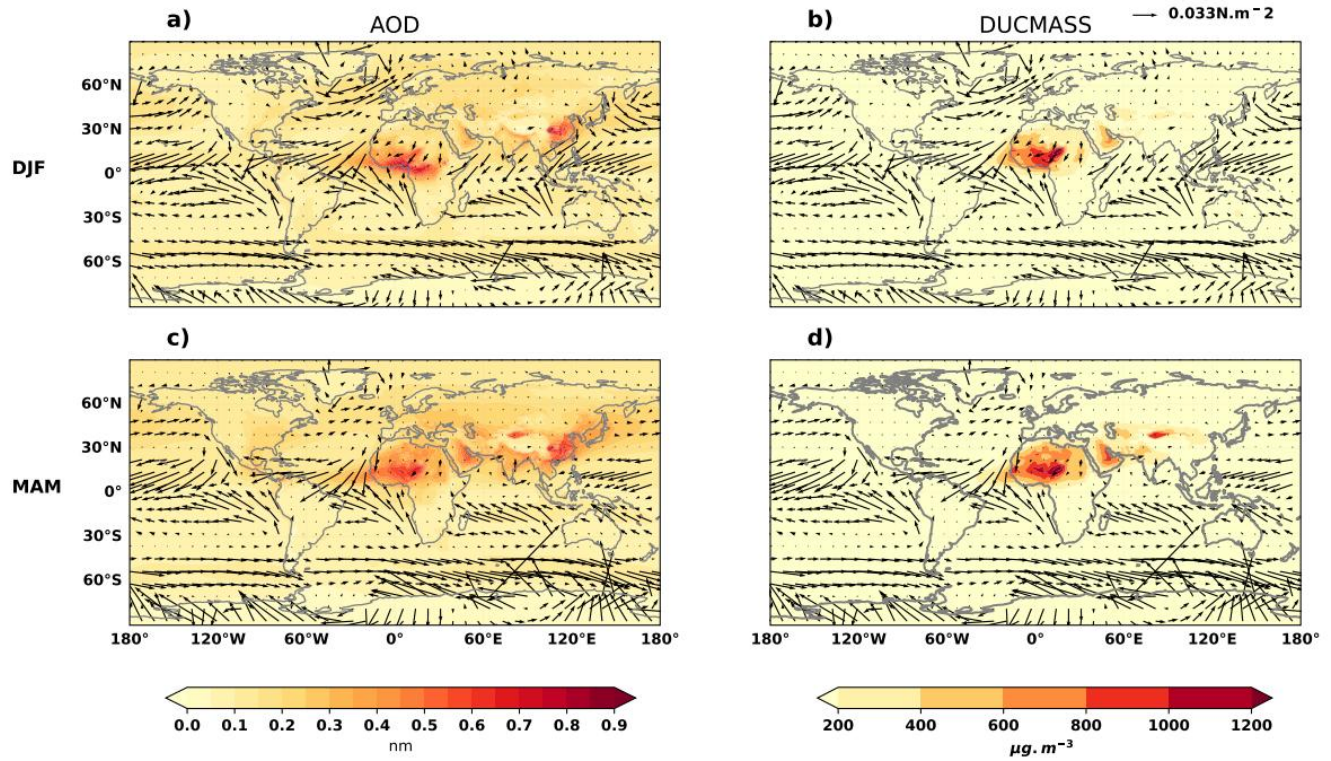


Figure 4.16: Variability of global dust mean (a-c) AOD and (b-d) DUCMASS averaged for the years 1980–2020, during the DJF (a-b) and MAM (c-d) seasons.

4.3.7 Impact of strong ENSO on Saharan dust in the North African desert.

This section addresses the composite analysis of global sea surface temperature (SST) (Figure. 4.17a–d) and the Saharan dust index, such as the aerosol optical depth (AOD) (Figure. 4.18a & c) and the dust convective mass (DUCMASS) (Figure. 4.18b & d) anomalies, during the ENSO and La Niña events (five each during 1980–2020). AOD anomalies are predominant in winter and positive during the dry season. Figures (4.17a & 4.18a) show that during EN years over the equatorial Pacific, the entire WA region was dominated by above-normal dust in both indices, peaking in the GG and over the equatorial Atlantic during DJF (Figure 4.18a–b). Meanwhile, the maximum dust anomalies above normal in MAM appeared over the Saharan and Sahelian countries (Figure 4.18c–d), particularly in the Sahara Desert (up to 0.17 nm and 160 $\mu\text{g}/\text{m}^3$). Additionally, during the event, a warm SST associated with a cool dipole in the subtropical Atlantic and around the equatorial Atlantic was observed over the West African coast. These conditions induce depressions in these latter two areas, where high dust concentrations are present. For the La Niña years (Figure 4.17b & d), the opposite was observed in terms of the SST pattern. While the dust distribution patterns over WA remain almost similar to those during EN events, a reduction in dust concentration is observed (Figure. 4.19a–d) compared to the pattern during EN events. MAM showed predominantly positive anomalies over the northern part of the Saharan region and the Sahelian band.

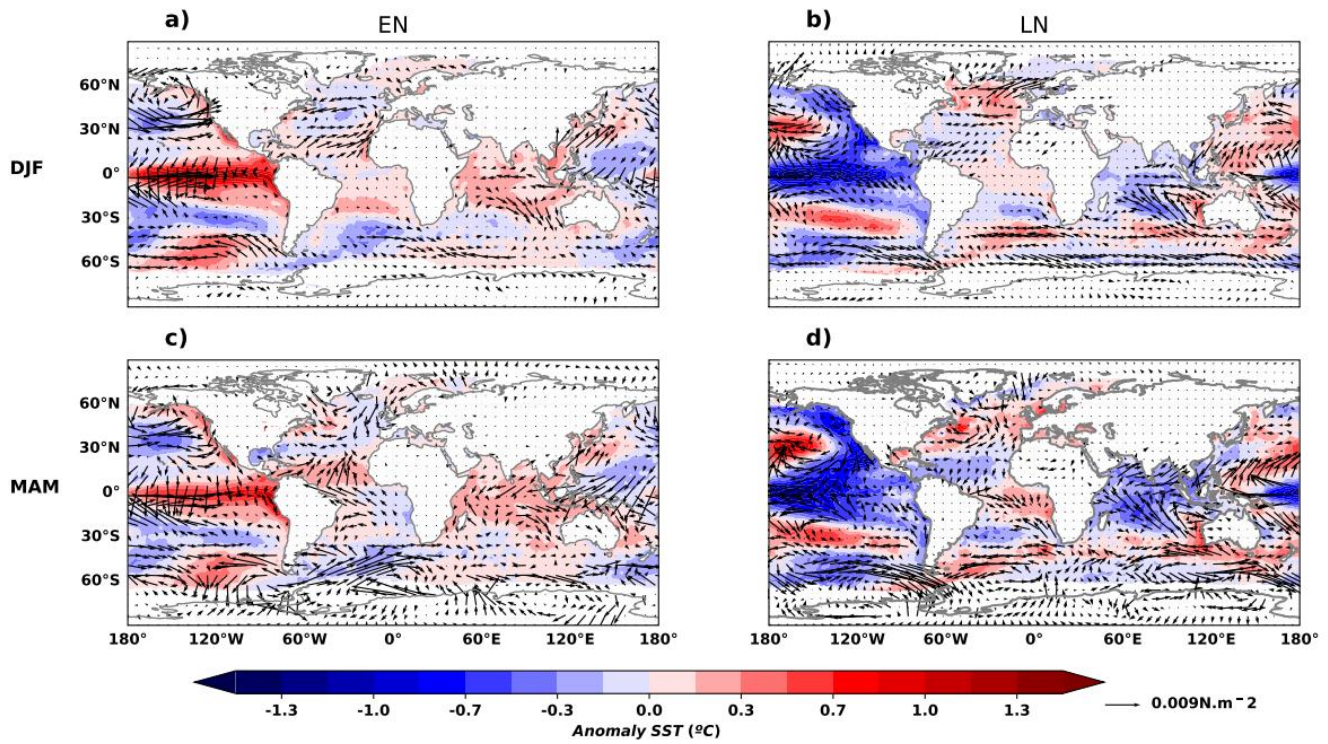


Figure 4.17: Composite of global sea surface temperature (SST) anomalies during El Niño–Southern Oscillation (ENSO) events from 1980 to 2020.

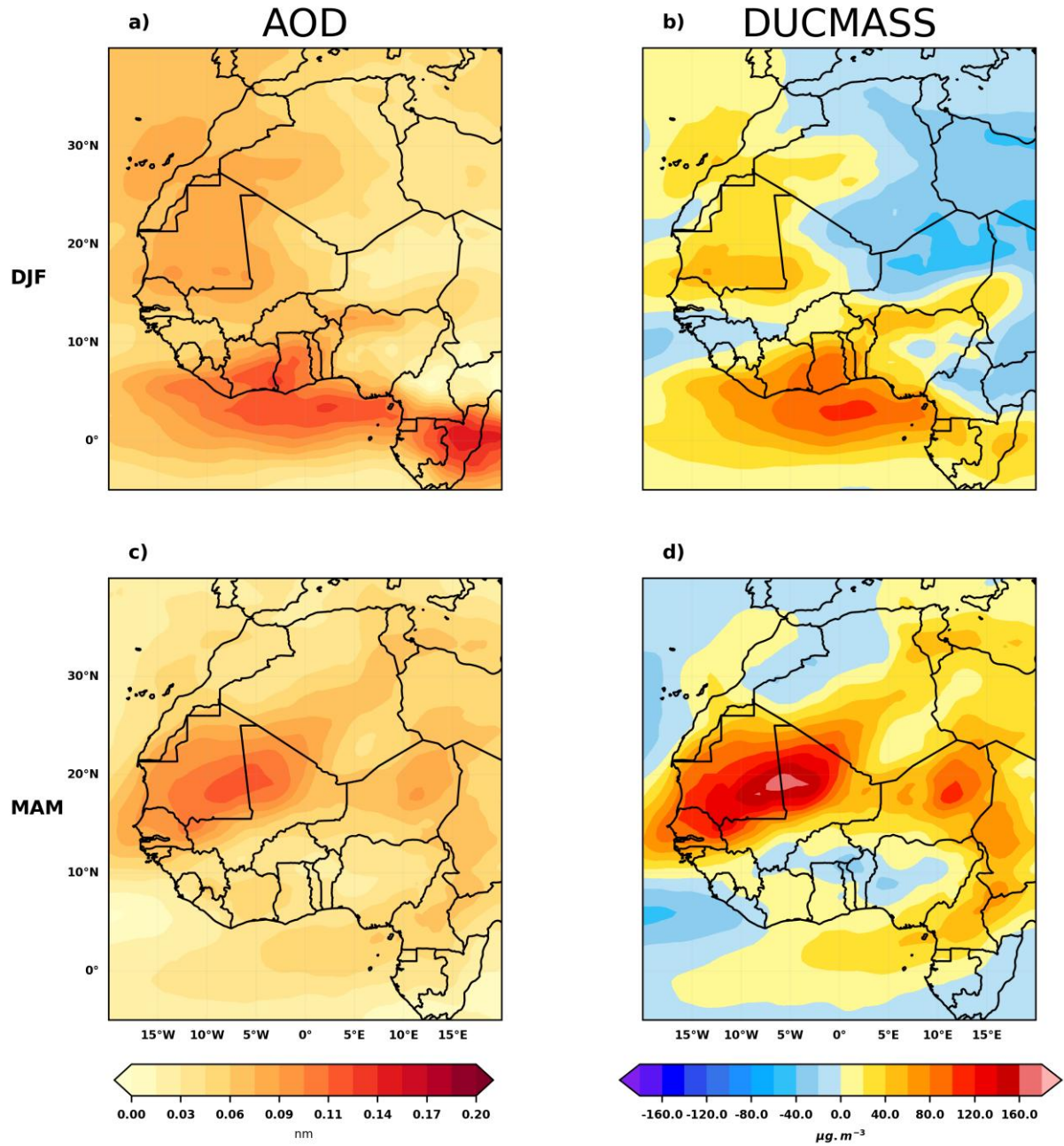


Figure 4.18: Composite of dust (AOD and DUCMASS) in the region (20°W–15°E and 4°N– 30°N) during El Niño events from 1980 to 2020.

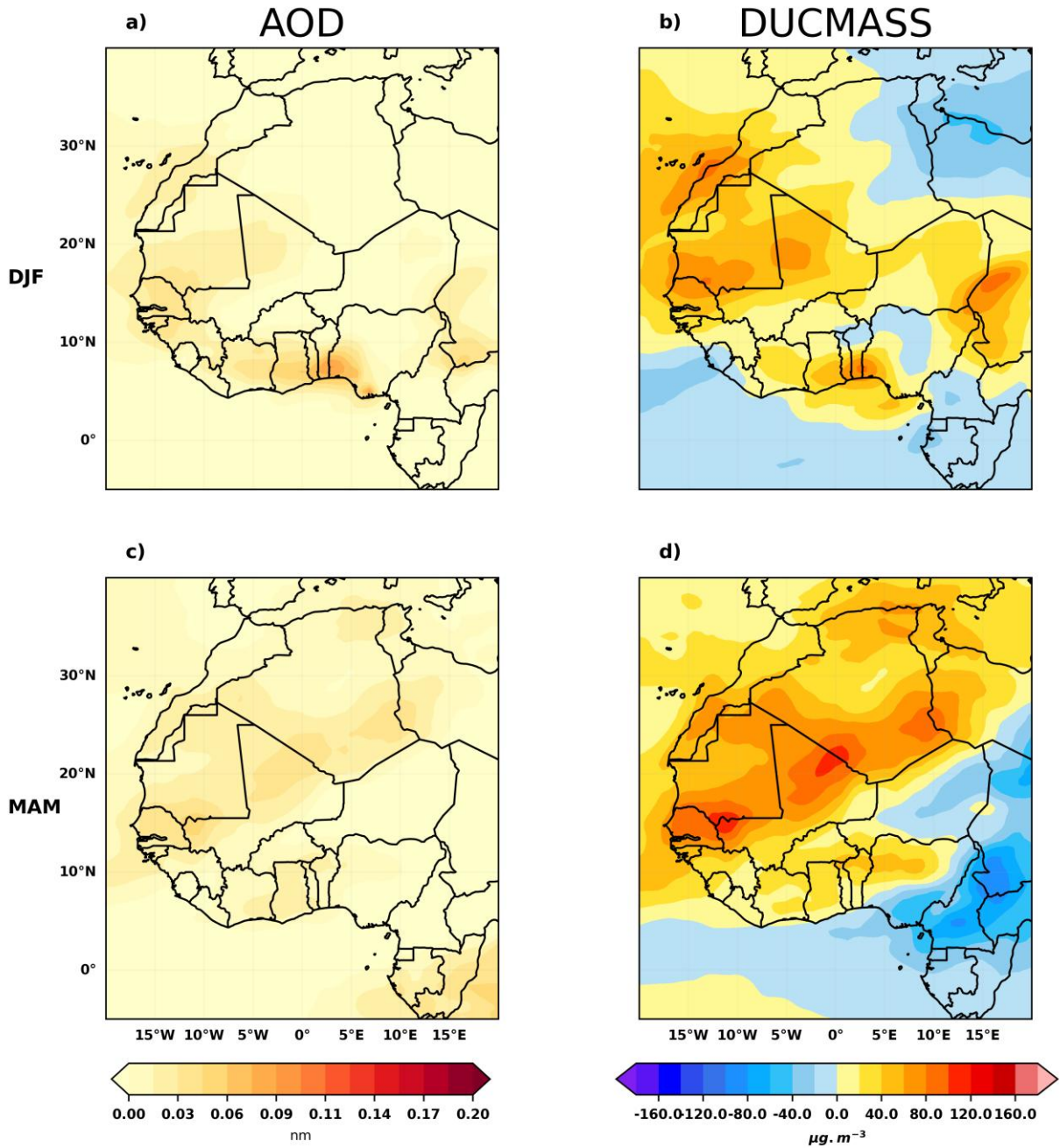


Figure 4.19: Composite of dust (AOD and DUCMASS) in the region (20°W–15°E and 4°N–30°N) during La Niña events from 1980 to 2020.

4.3.8 Influence of the ENSO event on wind and dust variability at regional scale: SAH and GG

Figures (4.20–4.23) show the relationship between equatorial Pacific SST anomalies and wind components that drive dust, including AOD and DUCMASS, during ENSO events between 1980 and 2020, across the DJF and MAM seasons. These are the periods during which dust events were driven to the surface over WA by southward trade winds. In the SAH region during an La Niña event (Figure. 4.21), the DJF season (Figure. 4.21a, c, e, g) is shown to be the period during which SST significantly influences wind behavior, particularly with regard to the zonal component (Figure. 4.21a, $R^2 = 0.82$) and is associated with high DUCMASS concentration ($R^2 = 0.51$). In contrast, during the MAM season (Figure. 4.21b, d, f, h), the relationship was mostly supported by the zonal component (Figure. 4.21d, $R^2 = 0.65$), which is associated with low dust concentrations. During ENSO events (Figure. 4.20), the moderate interaction between equatorial Pacific SST and the zonal wind during the DJF season (Figure. 4.20c, $R^2 = 0.48$) leads to a high concentration of AOD over the SAH region during the MAM season (Figure. 4.20f, $R^2 = 0.64$).

Regarding, the Figure 4.23, during La Niña event, SST anomalies in the ENSO region seem to monitor wind fluctuations and dust concentrations over the GG region during the DJF season (Figure. 4.23a, c, e, g). Through significant interactions dominated by zonal winds (Figure. 4.23a, $R^2 = 0.68$) and meridional winds (Figure. 4.23c, $R^2 = 0.56$), high dust concentrations, particularly DUCMASS (Figure. 4.23g, $R^2 = 0.67$), are observed. In the MAM season (Figure. 4.23b, d, f, h), the zonal wind (Figure. 4.23b, $R^2 = 0.49$) remains the main driver of DUCMASS

concentration, albeit with a moderate decrease (Figure. 4.23h, $R^2 = 0.36$) compared to the DJF season.

Similarly to the results obtained in the SAH during ENSO events (Figure. 4.22), a moderate interaction between the SST in the equatorial Pacific and the zonal wind during the DJF season (Figure. 4.22c, $R^2 = 0.39$) leads to a high concentration of AOD over the SAH during the MAM season (Figure. 4.22f, $R^2 = 0.44$).

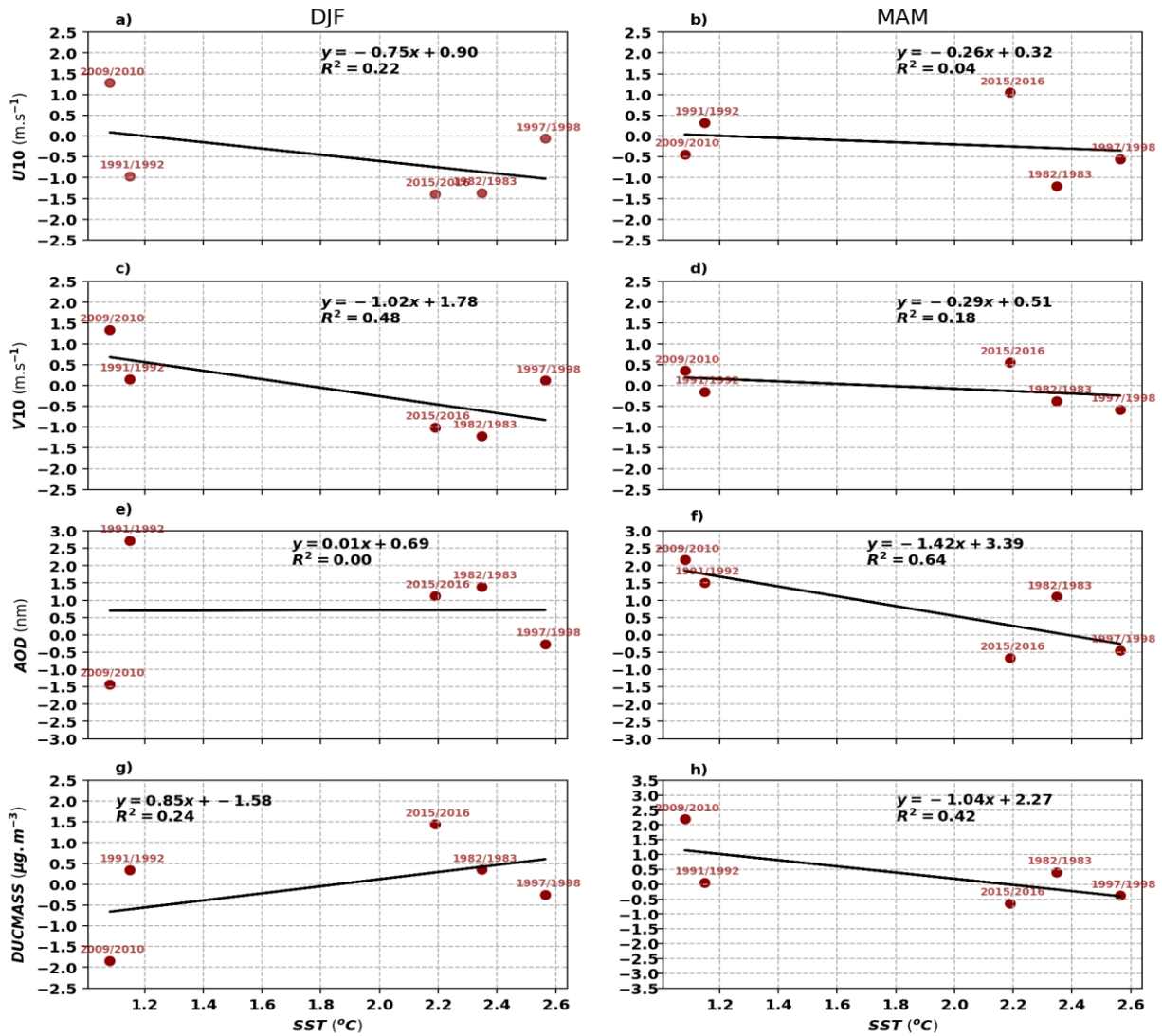


Figure 4.20: Composite of the SST anomalies in the Nino3.4 region (5°N–5°S, 120°W–170°W), the zonal wind (U10: a–b), the meridional wind (V10: c–d), and dust indices such as AOD (e–f) and DUCMASS (g–h), all averaged over the SAH region (12.22°W–16.04°E and 4.27°N–25.02°N) across the DJF (a, c, e, g) and MAM (b, d, f, h) seasons during the Nino events.

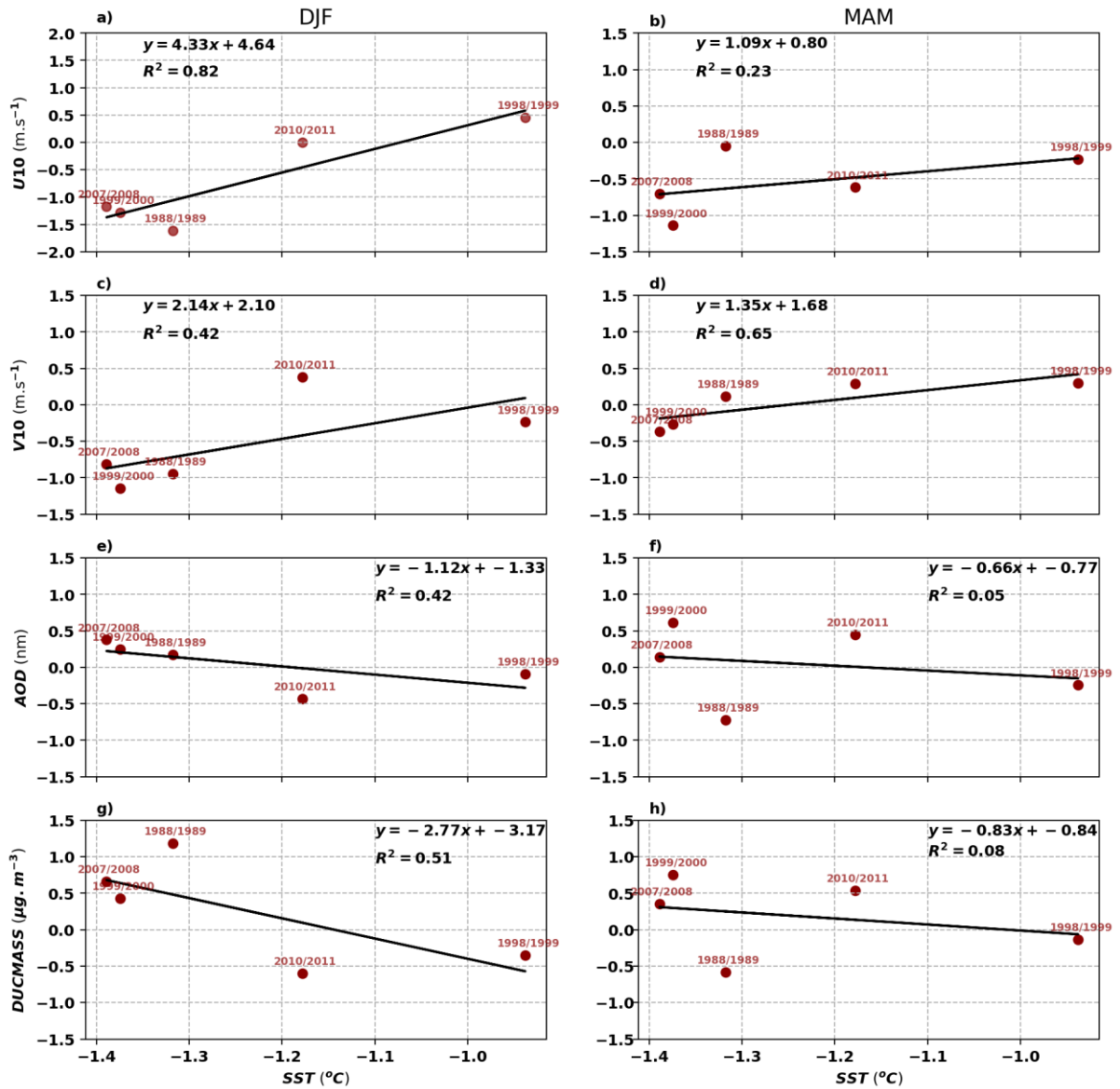


Figure 4.21: Composite of the SST anomalies in the Niño3.4 region (5°N–5°S, 120°W–170°W), zonal wind (U10: a–b), meridional wind (V10: c–d), and dust indices such as AOD (e–f) and DUCMASS (g–h), all of which are averaged over the SAH region (12.22°W–16.04°E and 4.27°N–25.02°N) across the DJF (a, c, e, g) and MAM (b, d, f, h) seasons during the Niña events.

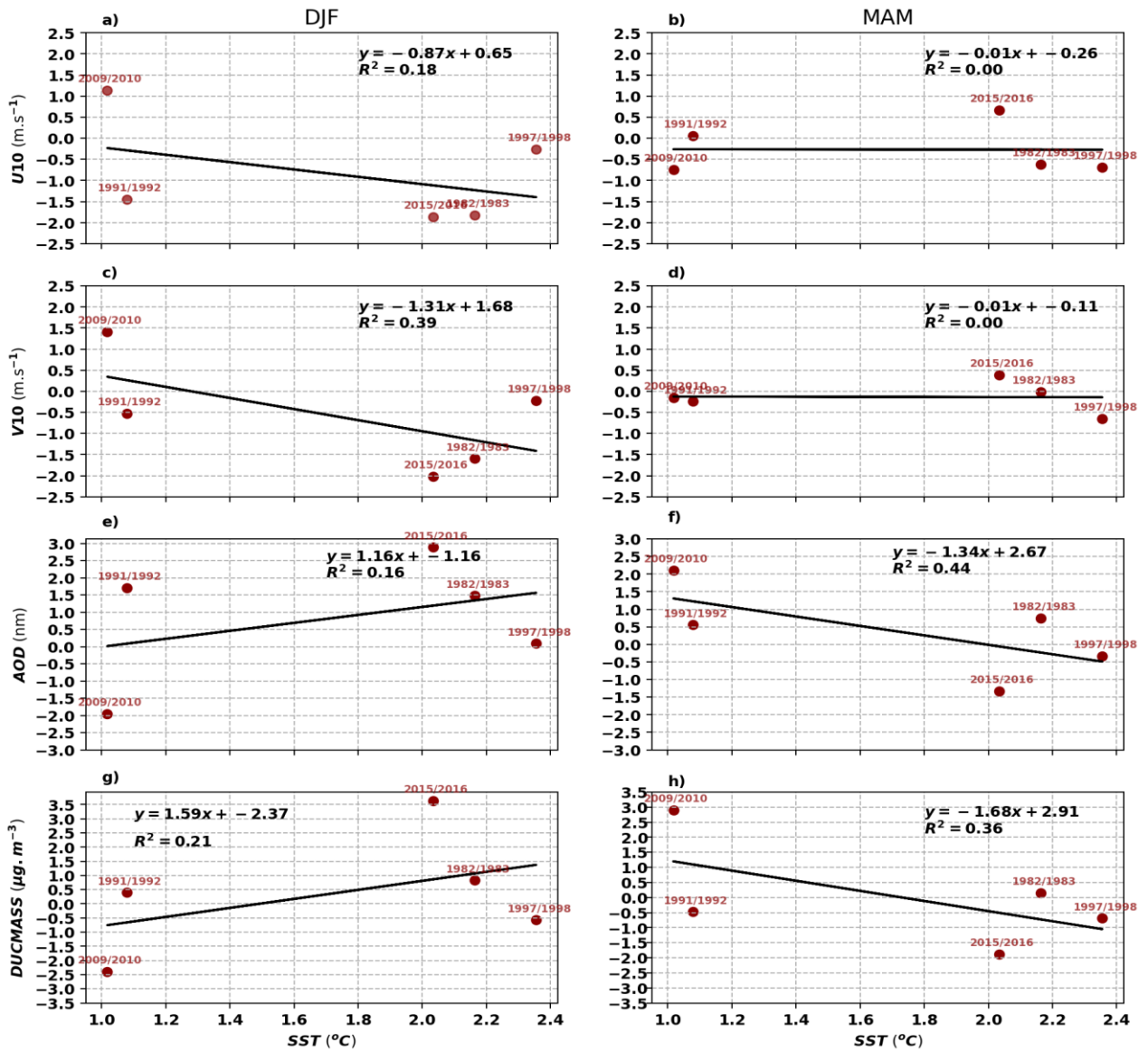


Figure 4.22: Composite of the SST anomalies in the Nino3.4 region (5°N–5°S, 120°W–170°W), zonal wind (U10: a–b), meridional wind (V10: c–d), and dust indices such as AOD (e–f) and DUCMASS (g–h), all of which are averaged over the GG region (8.55°W – 3.88°E and 4.35°N – 12.40°N) across the DJF (a, c, e, g) and MAM (b, d, f, h) seasons during the Nino events.

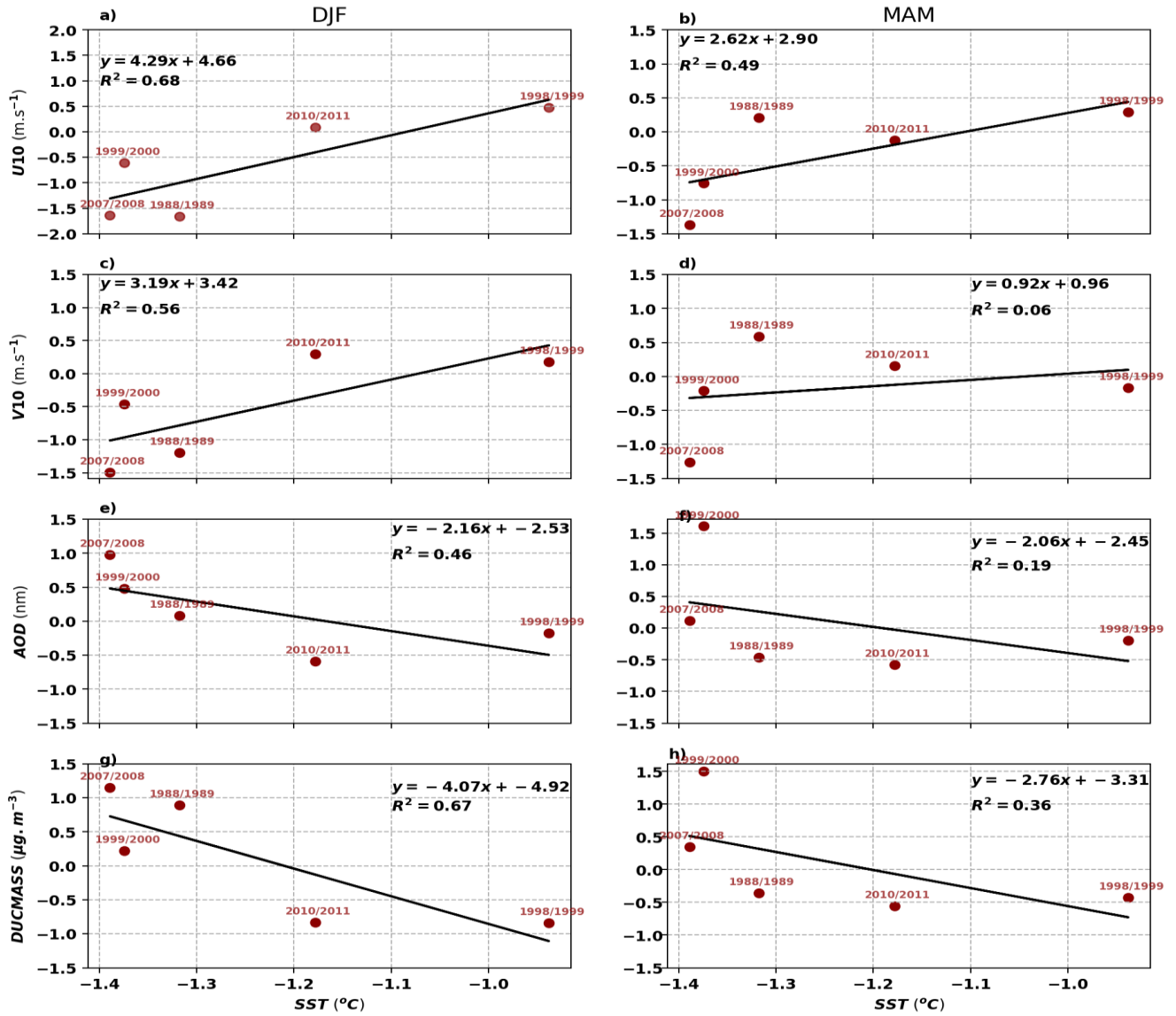


Figure 4.23: Composite of the SST anomalies in the Nino3.4 region (5°N–5°S, 120°W–170°W), zonal wind (U10: a–b), meridional wind (V10: c–d), and dust indices such as AOD (e–f) and DUCMASS (g–h), all of which are averaged over the GG region (8.55 °W - 3.88°E and 4.35°N – 12.40°N) across the DJF (a, c, e, g) and MAM (b, d, f, h) seasons during the Nina events.

4.3.9 Seasonal fluctuation of SST in the ENSO region, winds and Sharan dust over SAH and GG

Figure 4.24 illustrates the normalised anomalies of the SST in the Niño 3.4 region (5°N – 5°S , 120°W – 170°W), zonal wind (zwind), meridional wind (mwind), aerosol optical depth (AOD) and dust mass concentration (DUCMASS) during El Niño (a–b) and La Niña (c–d) events across the SAH and GG.24b), averaged respectively over the regions 12.22°W – 16.04°E , 4.27°N – 25.02°N , and 8.55°W – 3.88°E , 4.35°N – 12.40°N , during the winter (DJF) and spring (MAM) seasons.

During El Niño years (Figure. 4.24a–b), SST anomalies are strongly positive across all seasons in both regions, reflecting the warm SST anomalies typical of ENSO events. Wind anomalies (zonal and meridional winds) during El Niño events in both regions in the DJF season are predominantly negative, suggesting strong Harmattan trade winds that increase dust mobilisation across the SAH regions towards the GG and around the equator. However, wind anomalies remain negative during MAM in both regions, while dust concentrations increase/decrease in the SAH and GG.

In contrast, during La Niña years (Figure. 4.24c–d), SST anomalies are consistently negative across all seasons in both regions, reflecting the cool SST anomalies typical of ENSO events. DUCMASS dominates during La Niña events in the GG during DJF, while decreasing in MAM. The opposite is observed regarding AOD variability, which dominates during El Niño events in the SAH region, where patterns and concentrations also increase.

Overall, the analysis reveals that El Niño years are associated with warmer SSTs and generally stronger Harmattan winds, which increase dust concentration to a maximum in winter over the GG, persisting over the SAH with a maximum in MAM. Conversely, La Niña conditions tend to

favour stronger winds and enhanced dust transport, particularly in spring, which is consistent with the known impacts of ENSO on the climate dynamics of West Africa.

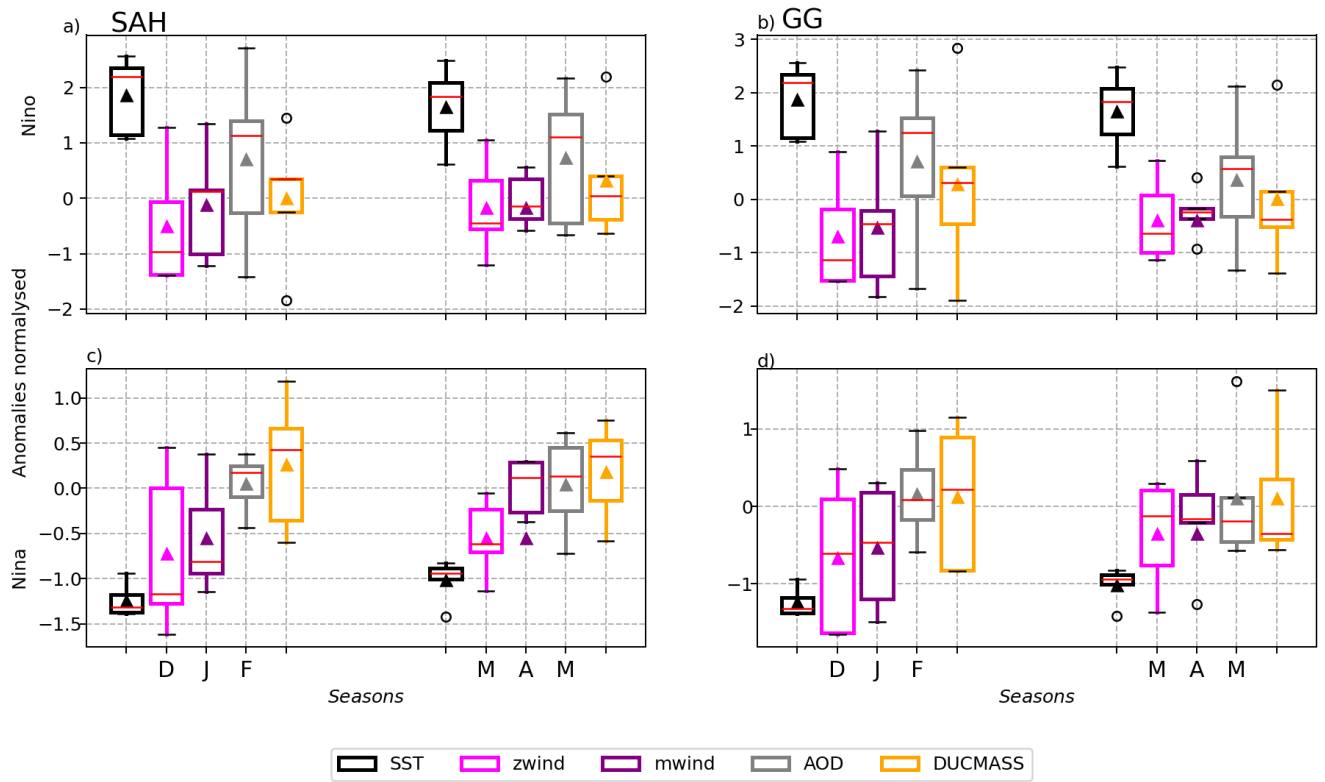


Figure 4.24: This boxplot shows the distribution of anomalies in sea surface temperature (SST), zonal wind (zwind), meridional wind (mwind), aerosol optical depth (AOD) and dust sixmass concentration (DUCMASS) during El Niño (a and b) and La Niña (c and d) years, across the SAH and GG regions for winter (DJF) and spring (MAM).

Summary

This study examined the intricate relationships between El Niño–Southern Oscillation (ENSO) anomalies, Saharan dust variability, and the incidence of bacterial meningitis in two regions of the African meningitis belt: the Sahel (SAH) and the Gulf of Guinea (GG). First, an EOF analysis was conducted to examine the variability of aerosol optical depth (AOD) during the dry season, taking into account the December–February (DJF), January–March (JFM), February–April (FMA) and March–May (MAM) seasons. JFM (70.8%) and MAM (70.5%) were identified as the main modes of variability. A Spearman correlation analysis then revealed that PC1 of AOD in DJF exhibited the strongest association with meningitis in GG ($r = 0.45$; p -value = 0.08) compared to other seasons. Meanwhile, PCs1 and PCs2 during the FMA season revealed a stronger significant relationship with meningitis in the SAH region during the FMA and MAM seasons. However, PC1 in MAM showed the highest correlation with SAH meningitis ($r = 0.85$; p -value = 0.02). Lastly, regression map analysis showed that warm (cool) sea surface temperature (SST) in the equatorial Pacific, often associated with El Niño (La Niña), seems to be the main precursor for aerosol optical depth (AOD) activities over North Africa through deep convection across areas of low (high) pressure, intensifying/weakening the Hadley and Walker cells. In addition to regression maps results, the composite analysis reveals that El Niño years are associated with warmer SSTs and generally stronger Harmattan winds, which increase dust concentration to a maximum in winter over the GG, persisting over the SAH with a maximum in MAM. However, La Niña conditions tend to favour stronger winds and enhanced dust transport, particularly in spring, which is consistent with the known impacts of ENSO on the climate dynamics of West Africa.

A lagged regression was associated with meningitis anomalies in the SAH during FMA and MAM, and in the GG during the JFM season. In the GG (Figure 4.12; lagging by around two months from JFM to NDJ), warm SST anomalies in the equatorial Pacific, indicative of El Niño conditions, precede elevated aerosol concentrations and meningitis cases in the GG. This sequence begins with low sea-level pressure over the tropical Pacific, evolving into a high-pressure anomaly over North Africa. This is accompanied by intensified northeasterly winds that promote the mobilization and transport of Saharan dust towards the Gulf of Guinea and the Sahel. Conversely, in the FMA and MAM seasons, regression patterns linked to Sahelian meningitis incidence (see Figure 4.13 and 4.14) are associated with cool SST anomalies in the equatorial Pacific indicative of La Niña conditions (see Figure 4.13: from lag 0 to lag -3 [FMA-NDJ] and Figure 4.14: from lag 0 to lag -4 [MAM-NDJ]). This is associated with low pressure around the equator and over West African coastal regions. Consequently, stronger variability in dust concentrations is observed in this region and at high altitudes. This suggests a strong environmental linkage between ENSO, climate, dust variability and meningitis outbreaks and incidence in WA by identifying early climatic signals likely to precede dust episodes and meningitis outbreaks. This information is essential for developing early warning systems and implementing targeted prevention strategies.

4.4 Application of AI models

4.4.1 Inter-annual and Seasonal cycle of meningitis

Figure 4.25 illustrates the variability of meningitis incidence in the Sahelian countries of Burkina Faso, Mali, Niger and Nigeria. The left panel (Figure. 4.25a) shows the patterns from

2006 to 2020, and the right panel (Figure. 4.25b) shows the seasonal cycle of the disease based on weekly data from January to June. Each country is represented by a different colour.

Regarding inter-annual variability (Figure. 4.25a), reported meningitis cases from 2006 to 2020 show a declining trend beginning in 2010, which coincided with the introduction of the MenAfriVac vaccine. Nigeria recorded the highest incidence, with over 40,000 cumulative cases in 2009, followed by Burkina Faso with 25,000 cumulative cases in 2007. Mali exhibited relatively regular periodicity in disease occurrence, whereas Niger reported over 7,500 cases in both 2009 and 2015. After 2010, a clear shift in the disease pattern emerges, with a significant reduction in reported cases attributed to vaccination efforts.

At the seasonal scale (Figure. 4.25b), Niger and Nigeria display a delayed disease onset, starting in the second week of February, whereas in Mali and Burkina Faso, the onset occurs before January. The highest disease burden was observed between March and April, with most cases recorded between the second and fourth weeks of February and May. Compared to the other countries, Mali shows a longer meningitis season. Epidemic peaks were recorded in weeks 4 and 5 of March, weeks 1 and 3 of April, and week 3 of May in Niger, indicating a prolonged and intensified outbreak in that country.

In summary, the temporal dynamics of meningitis in these countries show notable changes before and after 2010 in terms of both annual trends and seasonal timing, with the overall burden decreasing significantly in the post-vaccination era.

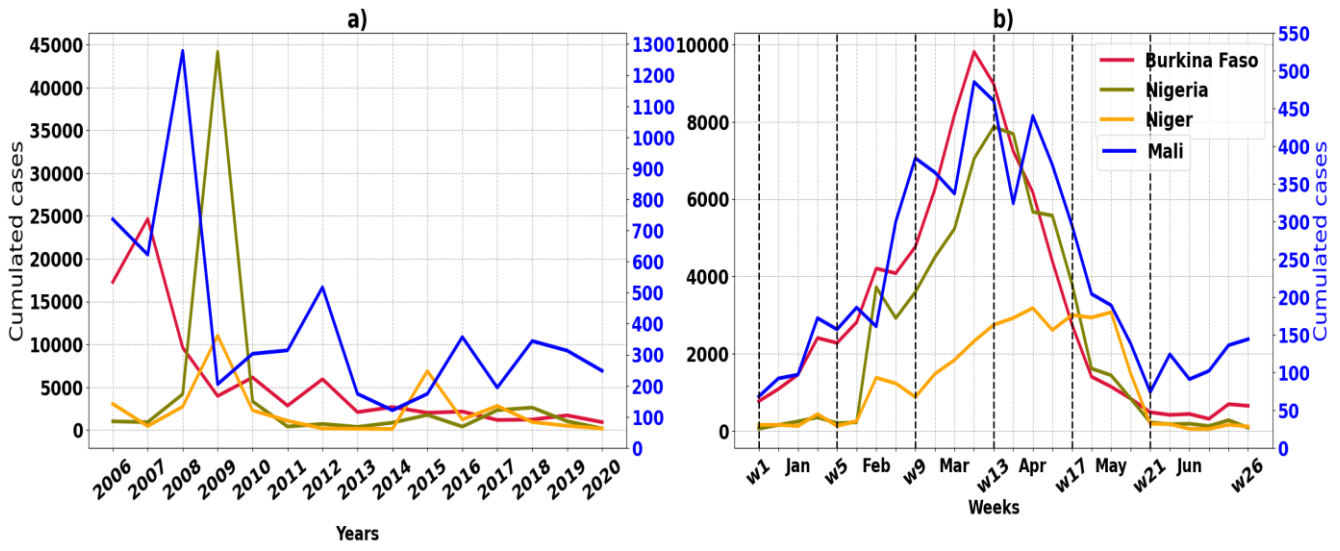


Figure 4.25: Variability in meningitis incidence across Sahelian countries: Burkina Faso, Mali, Niger and Nigeria.

4.4.2 Environmental precursors of meningitis

Due to the complexity of the relationships between environmental variables and meningitis prevalence, a Spearman correlation analysis was conducted to evaluate the associations among the explanatory variables, as well as between these variables and meningitis incidence (the dependent variable). The results indicate that zonal wind is highly correlated with both meridional wind and relative humidity (RH) across all countries. This justifies the use of regularization models to address multicollinearity issues.

In Burkina Faso (Figure. 4.26a), all environmental variables, including temperature, RH and aerosols (AOD and PM10), which are influenced by the Harmattan trade winds, were significantly correlated with meningitis incidence. Temperature also showed a weak but notable correlation with the disease in Mali (Figure. 4.26d). In Niger (Figure. 4.26c), all environmental variables except temperature exhibited a significant relationship with meningitis incidence. In Nigeria and Mali (Figure. 4.26b & d), the correlation between the disease and the zonal wind was relatively weak.

In conclusion, the Spearman correlation results suggest that the climatic drivers of meningitis vary by country. This indicates that country-specific environmental conditions play a key role in influencing the occurrence and prevalence of the disease.

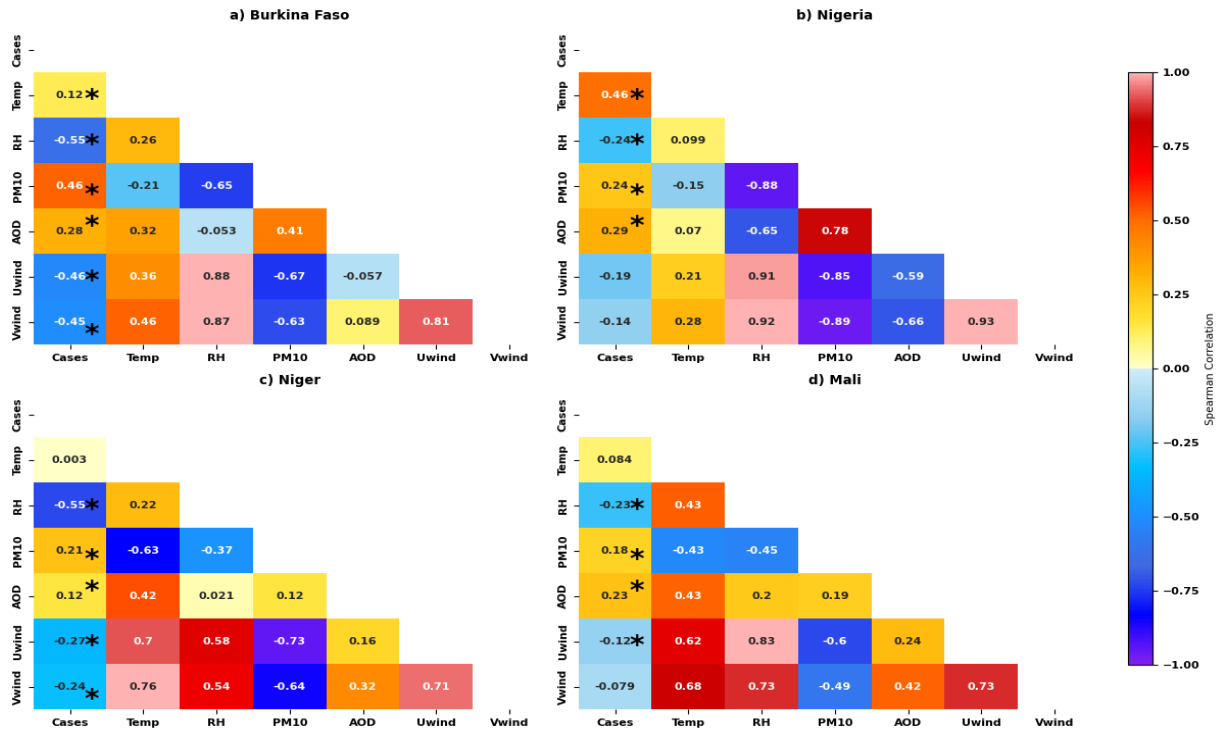


Figure 4.26: Spearman's rank correlation coefficients between the normalised anomalies of environmental variables and meningitis cases in Burkina Faso (a), Nigeria (b), Niger (c) and Mali (d). A star (*) indicates statistical significance at the 95% confidence level based on a t-test.

4.4.3 Relationships between Observed and predicted meningitis

Regarding Burkina Faso (Figure. 4.27a), CatBoost, Random Forest and linear regression show that the observed and predicted patterns are closely similar in terms of timing and magnitude. In Nigeria (Figure. 4.27b), ensemble models, particularly XGBoost and CatBoost, performed better than the other models, but failed to reproduce the amplitude of the outbreaks. Regularisation models, however, are very weak at representing disease patterns in Nigeria and Niger (Figure. 4.28.c), where ensemble models perform better, particularly Random Forest, Gradient Boosting and CatBoost, especially with regard to timing and intensity. Unlike in other countries, the regularisation model and Random Forest capture general trends, but tend to lag behind and underestimate outbreak intensity in Mali (Figure. 4.28.d).

Overall, linear models fail to capture the rapid transitions in Niger and Nigeria, highlighting the non-linearity of the relationship between meningitis and environmental variables. In Mali, however, this relationship appears to be linear in terms of outbreak dynamics.

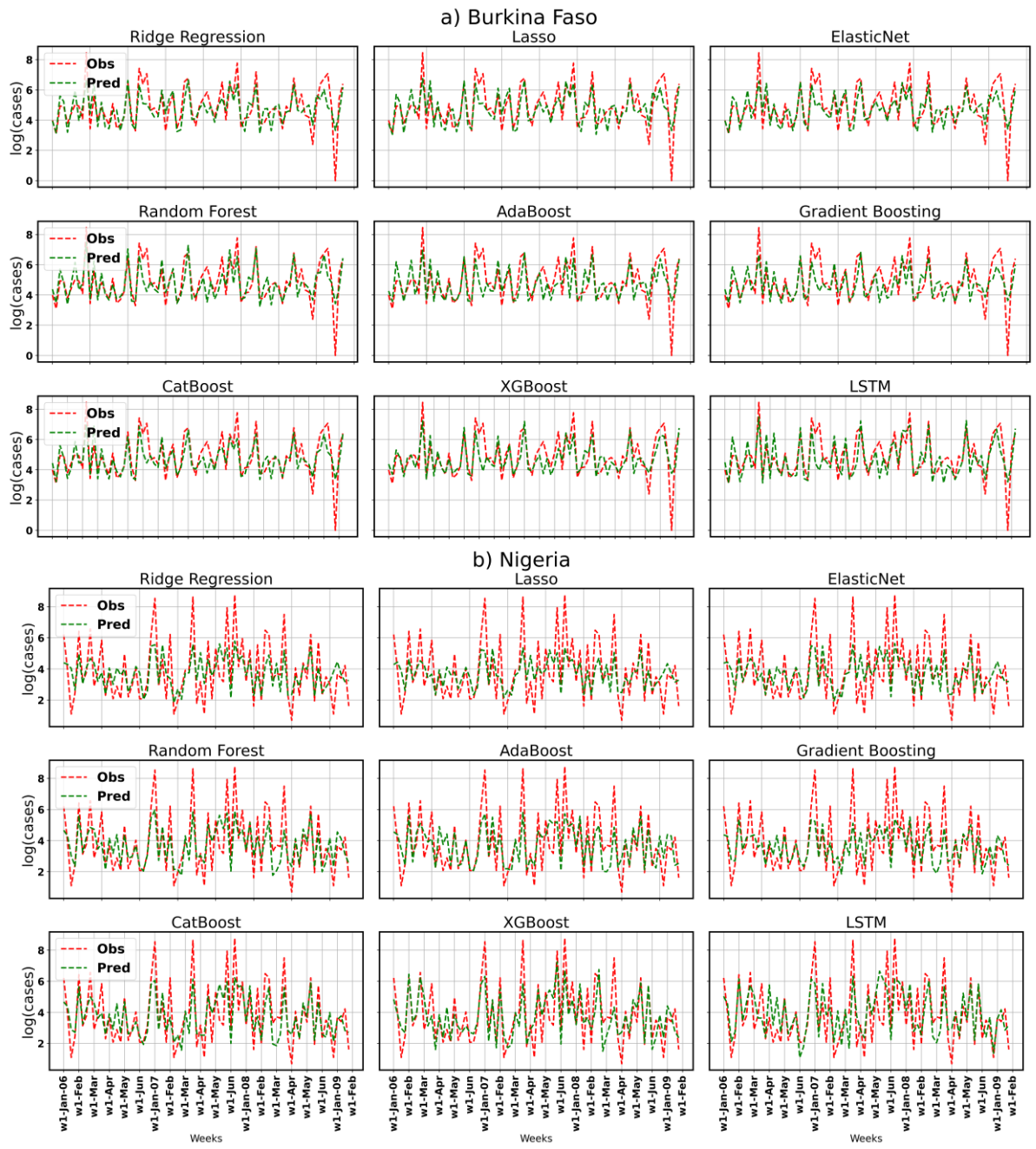


Figure 4.27: Comparison between the recorded and predicted meningitis prevalence in Burkina Faso (a) and Nigeria (b).

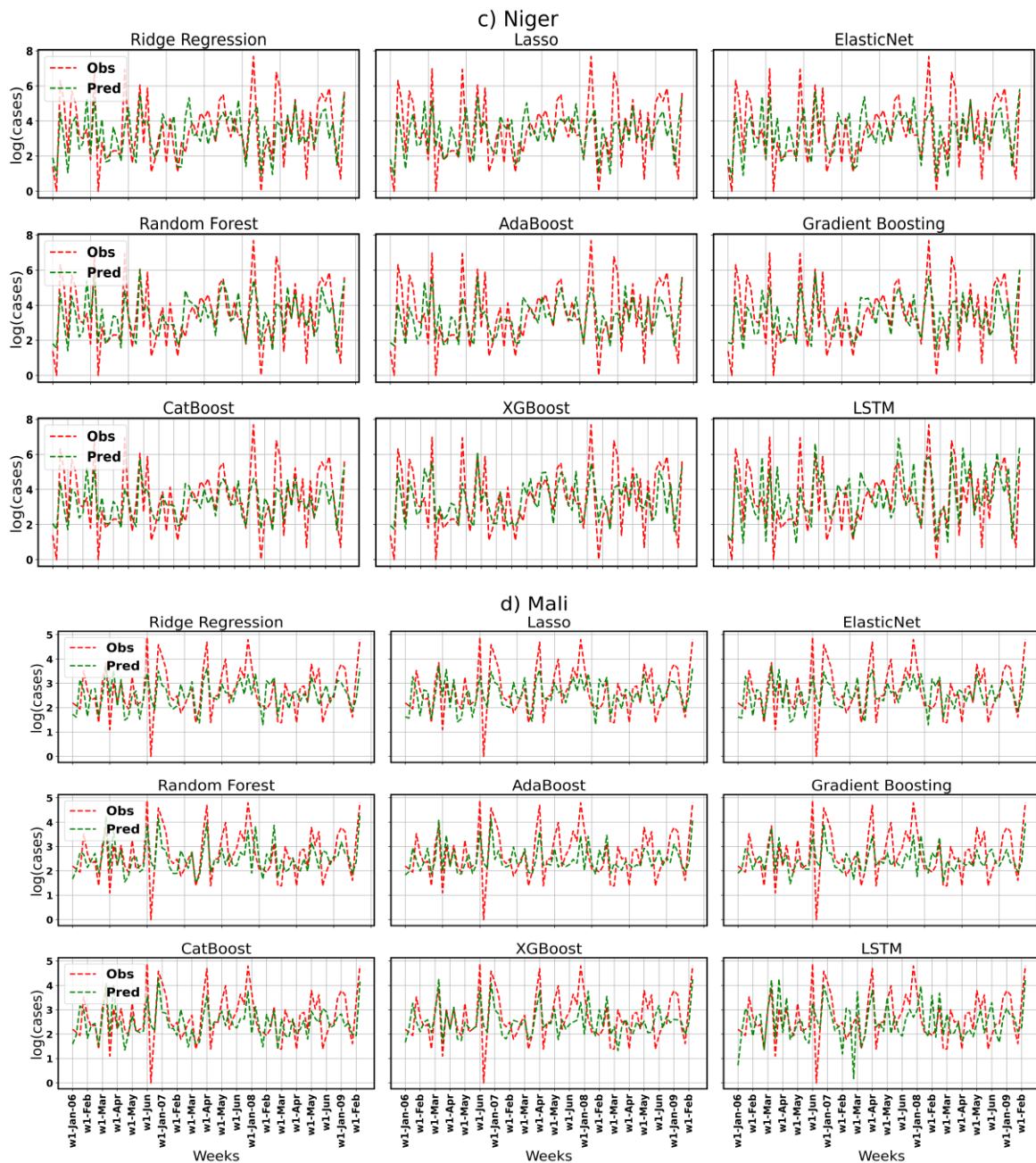


Figure 4.28: Comparison between the recorded and predicted meningitis prevalence in Niger (c) and Mali (d).

4.4.4 Performance of Machine Learning models

Figures (4.29, 4.30) show that the performance of the three types of models used in this study such as Regularization models, Ensemble learning models and deep learning (Long Short-Term Memory Networks; LSTMs) varies by country. The XGBoost model is shown to be the best in Nigeria (Figure. 4.29b), with an R^2 value of 0.638, while the CatBoost model is the best in Burkina Faso (Figure. 4.29a), with an R^2 value of 0.619. Figures (4.30c & 4.30d) and d illustrate that the Random Forest model performs better than the others in Niger and Mali, with R^2 values of 0.505 and 0.367 respectively. Furthermore, Mali shows the weakest performance of all the countries and models. Furthermore, ensemble learning models, except Random Forest, perform worse than regularization models in Mali.

It should be noted that machine learning models, particularly ensemble tree-based methods and regularized linear models, demonstrate strong predictive capability for meningitis incidence in certain regions, where model performance varies substantially across countries. This is likely due to differences in data quality, reporting practices and underlying epidemiological and environmental factors.

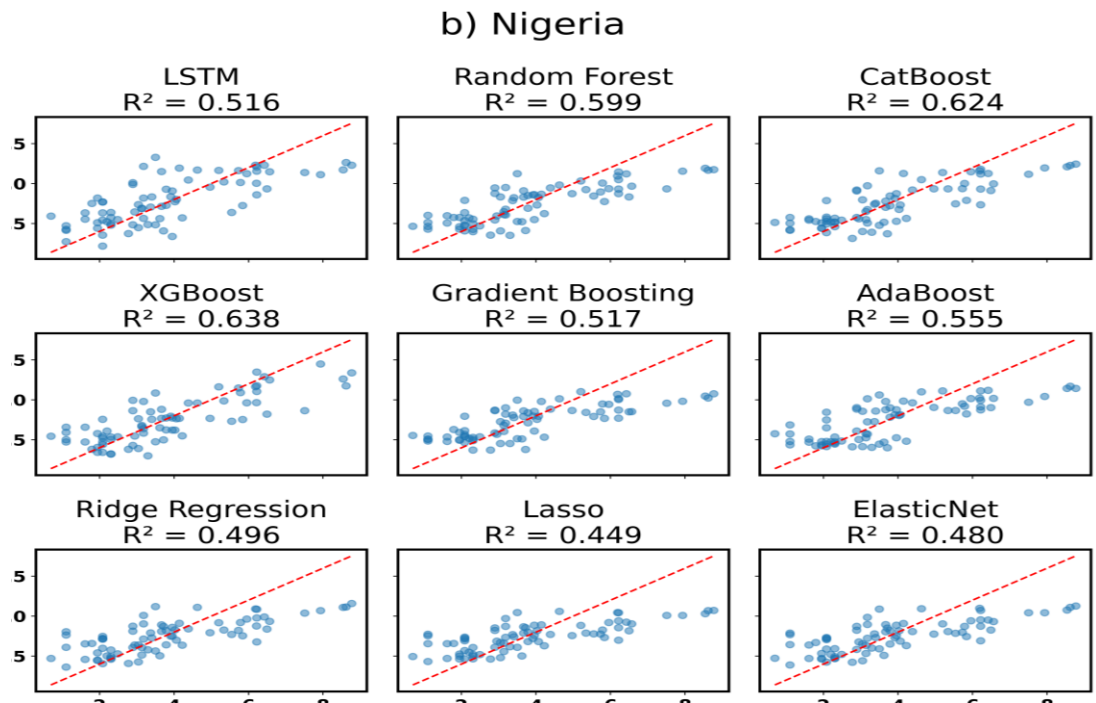
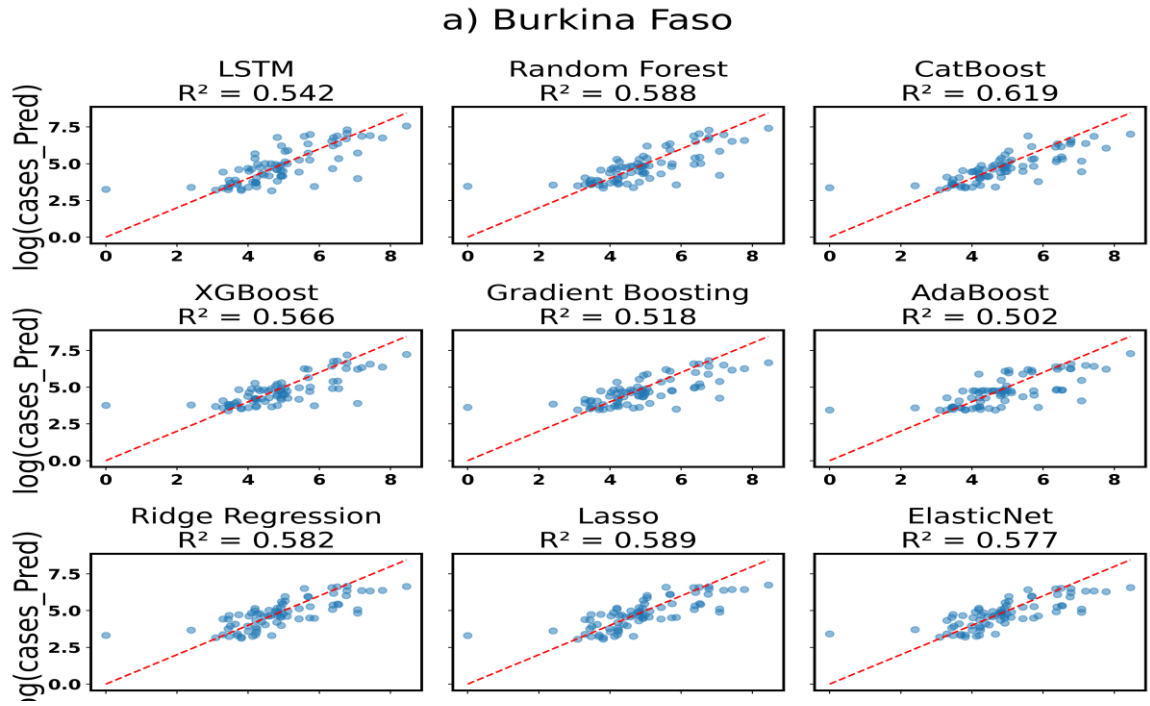


Figure 4.29: The potential of ML models evaluated and compared in terms of prediction and performance in Burkina (a) and Nigeria (b).

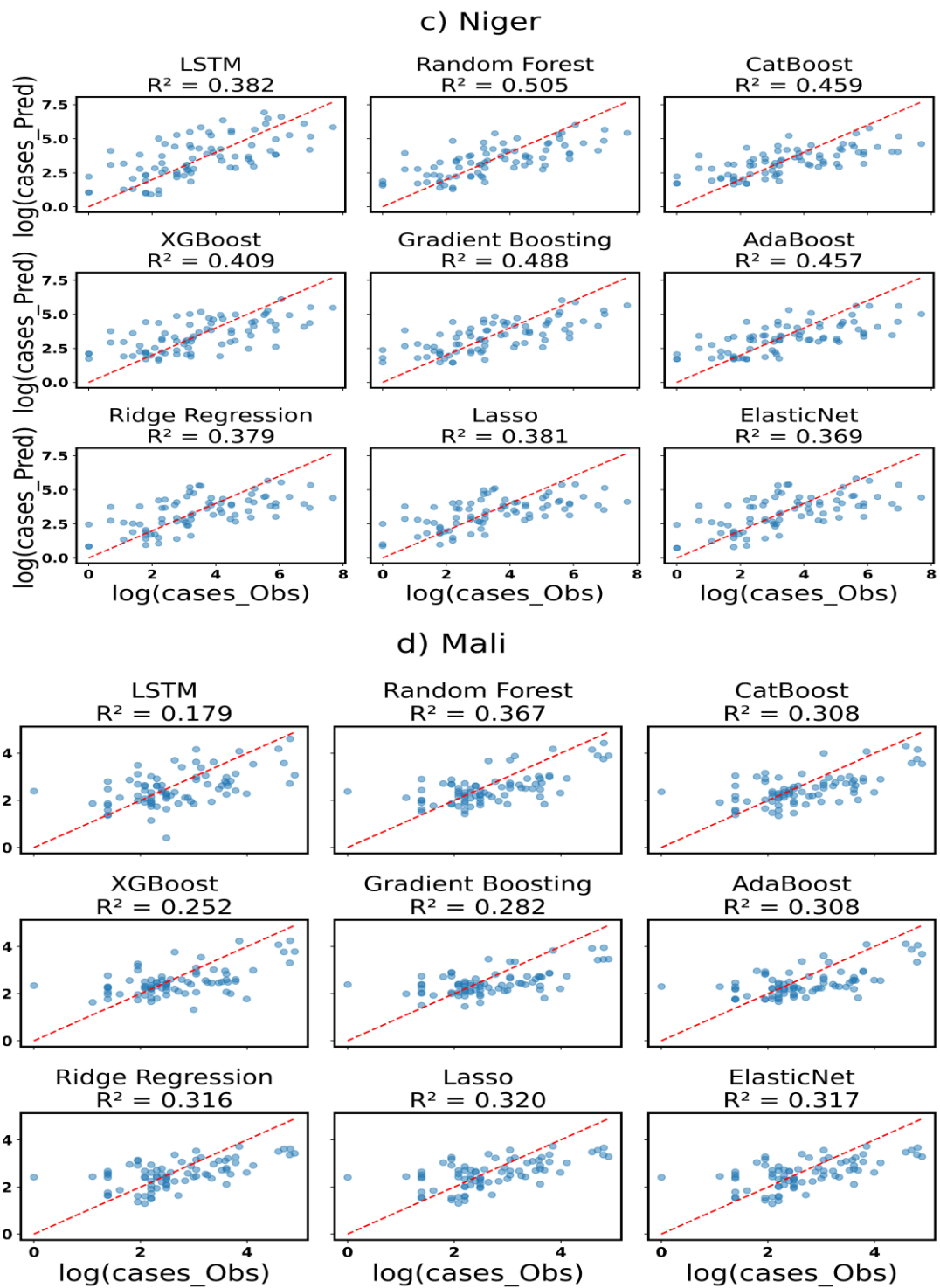


Figure 4.30: The potential of ML models evaluated and compared in terms of prediction and performance in Niger (c) and Mali (d).

4.4.5 Distributions of observed and predicted meningitis incidences

Figure 4.31 illustrates the comparison between the number of observed and predicted log-transformed weekly meningitis cases for each country and model.

In Burkina Faso (red), CatBoost closely replicated the median and distribution of observed cases, showing strong alignment with the interquartile range. Similarly, XGBoost captured the observed spread well in Nigeria (olive colour), though with slightly lower central tendency. In Niger (orange), Gradient Boosting followed the overall pattern, but tended to underestimate median values slightly. Random Forest showed the weakest alignment in Mali (blue), with both median and mean predictions falling below observed values and limited capture of peak extremes.

Overall, the top-performing tree-based ensemble models successfully mirrored temporal distributions, demonstrating their effectiveness in modeling complex nonlinear relationships. However, slight underestimations during outbreak peaks, particularly in Mali and Niger, highlight the ongoing challenge of modeling extreme events.

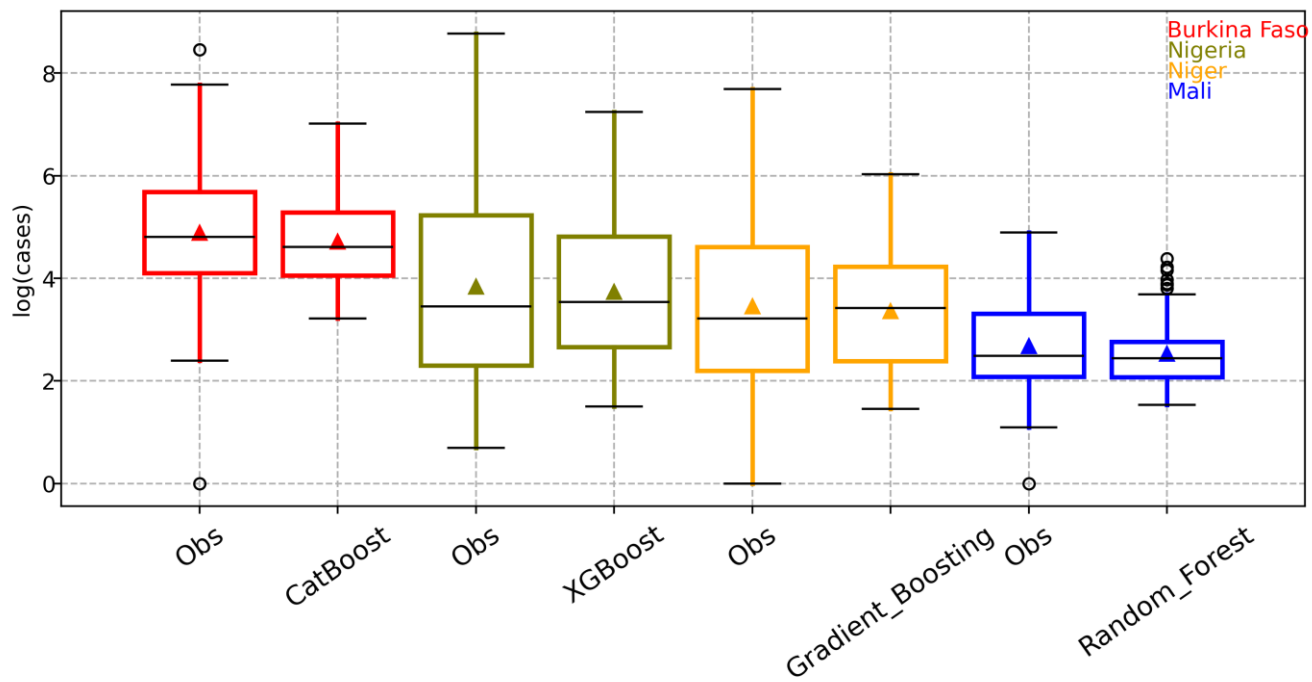


Figure 4.31: The boxplots of the observed and predicted meningitis incidence in (a) Burkina Faso, (b) Nigeria, (c) Niger and (d) Mali.

4.4.6 Model Shapley Additive exPlanations (SHAP) Value Interpretability Analysis

Figure 4.32 illustrates the influence of vaccination status and environmental variables on model performance. It shows that, in all regions, vaccination is the most effective predictor of reduced meningitis risk, particularly at two- and four-week moving averages. Meanwhile, environmental variables with lags of 2 and 4 weeks are shown to contribute significantly to model predictions.

Vaccination has a negative impact on the model output, meaning higher vaccination coverage is associated with lower predicted case numbers. Nigeria and Niger (Figure. 4.32b & c) show negative values for relative humidity (RH). This suggests that drier conditions during the Harmattan season facilitate increased disease transmission. Zonal winds bringing PM10 and AOD were associated with elevated values in most models, particularly in Mali (Figure. 4.32d), Burkina Faso (Figure. 4.32a) and Nigeria. These winds were positively associated with meningitis incidence with a lag of four weeks. This further emphasizes the significant impact of particulate matter on the seasonal cycle of meningitis. Temperature showed a more nuanced effect.

In summary, these findings highlight that:

- A vaccination campaign against meningitis, in order to reduce the disease burden across the African meningitis belt, is effectively supported by this result.

Strong winds support the formation of aerosols, which, at high concentrations, can carry pathogens or increase community susceptibility by damaging the respiratory tract and exacerbating mucosal irritation, thereby making communities more susceptible to bacterial meningitis.

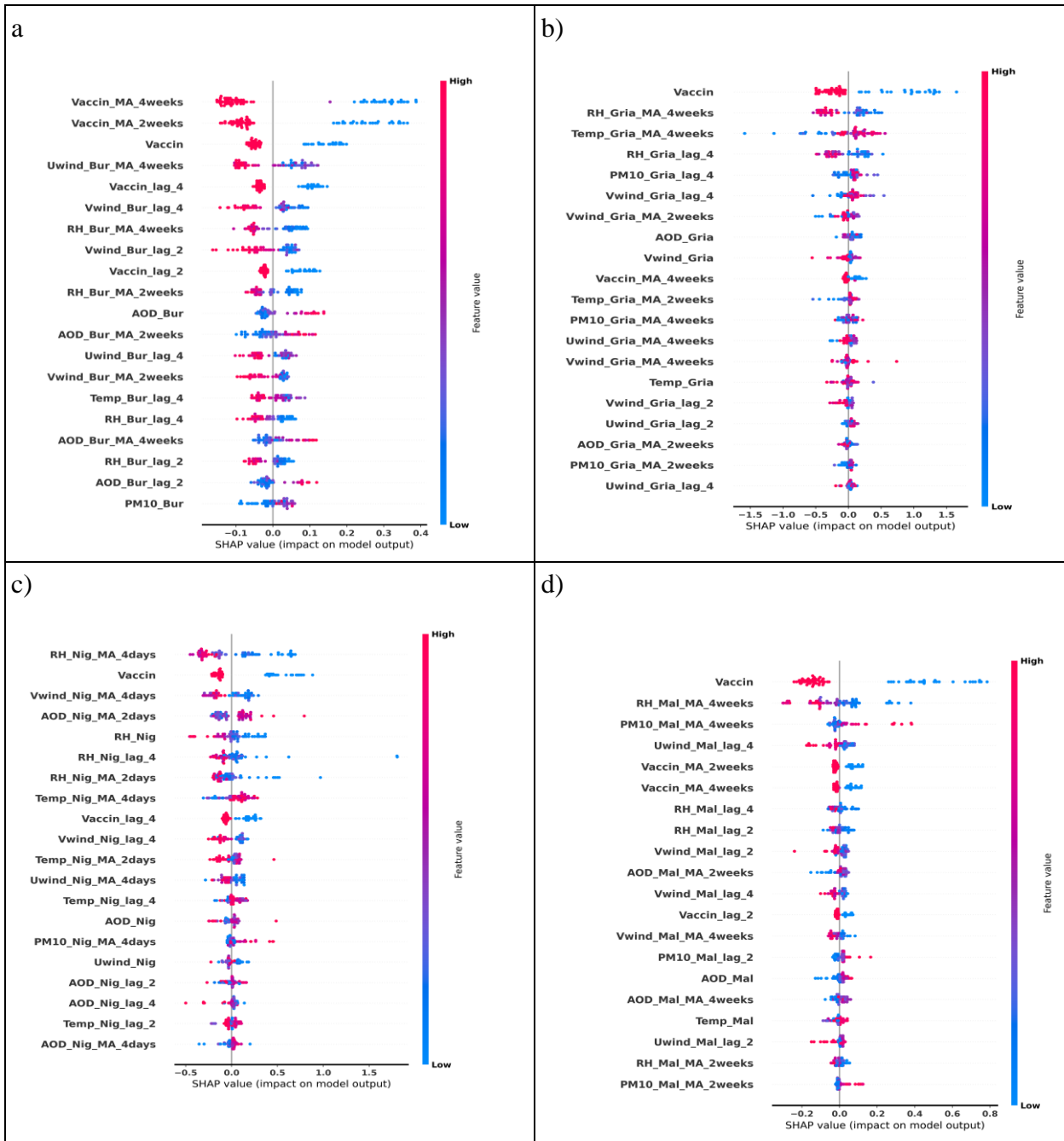


Figure 4.32: The summary plots of the high-ranked SHAP (Shapley) of feature importance for each variable in: (a) Burkina Faso, (b) Nigeria, (c) Niger, (d) Mali.

Summary

This study shows that tree-based ensemble models provide reliable baseline predictions of meningitis incidence, especially in Niger and Nigeria, whereas regularization models tend to underestimate variability, except in Mali and Burkina Faso. The performance of the LSTM model was weak across all countries. However, models do not capture extreme values and outbreak peaks well, indicating a limitation in forecasting severe epidemic events.

SHAP analysis enabled us to interpret the influence of environmental variables; model performance varied by country, likely reflecting differences in climatic signal strength, data quality and reporting systems.

Despite these differences, the performance gap between boosting algorithms was often small. The same remark applies to regularization models as well. While promising, the LSTM model requires further hyperparameter optimization to enhance its sensitivity to outbreak patterns.

Nevertheless, the models presented here could form the basis of early warning systems in regions prone to meningitis, helping to anticipate seasonal outbreaks and allocate resources proactively. Models that integrate environmental and health data could particularly support targeted vaccination campaigns, risk communication and preparedness planning in high-burden areas such as countries in the African meningitis belt. Therefore, predictive models can be transformed into operational decision-support tools for climate-informed health systems in West Africa.

4.5 Discussion of Results

This study provides a comprehensive assessment of the relationship between climate and meningitis in West Africa by exploring the interactions between ENSO variability, Saharan dust dynamics and bacterial meningitis incidence in two climatically distinct regions: the Sahel

(SAH), a vast and highly vulnerable semi-arid region and the Gulf of Guinea (GG) which is a humid tropical savanna zone. In addition to the difference in climate conditions, these regions has undergone several vaccination campaigns since 2010. Based on that, we first examine the influence of regional environmental condition on meningitis prevalence in both areas at seasonal and interannual scale and weekly time step considering the period 2006-2020. Results show that, between 2006–2009 and 2010–2020 notable changes in meningitis patterns, both in terms of weekly case numbers and the overall magnitude of the disease from onset to ending. Dust episodes in January are identified as triggers for the meningitis season, a finding consistent with Martiny & Chiapello (2013) and Sultan et al. (2005), who demonstrated that dust plays a key role in the onset of meningitis. High temperatures and low relative humidity, along with peak dust levels in March, are closely associated with epidemic progression. During the post-vaccination period, meningitis peaks occur in March and April, aligning with Deroubaix et al. (21). In the SAH region, the persistence of high temperatures, low relative humidity (<20%), and intensified surface dust concentrations prolongs disease prevalence. Meanwhile, in the GG region, PM10, moderate relative humidity (<45%), and maximum temperatures though generally lower than in SAH are critical factors shaping the meningitis season. The inter-annual variability of environmental variables reveals a dominant mode characterized by northeasterly winds transporting high dust concentrations to the SAH and GG regions, where dry and warm conditions prevail. This mode persists before and after the vaccination period, suggesting a strong link between climatic conditions and meningitis outbreaks.

In summary, surface winds, dust concentrations, and relative humidity serve as key precursors of meningitis outbreaks. Therefore, in this context of climate change, through a large-scale

atmospheric circulation influenced by local and remote climatic forces such as ENSO, ITCZ and NAO, changes in surface winds will directly impact dust activities (emission, transport and deposit) and consequently influence meningitis occurrence in the WAMB.

Based on these possible conditions, this study aimed to investigate the mechanisms linking El Niño–Southern Oscillation (ENSO) anomalies and modes of variability in Saharan dust during dry periods associated with bacterial meningitis in the SAH and GG regions. Countries in the African meningitis belt have different calendars for bacterial meningitis (onset, offset and intensity) and significant differences in atmospheric conditions, which are induced by atmospheric and oceanic teleconnections through various climate indices particularly the effects of ENSO. Atmospheric and oceanic observation and reanalysis datasets, as well as meningitis data, were analysed using statistical methods to improve preparedness for and prevention of infectious diseases, particularly bacterial meningitis, which is highly correlated with Saharan dust.

Typically, two dust seasons (winter and spring) are observed during the dry season in West Africa. Consequently, this study considered the DJF, JFM, FMA and MAM seasons, including the meningitis seasons, in both the SAH and GG regions, to investigate the impact of ENSO events on Saharan dust variability and its influence on bacterial meningitis.

The results reveal that the period of maximum AOD variability in the GG coincides with the meningitis incidence peak in that area during the winter months (December–March) (see Figures 4.7d and 4.8a). Meanwhile, in the SAH, dust concentration variability increases from winter to spring (MAM), peaking in March and April (see Figure. 4.7j and 4.8d). Interestingly, the meningitis season in the SAH also exhibits similar variability. These results are consistent

with those of previous studies (Sultan et al., 2005; Yaka et al., 2008; Martiny & Chiapello, 2013; Diouf et al., 2025), which identified dry, dusty, windy conditions as conducive to meningitis epidemics in the African meningitis belt. For instance, warm (cool) sea surface temperatures (SSTs) in the equatorial Pacific, often associated with El Niño (La Niña), appear to be the primary precursor of AOD activities in North Africa, particularly in the Sahara Desert. This occurs through deep convection across areas of low (high) pressure, which intensifies/weakens the Hadley and Walker cells. These findings are consistent with those of Zhang et al. (2023), who demonstrated that the phase shift in the North Atlantic Oscillation during the late winter ENSO period is primarily caused by the development of the ENSO-associated North Tropical Atlantic (TNA) SST anomaly through enhanced convection in the subtropical Atlantic. SST anomalies (Figure. 4.10: lag-1 and Figure. 4.11: lag-2) show that warming SST in the tropical north Atlantic from January to March (JFM) coincides with cooling SST around the equator and high dust variability over the sub-Saharan region. These results corroborate those of Vallès et al. (2025), who demonstrated that significant SST warming occurs in the TNA adjacent to West Africa, peaking off the coast of Senegal during JFM and spreading southwestward in MAM. This warming occurs alongside equatorial cooling and anomalous southerly winds over the eastern TNA. Furthermore, an El Niño event is associated with a reduction in sea level pressure (SLP) over the tropical Pacific and a reorganization of the global atmospheric circulation. This enhances the northeasterly winds across West Africa (WA) and promotes the southward movement of dust-laden air masses towards the Gulf of Guinea. Additionally, converging winds typically incorporate processes such as dry deep convection, favoring dust emission by enhancing near-surface turbulence. The lagged regression patterns associated with meningitis anomalies in the SAH during the FMA

and MAM seasons and in the GG during the JFM season exhibit striking similarities to the AOD-PC1 regression results. This suggests a strong environmental link between climate variability, dust transport, and meningitis outbreaks.

The composite analysis results are consistent with those obtained through a regression map analysis. It is shown that during El Niño years, both aerosol optical depth (AOD) and dust convective mass (DUCMASS) anomalies show elevated dust concentrations, especially in the GG region during DJF and in the Saharan and Sahelian regions during MAM, coinciding with warm SST anomalies and atmospheric depressions over the Atlantic. Conversely, La Niña events produce opposite SST patterns and are associated with reduced dust levels, although the spatial dust distribution remains similar. Wind components particularly the zonal wind demonstrate strong correlations with SST anomalies, especially during DJF (e.g., $R^2 = 0.82$ for zonal wind in SAH during La Niña), influencing dust concentrations across both DJF and MAM seasons. These interactions are most pronounced in DJF, where SST-driven changes in wind dynamics lead to elevated DUCMASS and AOD levels, especially in the SAH and GG regions.

These results highlight the significant role of the El Niño–Southern Oscillation (ENSO) phenomenon in modulating dust activity and meningitis incidence in areas such as the SAH and GG by enhancing our understanding of the climate drivers of dust variability and the associated mechanisms. Overall, this study reinforces the concept that ENSO plays a predictive role in dust climatology over West Africa and could potentially provide a framework for early warning systems.

This study emphasises the significant impact of local climatic conditions and large-scale phenomena, such as El Niño, on bacterial meningitis (BM) patterns. It reveals how Saharan dust events can trigger epidemics and emphasises the complexity of meningitis dynamics, which are influenced by interrelated climatic, environmental and socio-demographic factors operating at different spatio-temporal scales. The challenge of predicting meningitis outbreaks can only be addressed by integrating multi-source spatialized data, including satellite and model outputs. Traditional statistical models, limited by linear assumptions, are unable to capture these nonlinear interactions. Therefore, the study advocates using advanced methods such as artificial intelligence (AI) to develop more robust and accurate risk assessment models that can forecast the timing, scale and potential pathogens of future outbreaks.

For that, various machine learning models performance were evaluated in predicting weekly cases of meningitis across Burkina Faso, Nigeria, Niger and Mali. The results obtained demonstrate variations in model performance. Ensemble models (Random Forest, XGBoost, AdaBoost and Gradient Boosting) demonstrated greater robustness in all countries except Mali. Advanced Boosting algorithms such as CatBoost and XGBoost demonstrated superior performance ($R^2 > 0.6$) due to their ability to exploit complex interactions between meningitis, environmental variables, and vaccination status. Random Forest models ($R^2 > 0.5$ and $R^2 > 0.3$) and regularization models such as Lasso, Ridge Regression and ElasticNet performed well in Burkina Faso and Mali. However, regularization models performed better in Burkina Faso ($R^2 > 0.5$) than in Mali ($R^2 < 0.33$).

These results are consistent with those of many previous studies that have explored the impact of climate on infectious diseases using artificial intelligence (AI) and machine learning (ML)

approaches. For instance, Wang et al. (2017) conducted a study in Inner Mongolia, China, in which they used an artificial neural network (ANN) model to identify the main environmental drivers of human brucellosis (HB) and predict epidemics of the disease. They found that the enhanced vegetation index was the most influential predictor of HB incidence, followed by land surface temperature and other climate-related variables such as temperature and precipitation. The model's predictions closely matched the reported cases during the learning and validation phases. Farooq et al. (2022) used the XGBoost classifier and explainable AI (XAI) methods to assess the factors behind West Nile virus epidemics in Europe. They found that climatic trends from the previous year, combined with climatic variables from the beginning of the year, accurately predict the transmission season. Similar AI approaches have been used to optimise intervention strategies for malaria (Agrebi et al., 2020; Wilder et al., 2018). Furthermore, in response to the urgent need for predictive tools to forecast Ebola epidemic patterns, researchers such as Colubri et al. (2016) and Agrebi et al. (2020) have employed various models, including artificial neural networks (ANNs), logistic regression, decision trees, and support vector machines (SVMs), to predict epidemic patterns. Our results highlight the value of AI/ML models in capturing the complex relationships between climatic variables and infectious disease dynamics.

CHAPTER FIVE

5. CONCLUSION AND RECOMMENDATIONS

5.1 Summary

This study investigated the complex interactions between large-scale climate variability, Saharan dust dynamics, and bacterial meningitis incidence in West Africa, focusing on two climatically distinct regions the Sahel (SAH) and the Gulf of Guinea (GG). The seasonal and interannual influences of meteorological conditions and particulate matter (PM₁₀, AOD) on meningitis outbreaks were assessed using observational and reanalysis data from 2006–2020. The research showed that January dust events are critical triggers for meningitis onset in both regions. However, persistence and intensity differ by region: in the SAH, extreme dryness (RH < 20%) and high dust concentrations drive longer outbreak durations, while in the GG, PM₁₀ levels, moderate RH (< 45%), and relatively high temperatures shape the season.

Empirical Orthogonal Function (EOF) and regression analyses revealed that ENSO-related sea surface temperature (SST) anomalies modulate atmospheric circulation patterns, influencing dust variability across West Africa. In particular, warm SSTs in the equatorial Pacific (El Niño) intensify dust transport via weakened Hadley and Walker cells, correlating with increased meningitis incidence with lead times of 3–6 weeks. In addition, during El Niño years, both aerosol optical depth (AOD) and dust convective mass (DUCMASS) anomalies show elevated dust concentrations, especially in the GG region during DJF and in the Saharan and Sahelian regions during MAM, coinciding with warm SST anomalies and atmospheric depressions over the Atlantic. Conversely, La Niña events produce opposite SST patterns and are associated with reduced dust levels, although the spatial dust distribution remains similar.

In parallel, tree-based machine learning models (XGBoost, CatBoost, Gradient Boosting) were developed to predict meningitis incidence. These models performed well, particularly in Nigeria and Burkina Faso, and identified vaccination status, humidity, and meridional winds as the most influential predictors. However, all models struggled to capture extreme outbreak peaks, especially in Mali and Niger.

5.2 Conclusion

This study provides a robust, multidisciplinary exploration of the environmental drivers of meningitis outbreaks in West Africa. It integrates climate diagnostics, dust dynamics and advanced machine learning techniques, and considers pre- and post-vaccination periods (2006–2009 and 2010–2020). The results reveal clear temporal and spatial shifts in meningitis patterns that are closely linked to regional atmospheric thresholds, particularly low relative humidity and elevated dust concentrations (PM10 and AOD). More severe outbreaks occur under drier and dustier conditions in the Sahel (RH <20%) and under moderately humid conditions in the Guinea Gulf (RH <45%). Seasonal analyses reveal peak disease incidence during JFM in the Guinea Gulf (GG) and during MAM in the Sahel (SAH), which aligns with periods of heightened AOD variability. Significantly, the study identifies substantial teleconnections between global sea surface temperature (SST) anomalies, particularly those associated with El Niño–Southern Oscillation (ENSO) and Atlantic warming, and dust transport over North Africa. These climatic signals influence the timing and intensity of dust intrusions that coincide with increased meningitis risk by modulating zonal and meridional winds. Moreover, composite analyses reveal that El Niño events intensify dust concentrations across West Africa through altered sea surface temperature (SST)-wind interactions, whereas La Niña events

produce weaker yet more consistent dust patterns. Machine learning models (XGBoost, CatBoost, Random Forest and Gradient Boosting) demonstrated strong predictive capabilities; XGBoost and CatBoost performed best in Nigeria and Burkina Faso, respectively. Key predictors across all models include vaccination status, relative humidity (RH) and wind components, though challenges remain in capturing outbreak extremes. Overall, this study provides valuable insights into the relationship between climate, dust and health, and highlights the importance of integrating climate indicators with epidemiological data to improve early warning systems and support public health adaptation. This will help to achieve the WHO's goal of eliminating meningitis by 2030.

5.3 Recommendations

1. Integrate ENSO monitoring into national and regional health surveillance systems to improve the anticipation of meningitis risk based on climate forecasts.
2. Operationalize machine learning models as part of decision-support tools for public health planning, particularly in high-risk countries within the African meningitis belt.
3. Strengthen intersectoral collaboration among meteorological services, health ministries, and data scientists to co-develop early warning systems.
4. Enhance data infrastructure through improved environmental and health data collection and sharing at finer temporal and spatial scales.
5. Focus vaccination campaigns and preparedness efforts based on climate-informed forecasts and model outputs to protect vulnerable populations more efficiently.

5.4 Contribution to Knowledge

Overall, this study makes a significant contribution to climate-health research by shedding light on the environmental triggers of meningitis outbreaks and providing a predictive framework to inform early warning systems and targeted public health interventions. Demonstrating a clear teleconnection between ENSO and dust activities shows how global climate patterns impact regional disease risk through changes in atmospheric circulation. Meanwhile, integrating climate indicators and vaccination status using a machine learning approach represents a valuable step towards improving disease surveillance and enhancing climate resilience in vulnerable regions. Applying the findings of this study to decision-making processes, medical systems and populations provides a powerful toolset for improving epidemic preparedness and supporting the WHO's "Defeating Meningitis by 2030" goals. This multi-method, interdisciplinary approach deepens our understanding of climate–health interactions significantly and offers a predictive framework for early warning systems that can be adapted to regional characteristics.

5.5 Suggestions for Further Studies

1. Investigate the combined influence of additional climate modes, such as the North Atlantic Oscillation (NAO) and the Madden–Julian Oscillation (MJO), on dust transport and meningitis dynamics.
2. Expand the model's input to include socio-economic and demographic variables such as population density, mobility and access to healthcare.
3. Explore hybrid modelling approaches that combine physical modelling with deep learning (e.g. optimised LSTM models) to improve the detection of outbreak extremes.

4. Improve the spatial resolution and local calibration of models to support region-specific public health responses.

5. Develop user-friendly interfaces for the operational deployment of machine learning models in health agencies and decision-making contexts.

References

- Abdussalam, A. F., Monaghan, A. J., Dukić, V. M., Hayden, M. H., Hopson, T. M., Leckebusch, G. C., & Thornes, J. E. (2014). Climate influences on meningitis incidence in northwest Nigeria. *Weather, Climate, and Society*, 6(1), 62-76. DOI: <https://doi.org/10.1175/WCAS-D-13-00004.1>
- Adebisi, Y. A., Alaran, A., Badmos, A., Bamisaiye, A. O., Emmanuella, N., Etukakpan, A. U., ... & Lucero-Prisno, D. E. (2021). How West African countries prioritize health. *Tropical medicine and health*, 49, 1-7.
- Adedokun, J. A., Emofurieta, W. O., & Adedeji, O. A. (1989). Physical, mineralogical and chemical properties of Harmattan dust at Ile-Ife, Nigeria. *Theoretical and Applied Climatology*, 40, 161-169.
- Aghababaeian, H., Ostadtaghizadeh, A., Ardalani, A., Asgary, A., Akbary, M., Yekaninejad, M. S., & Stephens, C. (2021). Global health impacts of dust storms: a systematic review. *Environmental health insights*, 15, 11786302211018390. DOI: [10.1177/11786302211018390](https://doi.org/10.1177/11786302211018390)
- Agier, L., Deroubaix, A., Martiny, N., Yaka, P., Djibo, A., & Broutin, H. (2013). Seasonality of meningitis in Africa and climate forcing: aerosols stand out. *Journal of the Royal Society Interface*, 10(79), 20120814.
- Agrebi, S., & Larbi, A. (2020). Use of artificial intelligence in infectious diseases. In *Artificial intelligence in precision health* (pp. 415-438). Academic Press. <https://doi.org/10.1016/B978-0-12-817133-2.00018-5>
- Al Shehhi, M. R., Gherboudj, I., & Ghedira, H. (2014). An overview of historical harmful algae blooms outbreaks in the Arabian Seas. *Marine pollution bulletin*, 86(1-2), 314-324. <https://doi.org/10.1016/j.marpolbul.2014.06.048>
- Alile, S. O., & Bello, M. E. (2020). A machine learning approach for diagnosing meningococcal meningitis. *Int. J. Sci. Res. in Computer Science and Engineering*, 8(3).
- Ayanlade, A., Nwayor, I. J., Sergi, C., Ayanlade, O. S., Di Carlo, P., Jeje, O. D., & Jegede, M. O. (2020). Early warning climate indices for malaria and meningitis in tropical ecological zones. *Scientific Reports*, 10(1), 14303. <https://doi.org/10.1038/s41598-020-71094-8>
- Barichello, T., Rocha Catalão, C. H., Rohlwick, U. K., Kuip, M. V. D., Zaharie, D., Solomons, R. S., ... & Namale, V. S. (2023). Bacterial meningitis in Africa. *Frontiers in neurology*, 14, 822575. Doi: [10.3389/fneur.2023.822575](https://doi.org/10.3389/fneur.2023.822575)
- Barreto, A. et al. Long-term characterisation of the vertical structure of the Saharan Air Layer over the Canary Islands using lidar and radiosonde profiles: implications for radiative

- and cloud processes over the subtropical Atlantic Ocean. *Atmos. Chem. Phys.* 22, 739–763 (2022).
- Bassat Orellana, Q., & GBD 2016 Meningitis Collaborators. (2018). Global, regional, and national burden of meningitis, 1990-2016: a systematic analysis for the Global Burden of Disease Study 2016. *The Lancet Neurology*, 2018, vol. 17, num. 12, p. 1061-1082.
- Batista, R. S., Gomes, A. P., Gazineo, J. L. D., Miguel, P. S. B., Santana, L. A., Oliveira, L., & Geller, M. (2017). Meningococcal disease, a clinical and epidemiological review. *Asian Pacific journal of tropical medicine*, 10(11), 1019-1029. <https://doi.org/10.1016/j.apjtm.2017.10.004>
- Ben-Ami, Y., Koren, I., Altaratz, O., Kostinski, A., & Lehahn, Y. (2012). Discernible rhythm in the spatio/temporal distributions of transatlantic dust. *Atmospheric Chemistry and Physics*, 12(5), 2253-2262.
- Breiman, L. Random forests. *Mach. Learn.* 2001, 45, 5–32. [Google Scholar] [CrossRef] [Green Version]
- Broutin, H., Thiongane, O., Agier, L., Van-Engelgem, I., Ghomsi, J. P. J., Ouattara, A., ... & Graham, J. E. (2018). Fighting Meningitis in Africa: A Call for a Multi Sectorial Action. *Journal of Tropical Medicine and Health Opinion*. DOI: 10.29011/JTMH-129.000029
- Cartwright, K. (2006). Historical aspects. *Handbook of Meningococcal Disease: Infection Biology, Vaccination, Clinical Management*, 1-13.
- Caruana R, Niculescu-Mizil A (2006) An empirical comparison of supervised learning algorithms. In: Proceedings of the 23rd international conference on machine learning, ICML'06. ACM Press, New York, pp 161–168
- Chacon-Cruz, E., Martinez-Longoria, C. A., Llausas-Magana, E., Luevanos- Velazquez, A., Vazquez-Narvaez, J. A., Beltran, S., et al. (2016). Neisseria meningitidis and Streptococcus pneumoniae as leading causes of pediatric bacterial meningitis in nine Mexican hospitals following 3 years of active surveillance. *Ther. Adv. Vaccines* 4 (1-2), 15–19. [doi: 10.1177/2051013616650158](https://doi.org/10.1177/2051013616650158)
- Chen, J., Jiao, Z., Liang, Z., Ma, J., Xu, M., Biswal, S., ... & Zhang, Z. (2023). Association between temperature variability and global meningitis incidence. *Environment international*, 171, 107649. <https://doi.org/10.1016/j.envint.2022.107649>
- Chen T, Guestrin C (2016) Xgboost: a scalable tree boosting system. In: Proceedings of the 22nd ACM SIGKDD international conference on knowledge discovery and data mining, KDD'16. ACM, New York, pp 785–794

- Chen, T. M., Chen, H. Y., Hu, B., Hu, H. L., Guo, X., Guo, L. Y., et al. (2021). Characteristics of Pediatric Recurrent Bacterial Meningitis in Beijing Children's Hospital 2006-2019. *J. Pediatr. Infect. Dis. Soc* 10 (5), 635–640. [doi: 10.1093/jpids/piaa176](https://doi.org/10.1093/jpids/piaa176)
- Chen, R. C., Caraka, R. E., Arnita, N. E. G., Pomalingo, S., Rachman, A., Toharudin, T., ... & Pardamean, B. (2020). An end to end of scalable tree boosting system. *Sylwan*, 165(1), 1-11.
- Colubri, A., Silver, T., Fradet, T., Retzepe, K., Fry, B., & Sabeti, P. (2016). Transforming clinical data into actionable prognosis models: machine-learning framework and field-deployable app to predict outcome of Ebola patients. *PLoS neglected tropical diseases*, 10(3), e0004549. <https://doi.org/10.1371/journal.pntd.0004549>
- Cook, K. H. (1999). Generation of the African easterly jet and its role in determining West African precipitation. *Journal of climate*, 12(5), 1165-1184.
- Cristea, D., Ciobanu, E., & Croitoru, C. (2024). The use of the specialized questionnaire for assessing the risks of global warming and the development of infectious diseases in the Republic of Moldova. *Bulletin Științific Supliment Cadet Inova*, (9), 289-298.
- De Longueville, F., Ozer, P., Doumbia, S., & Henry, S. (2013). Desert dust impacts on human health: an alarming worldwide reality and a need for studies in West Africa. *International journal of biometeorology*, 57, 1-19. <https://doi.org/10.1007/s00484-012-0541-y>
- DeFlorio, M. J., Goodwin, I. D., Cayan, D. R., Miller, A. J., Ghan, S. J., Pierce, D. W., ... & Singh, B. (2016). Interannual modulation of subtropical Atlantic boreal summer dust variability by ENSO. *Climate Dynamics*, 46, 585-599.
- Deng, L., Xu, H., Liu, P., Wu, S., Shi, Y., Lv, Y., & Chen, X. (2020). Prolonged exposure to high humidity and high temperature environment can aggravate influenza virus infection through intestinal flora and Nod/RIP2/NF-κB signaling pathway. *Veterinary Microbiology*, 251, 108896. <https://doi.org/10.1016/j.vetmic.2020.108896>
- Deroubaix, A., Martiny, N., Chiapello, I., & Marticorena, B. (2013). Suitability of OMI aerosol index to reflect mineral dust surface conditions: Preliminary application for studying the link with meningitis epidemics in the Sahel. *Remote sensing of environment*, 133, 116-127.
- Diokhane, A. M., Jenkins, G. S., Manga, N., Drame, M. S., & Mbodji, B. (2016). Linkages between observed, modeled Saharan dust loading and meningitis in Senegal during 2012 and 2013. *International journal of biometeorology*, 60, 557-575.
- Dione, C., Talib, J., Bwaka, A. M., Kamga, A. F., Fouda, A. A. B., Hirons, L., ... & Woolnough, S. J. (2022). Improved sub-seasonal forecasts to support preparedness action for meningitis outbreak in Africa. *Climate Services*, 28, 100326.

- Diop, A. B., Wade, M., Sy, A., Mbodji, A. K., Farota, A. K., Deme, E. H., ... & Diakhaby, A. (2022). Atmospheric Conditions for Uplift and Dust Transport in the Latitudinal 10° North–20° North Band In Africa. *Atmosphere*, 13(7), 1083. <https://doi.org/10.3390/atmos13071083>
- Diouf D, Martín-Rey M, Rodríguez-Fonseca B, Diouf I, Dione C, Akinbobola A and Gaye AT (2025) Influence of environmental variability on meningitis in West African countries: pre- and post-vaccination. *Front. Environ. Health* 4:1531076. DOI:[10.3389/fenvh.2025.1531076](https://doi.org/10.3389/fenvh.2025.1531076)
- Dominguez-Rodriguez, A., Baez-Ferrer, N., Rodríguez, S., Avanzas, P., Abreu-Gonzalez, P., Terradellas, E., ... & Werner, E. (2020). Saharan dust events in the dust belt-Canary Islands-and the observed association with in-hospital mortality of patients with heart failure. *Journal of Clinical Medicine*, 9(2), 376. <https://doi.org/10.3390/jcm9020376>
- Ebi, K. L., Vanos, J., Baldwin, J. W., Bell, J. E., Hondula, D. M., Errett, N. A., ... & Berry, P. (2021). Extreme weather and climate change: population health and health system implications. *Annual review of public health*, 42(1), 293-315.
- El-Shafay, A. S., Hegazi, A. A., Zeidan, E. S. B., El-Emam, S. H., & Okasha, F. M. (2020). Experimental and numerical study of sawdust air-gasification. *Alexandria Engineering Journal*, 59(5), 3665-3679.
- Fanny, R., Djuraidah, A., & Alamudi, A., 2018. Pendugaan Produktivitas Bagan Perahu dengan Regresi Gulud, LASSO dan Elastic-net. *Xplore: Journal of Statistics*, Vol. 2, No 2,7–14.
- García-Serrano, J., Cassou, C., Douville, H., Giannini, A. & Doblus- Reyes, F. J. Revisiting the ENSO teleconnection to the tropical North Atlantic. *J. Clim.* 30, 6945–6957 (2017).
- Greenwood, B. M., Bradley, A. K., Blakebrough, I. S., Wali, S., & Whittle, H. C. (1984). Meningococcal disease and season in sub-Saharan Africa. *The Lancet*, 323(8390), 1339-1342.
- Hochreiter, S., & Schmidhuber, J. (1997). Long short-term memory. *Neural computation*, 9(8), 1735-1780.
- Jegede, A., Conteh, A., Sow, K., Boyon, M., Grant, C., Schmidt-Sane, M., & Leach, M. (2024). SSHAP West Africa Hub: Health Emergency Cycles and Social Context in West Africa. <https://doi.org/10.19088/SSHAP.2024.023>
- Jenkins, G. S., Gaye, A. T., & Sylla, B. (2005). Late 20th century attribution of drying trends in the Sahel from the Regional Climate Model (RegCM3). *Geophysical Research Letters*, 32(22).

- Jordan et al., 2020) A. K., Zaitchik, B. F., Gnanadesikan, A., Kim, D., & Badr, H. S. (2020). Strength of linkages between dust and circulation over North Africa: Results from a coupled modeling system with active dust. *Journal of Geophysical Research: Atmospheres*, 125, e2019JD030961. <https://doi.org/10.1029/2019JD030961>
- Jusot, J. F., Neill, D. R., Waters, E. M., Bangert, M., Collins, M., Moreno, L. B., ... & Kadioglu, A. (2017). Airborne dust and high temperatures are risk factors for invasive bacterial disease. *Journal of Allergy and Clinical Immunology*, 139(3), 977-986.
- Kekeisen-Chen, J. F., Tarbangdo, F. T., Sharma, S., Marasini, D., Marjuki, H., Kibler, J. L....McNamara, L. A. (2024). Expansion of *Neisseria meningitidis* Serogroup C Clonal Complex 10217 during Meningitis Outbreak, Burkina Faso, 2019. *Emerging Infectious Diseases*, 30(3), 460-468. <https://doi.org/10.3201/eid3003.221760>.
- Kwambana-Adams, B. A., Liu, J., Okoi, C., Mwenda, J. M., Mohammed, N. I., Tsolenyanu, E., ... & Houpt, E. (2020). Etiology of pediatric meningitis in West Africa using molecular methods in the era of conjugate vaccines against *Pneumococcus*, *Meningococcus*, and *Haemophilus influenzae* Type b. *The American journal of tropical medicine and hygiene*, 103(2), 696.
- Kamwamba, T. E. (2017). *Synergistic Interactions of Selected Medicinal Plants Traditionally Used to Treat Meningitis* (Doctoral dissertation, Nelson Mandela Metropolitan University).
- Lapeyssonnie, L. (1963). Cerebrospinal meningitis in Africa. *Bulletin of the world Health organization*, 28, 1-114.
- Le, T., & Bae, D. H. (2022). Causal influences of El Niño–Southern Oscillation on global dust activities. *Atmospheric Chemistry and Physics*, 22(8), 5253-5263. <https://doi.org/10.5194/acp22-5253-2022>
- Lee, D. S., Kwak, J. H., Hong, J. H., et al. (2023). Development and validation of an artificial intelligence model for the early classification of the aetiology of meningitis and encephalitis. *EclinicalMedicine*, 61, 102044. <https://doi.org/10.1016/j.eclinm.2023.102044>
- Lee, E. C., Asher, J. M., Goldlust, S., Kraemer, J. D., Lawson, A. B., Bansal, S., & Moritz, S. (2022). A comparison of infectious disease forecasting methods across locations, diseases, and time. *BMC Infectious Diseases*, 22, 238. <https://doi.org/10.1186/s12879-022-07161-8>
- Liu, Y.; Yang, T.; Tian, L.; Huang, B.; Yang, J.; Zeng, Z. Ada-XG-CatBoost: A Combined Forecasting Model for Gross Ecosystem Product (GEP) Prediction. *Sustainability* 2024, 16, 7203. <https://doi.org/10.3390/su16167203>
- Liu, Y., Zhang, S., Li, H., et al. (2023). Development and validation of a machine learning model to predict prognosis in HIV-negative cryptococcal meningitis patients: A

- multicenter study. *Frontiers in Public Health*, 11, 1211354. <https://doi.org/10.3389/fpubh.2023.1211354>
- Lucas, M. J., Brouwer, M. C., & van de Beek, D. (2016). Neurological sequelae of bacterial meningitis. *Journal of Infection*, 73(1), 18-27. <https://doi.org/10.1016/j.jinf.2016.04.009>
- Lou, S., Russell, L. M., Yang, Y., Liu, Y., Singh, B., & Ghan, S. J. (2017). Impacts of interactive dust and its direct radiative forcing on interannual variations of temperature and precipitation in winter over East Asia. *Journal of Geophysical Research: Atmospheres*, 122(16), 8761-8780.
- Mahowald, N., Albani, S., Kok, J. F., Engelstaeder, S., Scanza, R., Ward, D. S., & Flanner, M. G. (2014). The size distribution of desert dust aerosols and its impact on the Earth system. *Aeolian Research*, 15, 53-71.
- Martín-Rey, M., Vallès-Casanova, I., & Pelegrí, J. L. (2023). Upper-ocean circulation and tropical Atlantic interannual modes. *Journal of Climate*, 36(8), 2625-2643. <https://doi.org/10.1175/JCLI-D-22-0184.1>
- Martiny, N., & Chiapello, I. (2013). Assessments for the impact of mineral dust on the meningitis incidence in West Africa. *Atmospheric Environment*, 70, 245-253.
- Mishra, S., Mishra, D., & Santra, G. H. (2020). Adaptive boosting of weak regressors for forecasting of crop production considering climatic variability: An empirical assessment. *Journal of King Saud University-Computer and Information Sciences*, 32(8), 949-964. <https://doi.org/10.1016/j.jksuci.2017.12.004>
- Mohammed, I., Iliyasu, G., & Habib, A. G. (2017). Emergence and control of epidemic meningococcal meningitis in sub-Saharan Africa. *Pathogens and global health*, 111(1), 1-6. doi: [10.1080/20477724.2016.1274068](https://doi.org/10.1080/20477724.2016.1274068)
- Molesworth, A.M., Cuevas, L.E., Connor, S.J., Morse, A.P., Thomson, M.C., 2003. Environmental risk and meningitis epidemics in Africa. *Emerg. Infect. Dis.* 9 (10), 1287–1293. <https://doi.org/10.3201/eid0910.030182>.
- Mueller, J. E., Woringer, M., Porgho, S., Madec, Y., Tall, H., Martiny, N., & Bicaba, B. W. (2017). The association between respiratory tract infection incidence and localised meningitis epidemics: an analysis of high-resolution surveillance data from Burkina Faso. *Scientific reports*, 7(1), 11570.
- Nalluri, M., Pentela, M., & Eluri, N. R. (2020). A scalable tree boosting system: XG boost. *Int.J. Res. Stud. Sci. Eng. Technol*, 7(12), 36-51.
- Oluwole OSA (2015) Climate regimes, El Niño-southern oscillation, and meningococcal meningitis epidemics. *Front. Public Health* 3:187. doi: [10.3389/fpubh.2015.00187](https://doi.org/10.3389/fpubh.2015.00187)

- Pandya, R., Hodgson, A., Hayden, M. H., Akweongo, P., Hopson, T., Forgor, A. A., ... & Semazzi, F. (2015). Using weather forecasts to help manage meningitis in the West African Sahel. *Bulletin of the American Meteorological Society*, 96(1), 103-115.
- Peng, X., Zhu, Q., Liu, J., Zeng, M., Qiu, Y., Zhu, C., et al. (2021). Prevalence and antimicrobial resistance patterns of bacteria isolated from cerebrospinal fluid among children with bacterial meningitis in China from 2016 to 2018: a multicenter retrospective study. *Antimicrob. Resist. Infect. Control.* 10 (1), 24. doi: 10.1186/s13756-021-00895-x
- Prospero, J. M., Ginoux, P., Torres, O., Nicholson, S. E., & Gill, T. E. (2002). Environmental characterization of global sources of atmospheric soil dust identified with the Nimbus 7 Total Ozone Mapping Spectrometer (TOMS) absorbing aerosol product. *Reviews of geophysics*, 40(1), 2-1. <https://doi.org/10.1029/2000RG000095>
- Prospero, J. M. (1996). Saharan dust transport over the North Atlantic Ocean and Mediterranean: An overview. *The impact of desert dust across the Mediterranean*, 133-151.
- Prospero, J. M., & Lamb, P. J. (2003). African droughts and dust transport to the Caribbean: Climate change implications. *Science*, 302(5647), 1024-1027.
- ResearchGate:<https://www.researchgate.net/publication/220579612DOI:10.1504/IJBIDM.2007.015485>
- ResearchGate: <https://www.researchgate.net/publication/376832547> DOI: 10.20956/j.v20i2.31632
- Ridley, D. A., Heald, C. L., & Prospero, J. M. (2014). What controls the recent changes in African mineral dust aerosol across the Atlantic?. *Atmospheric Chemistry and Physics*, 14(11), 5735-5747. <https://doi.org/10.5194/acp-14-5735-2014>
- Rodríguez-Fonseca, B., Suárez-Moreno, R., Ayarzagüena, B., López-Parages, J., Gómara, I., Villamayor, J., ... & Castaño-Tierno, A. (2016). A review of ENSO influence on the North Atlantic. A non-stationary signal. *Atmosphere*, 7(7), 87. doi:10.3390/atmos7070087
- Roy, C., & Reason, C. (2001). ENSO related modulation of coastal upwelling in the eastern Atlantic. *Progress in Oceanography*, 49(1-4), 245-255.
- Sartika, I., Naomi Nessyana, D., & Nurfitri, I., 2020. Analisis Regresi Dengan Metode Least Absolute Shrinkage and Selection Operator (Lasso) Dalam Mengatasi Multikolinearitas. *Bimaster : Buletin Ilmiah Matematika, Statistika Dan Terapannya*, Vol. 9, No. 1, 31–38.

- Schiess, N., Groce, N. E., & Dua, T. (2021). The impact and burden of neurological sequelae following bacterial meningitis: a narrative review. *Microorganisms*, 9(5), 900.
- Shao, Z., Ahmad, M. N., & Javed, A. (2024). Comparison of random forest and xgboost classifiers using integrated optical and sar features for mapping urban impervious surface. *Remote Sensing*, 16(4), 665.
- Sultan, B., Labadi, K., Guégan, J. F., & Janicot, S. (2005). Climate drives the meningitis epidemics onset in West Africa. *PLoS medicine*, 2(1), e6.
- Sylla, M. B., Giorgi, F., Ruti, P. M., Calmanti, S., & Dell'Aquila, A. (2011). The impact of deep convection on the West African summer monsoon climate: a regional climate model sensitivity study. *Quarterly Journal of the Royal Meteorological Society*, 137(659), 1417-1430.
- Tang, C., Han, R., Yang, J., Wu, N., & He, D. (2025). Comprehensive analysis of the Global Burden and epidemiological trends of meningitis from 1990 to 2021. *Infection*, 1-17.
- Thiam, M., Oruba, L., de Coetlogon, G., Wade, M., Diop, B., & Farota, A. K. (2024). Impact of the Sea Surface Temperature in the North-Eastern Tropical Atlantic on Precipitation Over Senegal. *Journal of Geophysical Research: Atmospheres*, 129(3), e2023JD040513.
- Thomson, M. C., Molesworth, A. M., Djingarey, M. H., Yameogo, K. R., Belanger, F., & Cuevas, L. E. (2006). Potential of environmental models to predict meningitis epidemics in Africa. *Tropical Medicine & International Health*, 11(6), 781-788. doi:10.1111/j.1365-3156.2006.01630.x
- Vallès-Casanova, I., Adam, O., & Martín Rey, M. (2025). Influence of winter Saharan dust on equatorial Atlantic variability. *Communications Earth & Environment*, 6(1), 31. <https://doi.org/10.1038/s43247-024-01926-2>
- Von Storch H., Frankignoul C. 1998. Empirical Modal Decomposition in coastal oceanography. In: Brink K.H., Robinson A.R. (eds.) *The Sea: Vol. 10, the Global Coastal Ocean*. John Wiley, p. 419-455.
- Wagner, R., Schepanski, K., Heinold, B., & Tegen, I. (2016). Interannual variability in the Saharan dust source activation—Toward understanding the differences between 2007 and 2008. *Journal of Geophysical Research: Atmospheres*, 121(9), 4538-4562.
- Washington, R., Todd, M., Middleton, N. J., & Goudie, A. S. (2003). Dust-storm source areas determined by the total ozone monitoring spectrometer and surface observations. *Annals of the Association of American Geographers*, 93(2), 297-313. <https://doi.org/10.1111/1467-8306.9302003>

- Wilder, B., Suen, S. C., & Tambe, M. (2018, April). Preventing infectious disease in dynamic populations under uncertainty. In *Proceedings of the AAAI Conference on Artificial Intelligence* (Vol. 32, No. 1).
- World Health Organization. (2024). *Investing to Defeat Meningitis and beyond*. World Health Organization.
- WHO (2023). <https://www.who.int/emergencies/disease-outbreak-news/item/2023-DON439>
- WHO (1998). Control of Epidemic Meningococcal Disease. WHO Practical Guidelines, 2nd edn. Geneva: World Health Organization.
- Woringer, M., Martiny, N., Porgho, S., Bicaba, B. W., Bar-Hen, A., & Mueller, J. E. (2018). Atmospheric dust, early cases, and localized meningitis epidemics in the African meningitis belt: an analysis using high spatial resolution data. *Environmental health perspectives*, 126(9), 097002.
- Wright, C., Blake, N., Glennie, L., Smith, V., Bender, R., Kyu, H., ... & Trotter, C. (2021). The global burden of meningitis in children: challenges with interpreting global health estimates. *Microorganisms*, 9(2), 377.
- Yaka, P., Sultan, B., Broutin, H., Janicot, S., Philippon, S., & Fourquet, N. (2008). Relationships between climate and year-to-year variability in meningitis outbreaks: a case study in Burkina Faso and Niger. *International journal of health geographics*, 7, 1-13. doi:10.1186/1476-072X-7-34
- Yarber, A. L., Jenkins, G. S., Singh, A., & Diokhane, A. (2023). Temporal relationships between Saharan dust proxies, climate, and meningitis in Senegal. *GeoHealth*, 7(2), e2021GH000574.
- Zhang, Y., Zhao, Z., Zheng, J., 2020. CatBoost: a new approach for estimating daily reference crop evapotranspiration in arid and semi-arid regions of northern China. *J. Hydrol.* 588, 125087
- <https://www.afro.who.int/sites/default/files/2017-09/Dashboard%20of%20Nigeria%20meningitis%20-%20EndF.pdf>

Data availability statement

Publicly available datasets were analyzed in this study. This data can be found at the following links:

WHO :

meningitis data: <https://www.menafri.net.org/who-meningitis-bulletins>

MERRA2:

AOD & DUCMASS: <https://disc.gsfc.nasa.gov/datasets?keywords=Aerosols&page=1>

CAMS:

PM10: <https://ads.atmosphere.copernicus.eu/datasets/cams-global-reanalysis-eac4?tab=download>

ERA5:

<https://cds.climate.copernicus.eu/datasets/reanalysis-era5-single-levels?tab=download>.

HadISST:

<https://climatedataguide.ucar.edu/climate-data/sst-data-hadisst-v11>

Appendices

Publication:

Title: **“Influence of environmental variability on meningitis in West African countries: pre- and post-vaccination”**

Diarra Diouf^{1,2*}, Marta Martín-Rey³, Belén Rodríguez-Fonseca^{3,4}, Ibrahima Diouf^{2,5}, Cheikh Dione⁶, Ademola Akinbobola¹ and Amadou T. Gaye²

Citation:

Diouf D, Martín-Rey M, Rodríguez-Fonseca B, Diouf I, Dione C, Akinbobola A and Gaye AT (2025) Influence of environmental variability on meningitis in West African countries: pre- and post-vaccination. Front. Environ. Health 4:1531076. DOI:[10.3389/fenvh.2025.1531076](https://doi.org/10.3389/fenvh.2025.1531076)